

Master thesis : INSULIN SENSITIVITY TESTING MODEL - BASED SUBCUTANEOUS - ORAL INSULIN SENSITIVITY TESTING

Auteur : Bekisz, Sophie

Promoteur(s) : Desaive, Thomas

Faculté : Faculté des Sciences appliquées

Diplôme : Master en ingénieur civil biomédical, à finalité spécialisée

Année académique : 2017-2018

URI/URL : <http://hdl.handle.net/2268.2/4594>

Avertissement à l'attention des usagers :

Tous les documents placés en accès ouvert sur le site le site MatheO sont protégés par le droit d'auteur. Conformément aux principes énoncés par la "Budapest Open Access Initiative"(BOAI, 2002), l'utilisateur du site peut lire, télécharger, copier, transmettre, imprimer, chercher ou faire un lien vers le texte intégral de ces documents, les disséquer pour les indexer, s'en servir de données pour un logiciel, ou s'en servir à toute autre fin légale (ou prévue par la réglementation relative au droit d'auteur). Toute utilisation du document à des fins commerciales est strictement interdite.

Par ailleurs, l'utilisateur s'engage à respecter les droits moraux de l'auteur, principalement le droit à l'intégrité de l'oeuvre et le droit de paternité et ce dans toute utilisation que l'utilisateur entreprend. Ainsi, à titre d'exemple, lorsqu'il reproduira un document par extrait ou dans son intégralité, l'utilisateur citera de manière complète les sources telles que mentionnées ci-dessus. Toute utilisation non explicitement autorisée ci-avant (telle que par exemple, la modification du document ou son résumé) nécessite l'autorisation préalable et expresse des auteurs ou de leurs ayants droit.



INSULIN SENSITIVITY TESTING

MODEL-BASED SUBCUTANEOUS-ORAL INSULIN SENSITIVITY TESTING

Master thesis conducted by

SOPHIE BEKISZ

with the aim of obtaining the degree of Master in Biomedical Engineering

Under the supervision of

Prof. Thomas DESAIVE

Prof. J. Geoffrey CHASE

ACADEMIC YEAR 2017-2018

"Any knowledge begins with feelings"

Leonardo Da Vinci

Abstract

The prevalence of diabetes, particularly Type 2 Diabetes (T2D), is dramatically rising and reaching epidemic proportions. Diabetes and its complications are thus become a major public health problem, with an economic cost of approximately 1 % of Growth Domestic Product (GDP), and equal social burden. Pathogenesis of type 2 diabetes includes insulin resistance, or low insulin sensitivity, describing the impaired capacity of the body to regulate glucose. Insulin resistance develops long before the final state of the disease. The diagnosis of pre-diabetes and eventual T2D is thus possible years before type 2 diabetes eventuates. Irreparable damage can be prevented by early detection, offering the opportunity to delay or eliminate development of diabetes, reducing cost and social burden.

Current diabetes tests do not use insulin sensitivity directly but detect the disease on the basis of late-appearing symptoms, particularly rising glucose levels, when it is already in a critical, near diabetes situation, or later. Among these diagnosis tools, the Oral Glucose Tolerance Test (OGTT) is the most recommended and able to detect pre-diabetes. In contrast, insulin sensitivity tests are either low resolution, and/or costly, invasive, time-consuming, and not adapted for a large population screening, However, the Dynamic Insulin Sensitivity and Secretion Test (DISST) is a power model-based diagnostic tool without these issues, but could potentially be made much simpler.

This master thesis is part of a larger research project at the University of Canterbury (Christchurch, New Zealand), aiming at translating the DISST model-based test to a less invasive version. The proposed protocol uses 35 g of oral glucose and 2 units of rapid-acting insulin. The insulin injection is performed subcutaneously with a needle free and painless injection device. The number of blood samples is reduced and some are extracted with less invasive finger-prick methods with an eye toward eventual needle free sensing technology under development. Blood samples are collected over a 2-hour period and assessed for blood glucose, C-peptide and insulin. This model-based subcutaneous-oral insulin sensitivity testing would allow direct identification of the insulin sensitivity and thus provide crucial information about diabetes status and progression. It would also enable the same low-cost hierarchy of tests like the DISST.

The DISST model is originally a glycaemic control model. It is modified in this research to consider oral glucose absorption and subcutaneous insulin injection kinetics as employed in this new test. A gastrointestinal glucose sub-model, a subcutaneous insulin delivery sub-model, and a glycaemic control sub-model are thus combined. Even

though these different sub-models have been validated separately, the overall system model needs validation, which is the main goal of this research.

A sensitivity analysis is performed to demonstrate the robustness of the model, as well as the potential accuracy of this new kind of Dynamic Insulin Sensitivity and Secretion Test (DISST). It identifies critical, sensitive model parameters in the context of the combined overall system model. This *in silico* investigation also provides a means to highlight any model and protocol weakness.

A single parameter sensitivity analysis is conducted first, where the effects of model parameters on model outcomes are analysed individually. Parameters with the biggest influence on blood glucose evolutions are identified. Changes of parameters always lead to a coherent modification of blood glucose evolution and no non-physiological behaviour is observed, providing initial model validation. Clinically significant modifications are not detected for most parameters.

The results of this single parameter sensitivity analysis are used to perform a multiple parameter Monte Carlo investigation. This study defines the potential range and resolution of the overall system model, as well as the inter-subject and intra-subject variability. This analysis consolidates the model validation. The multiple parameter sensitivity analysis is then applied to the now validated model to assess protocol safety.

Because the trial received ethics approval during the writing of this master thesis (April 30, 2018), I have been able to assist the first experimental assay practically using the model. The first clinical pilot test, carried on subject 1, is described. With the results obtained, a rapid parametric identification is performed to assess insulin sensitivity and further validate the model developed. However, as those experiments are still in their early days, the aim of this part of the project is more related to a proof of concept of the model, as well as a personal achievement, to see how could the model be useful for real clinical experiments.

Acknowledgements

In order to complete this master thesis, many people helped and supported me. I would like to thank all of them for everything they did for me. Indeed, I had never been asked to carry out such a considerable work before and I certainly would not have been able to conclude this task without their assistance.

First and foremost, I would like to express all my gratitude to my Professor Mr Thomas Desaive, my supervisor at the University of Liège. Besides giving me the opportunity to take part in a very attractive study at the University of Canterbury (Christchurch, New Zealand), he was all along responsive and prepared to answer my many questions. His opinion and advice always provided me a valuable assistance and allowed me to view the remaining labour enthusiastically. Motivation and rigour being his keywords, I consider myself lucky to have had him as my supervising professor.

Then, I would like to thank my supervisor at the University of Canterbury, the Professor Mr J. Geoffrey Chase, for welcoming and including me in his school and researches. His office was consistently open and he was always available to clarify my misunderstandings, even several times if it was necessary. Thanks to him, I really felt integrated in this large scale project and not just like a student in whom we do not trust.

Thereafter, I would like to express my thanks to Lui Pearson, the PhD student with whom I have worked all along my internship. He agreed that I use his codes for my own task, always answered my questions and took care of my issues.

Afterwards, I would like to emphasize my gratefulness to the simple and doctoral students I have met during the achievement of my master thesis. First, I would like to mention Vincent Uyttendaele who introduced and explained me some concepts about my subject. Then, I would not forget all the PhD students of my office who made this place very convivial and pleasant to work. Lastly, I would like to thank the students I have met during my internship and who encouraged me throughout critical periods.

Finally, I am thankful to my family and my friends who encouraged me during this project.

Contents

Abstract	I
Acknowledgements	IV
Contents	VI
1 Introduction	1
2 Background	4
2.1 Glucose and glycaemia	4
2.2 Insulin	6
2.3 Natural glucose regulation	8
2.4 Insulin sensitivity	8
2.5 Diabetes	9
2.5.1 Type 1 diabetes (T1D)	11
2.5.2 Type 2 diabetes (T2D)	11
2.6 Diagnosis	11
2.6.1 Diabetes testing	12
▷ FPG / FGT	12
▷ OGTT	13
▷ HbA _{1c}	15
2.6.2 Insulin secretion or sensitivity testing	16
▷ Clamp	17
▷ IVGTT	19
▷ IM-IVGTT	24
▷ DISST	24
▷ DISTq	27
2.7 Summary	27

3	The SC-OG-ICING-2 model	28
3.1	Sub-model 1 : Glycaemic control model	28
3.2	Sub-model 2 : Gastrointestinal model	34
3.3	Sub-model 3 : Subcutaneous insulin injection model	37
3.4	Summary	38
4	Single parameter sensitivity analysis	39
4.1	Parameters of interest	39
4.2	Physiological ranges	40
4.3	Results and Discussion	43
4.4	Summary	52
5	Multiple parameter sensitivity analysis	54
5.1	Parameters of interest	54
5.2	Methodology	55
5.3	Results and Discussion	56
5.3.1	Consolidation of model validity	56
5.3.2	Verification of protocol safety	63
5.4	Summary	69
6	Clinical trial	71
6.1	Protocol	71
6.1.1	Initial protocol	71
6.1.2	Possible changes	75
6.2	Ethics approval	76
6.3	Test results	76
6.4	Analysis	79
6.5	Summary	80
7	Conclusions	82
7.1	General conclusions	82
7.2	Perspectives and Future work	84
	Appendices	85
	Bibliography	93

List of abbreviations

ACRONYMS

BG	Blood Glucose
BGL	Blood Glucose Level
CNS	Central Nervous System
DISST	Dynamic Insulin Sensitivity and Secretion Test
DISTq	quick Dynamic Insulin Sensitivity Testing
EGP	Endogenous Glucose Production
FPG	Fasting Plasma Glucose
FGT	Fasting Glucose Test
FS-IVGTT	Frequent Sampling IntraVenous Glucose Tolerance Test
GDP	Growth Domestic Product
GTT	Glucose Tolerance Test
HbA	Haemoglobin A
HEC	Hyperinsulinaemic Euglycaemic Clamp
ICING	Intensive Control Insulin-Nutrition-Glucose
IFG	Impaired Fasting Glucose
IGT	Impaired Glucose Tolerance
IM-IVGTT	Insulin-Modified IntraVenous Glucose Tolerance Test
ISI	Insulin Sensitivity Index
IV	IntraVenous
ITT	Intensive Insulin Therapy
IVGTT	IntraVenous Glucose Tolerance Test
MI	Monomeric Insulin
MM	Minimal Model

NFIT	Needle Free Injection Technology
NGT	Normal Glucose Tolerance
NHGB	Net Hepatic Glucose Balance
NPH	Neutral Protamine Hagedorn
NZSSD	New Zealand Society for the Study of Diabetes
OGTT	Oral Glucose Tolerance Test
RER	Rough Endoplasmic Reticulum
RI	Regular Insulin
SC	SubCutaneous
T1D	Type 1 Diabetes
T2D	Type 2 Diabetes
TGC	Tight Glycaemic Control
TGN	Trans-Golgi Network
WHO	World Health Organisation

Chapter 1

Introduction

Many people think diabetes is a mild illness linked to a poor glucose metabolism, which can be treated by some insulin injections. Regrettably, they are inaccurate, perhaps due to the increasing prevalence of it in people who may appear otherwise normal. Equally, they may never have witnessed the significant health and life impacts of this disease.

During the time needed to read this sentence, one patient with diabetes died. Indeed, one person passes away every six seconds from diabetes. It is one of the primary sources of death worldwide [1, 2]. Unfortunately, it will keep on evolving and happening in the future, because of the increasingly ageing population and prevalence of obesity.

More than 422 millions of individuals suffer from diabetes and this number is expected to rise to 622 millions by 2040 [2]. One in eleven individuals is affected. Diabetes generates complications, such as cerebrovascular incidents and stroke, blindness, heart attack, renal failure, and amputation [2]. The total health expenditures to treat these complications are very high, approaching 1 % of GDP in western countries [3]. This disease and its long-term complications are thus a major public health problem, which has to be closely studied, treated and regulated.

Diabetes is a disease characterised by hyperglycaemia. Causes of this hyperglycaemia vary and diabetes is thus distinguished by types. Type 1 Diabetes (T1D) is described by a destruction of pancreatic beta cells responsible of insulin production. The body does not produce enough insulin to regulate glycaemia and all insulin must be given exogenously. In contrast, Type 2 Diabetes (T2D) is characterised by a dysfunction of insulin target cells. Despite insulin production, glucose is not able to enter the cells, preventing uptake and causing hyperglycaemia [4].

Type 2 diabetes is thus described by a resistance to insulin. This disease is more incremental in its appearance and evolution than type 1 diabetes. The pathogenesis of this disease is first described by Normal Glucose Tolerance (NGT), followed by a pre-diabetic state, and eventually by type 2 diabetes. Deviation from NGT to pre-diabetes is characterised by a decrease in insulin sensitivity (S_I), supported by a compensatory increase in endogenous pan-

cretic insulin secretion. Normal blood glucose levels are thus maintained. When the pancreas is exhausted and no longer able to produce enough insulin to compensate the decrease in insulin sensitivity, glucose levels rise and type 2 diabetes appears [5].

As insulin resistance developed long before the final appearance of the disease, its diagnosis is thus potentially possible years before type 2 diabetes occurs. Irreparable damage could thus be prevented by early detection. However, the most common diagnosis tests assess the ability of the body to regulate blood glucose and examine glucose levels, which are the last markers to change. Thus, normal blood glucose levels are maintained during pre-diabetes.

Detection of a decreasing insulin sensitivity is thus not possible by simple blood glucose measurements. These tests only detect the disease on the basis of late-appearing symptoms, when it is already at a more critical situation. Among these tests, the Oral Glucose Tolerance Test (OGTT) best detects later stages of the pre-diabetic state [6]. In contrast, insulin sensitivity tests are either low resolution, and/or costly, invasive, time consuming and limited to clinical applications [7], such as the Dynamic Insulin Sensitivity and Secretion Test (DISST) and the IntraVenous Glucose Tolerance Test (IVGTT). Development of tests which are accurate, low-cost, less invasive, and adaptable for economic population screening are thus needed.

This master thesis is part of a larger research project at the University of Canterbury (Christchurch, New Zealand), aiming at developing a new insulin sensitivity test for an efficient monitoring of the pathogenesis of diabetes. This new test translates the DISST model-based test [8, 9, 10] to a far less invasive version. The DISST is based on a glycaemic control model and assesses insulin sensitivity and secretion. It is nonetheless quite invasive because its protocol includes intravenous glucose and insulin injections, as well as several intravenous blood extractions.

The new proposed protocol uses 35 g of oral glucose and 2 units of rapid-acting insulin. The insulin injection is performed subcutaneously with a needle free injection device, 15 minutes after the beginning of the test. The number of blood samples is reduced and some are even extracted with a less invasive finger-prick method than the intravenous route, in preparation for needle free glucose detection technology under development. Blood samples are collected over a 2-hour period and assessed for blood glucose, C-peptide and insulin. This model-based subcutaneous-oral insulin sensitivity testing would allow direct identification of the insulin sensitivity and thus provide crucial information about diabetes status and progression.

First, in this master thesis, biological and physiological basis around diabetes is addressed in Chapter 2. Then, initial DISST model is modified to consider oral glucose absorption and subcutaneous insulin injection. This new model is thus explained in Chapter 3. The main goal of this research project is to validate the overall system model, as well as the protocol, to investigate the potential accuracy of this new test. Chapter 4 performs a single parameter sensitivity analysis, where the effects of model parameters on model outcomes are analysed individually. The aim is to identify the parameters with the biggest influence on blood glucose evolution. Chapter 5 carries out a multiple

parameter Monte Carlo sensitivity analysis to investigate the effect of several parameters on the model and thus to complete the previous analysis. By studying the potential range and resolution of the overall system model, this Monte Carlo analysis aims at consolidating the model validity. Safety of the protocol is also studied in this chapter. Finally, Chapter 6 describes the first clinical pilot trial, practically using this new overall system model.

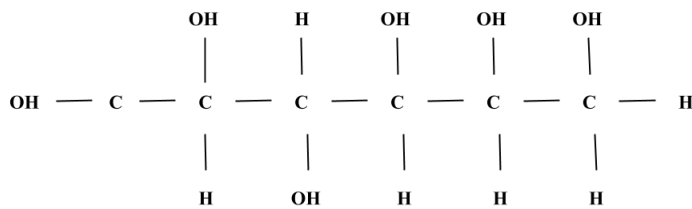
Chapter 2

Background

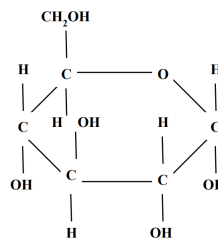
This chapter highlights the background of this project. The biological and physiological basis around diabetes is addressed, including information about glucose, insulin and the natural regulation of glucose. The concept of insulin sensitivity, or its inverse, insulin resistance, is also developed. In addition, the different types of diabetes, their causes and basic effects are explained. Thereafter, methods for the prediction and diagnosis of diabetes are reviewed. In particular, a distinction between diabetes testing and insulin secretion or sensitivity testing is made, as these are the key elements in how early diabetes is diagnosed.

2.1 Glucose and glycaemia

Glucose is a simple sugar whose molecular formula is $C_6H_{12}O_6$. Specifically, because of its hydrogen, carbon and oxygen content, it can be considered as a monosaccharide. Like all the other six-carbon molecules, glucose is an hexose [4]. It can be represented linearly, as shown in Figure 2.1a, but in water and physiological solutions, glucose tends to become withdrawn and thus has a cyclic form (Figure 2.1b) [11].



(a) *Glucose linear form.*



(b) *Glucose cyclic form.*

Figure 2.1 :
Glucose molecular form [11].

Glucose is essential : it is the principal human body power supply. It is converted into an easily accessible form of energy (ATP) via the Krebs Cycle [4], and is used by our cells to achieve fundamental tasks.

Our body does not directly use all absorbed glucose. Some is stored in the liver as glycogen for later use. As illustrated in Figure 2.2, glycogen is a glucose polymer (a polysaccharide). The transformation of glucose into glycogen is called the glycogenesis. The inverse reaction is named glycogenolysis and occurs when the cells need glucose, which is then released in gluconeogenesis [12].

Excess glucose can also be stored in fat in the liver or periphery. Once again, this process can be reversed if energy is required. This mechanism is another form of gluconeogenesis [12]. The result of all these transformations which release glucose stores is called Endogenous Glucose Production (EGP).

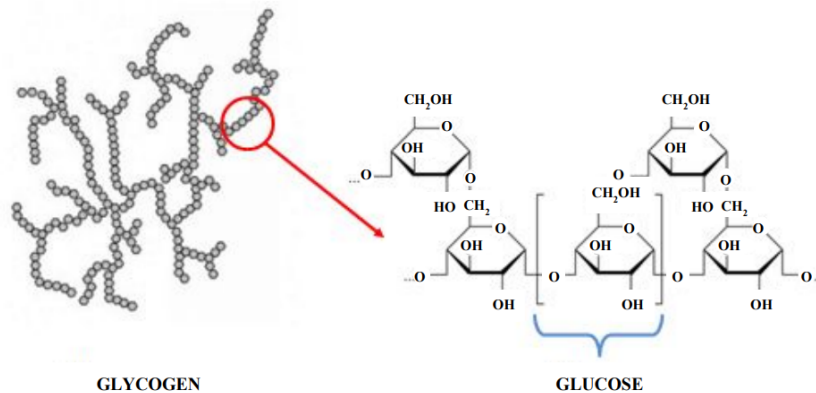


Figure 2.2 :
Glycogen [13, 14].

The brain is the largest user of glucose. However, for the Central Nervous System (CNS), glucose molecules can directly enter these tissue cells by diffusion, in what it is denoted non-insulin mediated glucose uptake [15]. In contrast, muscle, liver and adipose tissue cells are not permeable to glucose and a hormone, the insulin, is thus used to regulate its uptake. One can therefore differentiate insulin-mediated and non-insulin-mediated uptake [16].

Glycaemia, also called the blood sugar level or Blood Glucose Level (BGL), can be defined as the amount of glucose in the blood. Because of the importance of glucose, regulation of blood sugar is necessary to ensure healthy functioning of the organism (see Section 2.3). If BGL is too low, it is called hypoglycaemia and, in contrast, the term hyperglycaemia is used when the blood contains too much glucose. Hypoglycaemic symptoms include tiredness, trembling and syncope. Frequent and extended hypoglycaemia can lead to irreversible damage, such as brain injury and even death [17, 18]. Indeed, neurons are very sensitive to a lack of glucose [15]. On the other hand, thirst and polyuria are symptoms of hyperglycaemia. Enhanced and common hyperglycaemia can have significant consequences, including increased risk of infection, ocular damage, cardiovascular injury and coma [19, 20]. Although glycaemia varies according to various parameters, it is considered normal between 80 mg/dL (4.4 mmol/L) and 126 mg/dL (7 mmol/L) [21]. Across countries, units of glucose concentration may vary between mg/dL and mmol/L, where 1 mmol/L \simeq 18 mg/dL.

2.2 Insulin

Insulin is a hormone produced in the pancreas by the beta cells located in the Islets of Langerhans [4]. Beta cells do not exactly produce insulin, but its precursor, Preproinsulin. It is a peptide of 109 amino acids and it comprises two parts : a signal peptide and the Proinsulin. The signal peptide guides the Preproinsulin towards the Rough Endoplasmic Reticulum (RER), where it is cleaved by a peptidase. Additionally, this enzyme enables the creation of three sulphur bridges in order to fold the Proinsulin in its final configuration. The Proinsulin is turned into mature insulin in the Trans-Golgi Network (TGN). Indeed, peptidases cut Proinsulin at two separates places, leading to the formation of two specific entities : C-peptide and insulin [22, 23].

Insulin comprises two different chains linked through sulphur bridges. Insulin and C-peptide exit the cell by exocytosis [22, 23]. C-peptide is secreted in the same molar amount as insulin, it can thus be used as an accurate marker for the secretion of this hormone. Indeed, this peptide is more stable in blood concentration than insulin because it is only cleared by the kidney, where insulin is cleared by the liver, kidney, and uptake in the periphery [24]. Figure 2.3 represents the different steps from Preproinsulin secretion to insulin and C-peptide formation. Finally, note that insulin is not directly secreted into the circulation, but first passes through the liver, which removes some in first pass extraction.

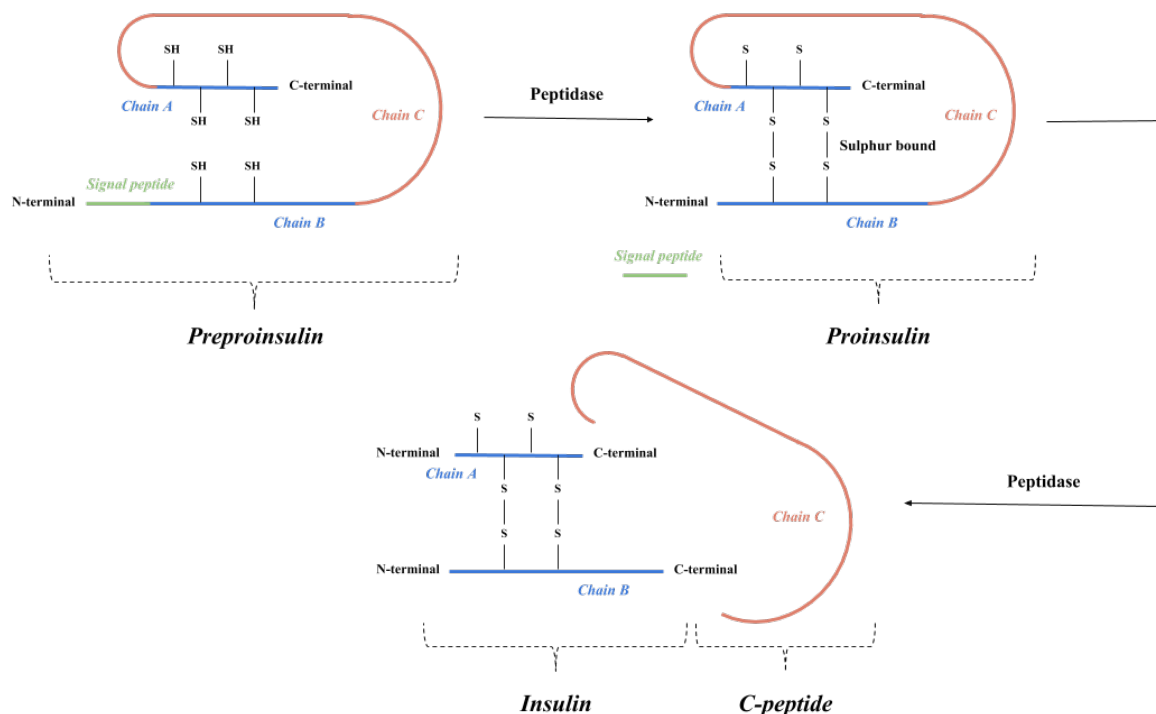


Figure 2.3 :

Different steps from Preproinsulin to insulin and C-peptide [24, 25].

Beta cells continuously produce small amount of insulin, but this synthesis may be stimulated by an increase in blood sugar level (e.g. after eating). Once insulin has been secreted in blood by pancreatic beta cells, it matches

with tyrosine kinase receptors located on target cell membranes. Once activated, this kind of receptor is able to induce a specific cell response. In this case, cells will enable more glucose to enter by activating glucose transporters, leading to a reduction of glycemia. Insulin also allows glucose storage in organs, muscle tissue and fat. It thus enables glycogen formation. Thus, one can conclude insulin enables the decrease of glycaemia by encouraging cells to capture glucose and by aiding its transformation into glycogen [4].

Because of its importance in glucose regulation, insulin has been widely studied and can be easily synthesised. One can therefore distinguish different sorts of insulin : animal, human, and analogue. Each type has specific uses and/or dynamic behaviours.

- ANIMAL INSULIN

Following the discovery of this hormone and its use in some diseases, bovine and porcine insulins have been extracted and exploited. Compared to human insulin, bovine insulin has three different amino acids. In contrast, porcine and human insulin only differ by one amino acid [26]. Before being used on humans, animal insulin is purified by chromatography. This laboratory technique allows to separate the different compounds of a mixture : specifically, non-appropriate substances for human from insulin [27]. Even if animal insulins helped many diabetic individuals, immune rejection was frequent. New methods of chromatography to obtain almost pure animal insulin have thus emerged [26].

Porcine insulin has also been humanised. The distinct amino acid between human and porcine insulins was replaced. In addition, modified animal insulins were created to better match with the physiological features of human insulin. Indeed, the duration of action of animal insulin can be shifted by adding a protein support, zinc or protamine [26].

- HUMAN INSULIN

It is now possible to produce human insulin by genetic engineering [28]. By inserting the human insulin-producing gene in a bacterium, it produces this hormone by proliferating. As for animal insulins, the kinetic properties of human insulin can be enhanced by adding zinc and protamine [29]. Zinc inclusion leads to an increase of the insulin resorption speed and faster appearance after a subcutaneous injection. In contrast, the addition of protamine improves the insulin duration of action by slowing the appearance after a subcutaneous injection.

- ANALOGUE INSULIN

Analogue insulins can be defined as modified human insulin, differing from it in specific amino acids. These sequence changes enable shifts in insulin kinetics. Very fast-acting insulins, as well as very long-acting ones, can thus be created [29]. One can notice that mixture of these different insulins is very interesting for developing insulins with several action peaks and thus better tailored to specific uses.

2.3 Natural glucose regulation

As mentioned earlier, glucose is crucial for the human body. The cells turn it into energy and it is one of the principal supplies of carbon to create organic compounds. Moreover, extended hypoglycaemia or hyperglycaemia can lead to harmful and irreversible damages. Therefore, glucose must be specifically and exactly regulated. Overall, insulin and a second hormone, named glucagon, are responsible for glucose regulation. Glucagon raises glycaemia and insulin lowers it (see Section 2.2). These two hormones have thus antagonist effects [4].

Glucagon causes the release of previously stored glucose (e.g. glycogen) in bloodstream. It is a hyperglycaemic hormone and, contrary to the insulin, is synthesised by alpha cells in the Islets of Langerhans. Production of glucagon is stimulated by hypoglycaemia [4].

Glucagon mainly acts on the liver, by coupling with specific receptors on the surface of liver cells. The principal function of glucagon is to degrade glycogen into glucose by encouraging the glycogenolysis and by inhibiting the glycogenesis. Glucagon thus enables the increase of blood glucose and thus the stabilisation of glycaemia [4]. Notably, although muscles also store glycogen, they are not equipped with glucagon receptors and thus do not feel the influence of this hormone. The degradation of the glycogen accumulated in muscle cells is preferably favoured by one other hormone called adrenaline, which is also stimulated in hypoglycaemia [30].

Figure 2.4 summarises the action of the insulin and the glucagon on the body. With this drawing, one can easily summarise the simultaneous antagonistic actions of these two hormones. In combination, they enable a good blood sugar balancing.

2.4 Insulin sensitivity

The concept of insulin sensitivity (S_I) has to be introduced because of its interest and importance in this thesis and in the overall diabetes framework. It is the inverse of insulin resistance. It can be defined as the body's cellular response to insulin. In other words, it determines the effect of insulin on glucose uptake.

For example, compared to non-insulin sensitive people, insulin sensitive ones need less insulin to help the cells take up glucose. From another point of view, insulin sensitive patients require less insulin to reach the same glycaemia. Individuals with diabetes have low insulin sensitivity and thus require more insulin.

Determining insulin sensitivity is of critical importance. First, it can enable identification of diabetic individuals before irreparable damage appear [5]. Second, for patients whose insulin sensitivity changes over time, such as critical care patients, it enables personalised adaptation of insulin dosing for glycaemic control [31, 32]. Insulin sensitivity computation can be conducted using mathematical models.

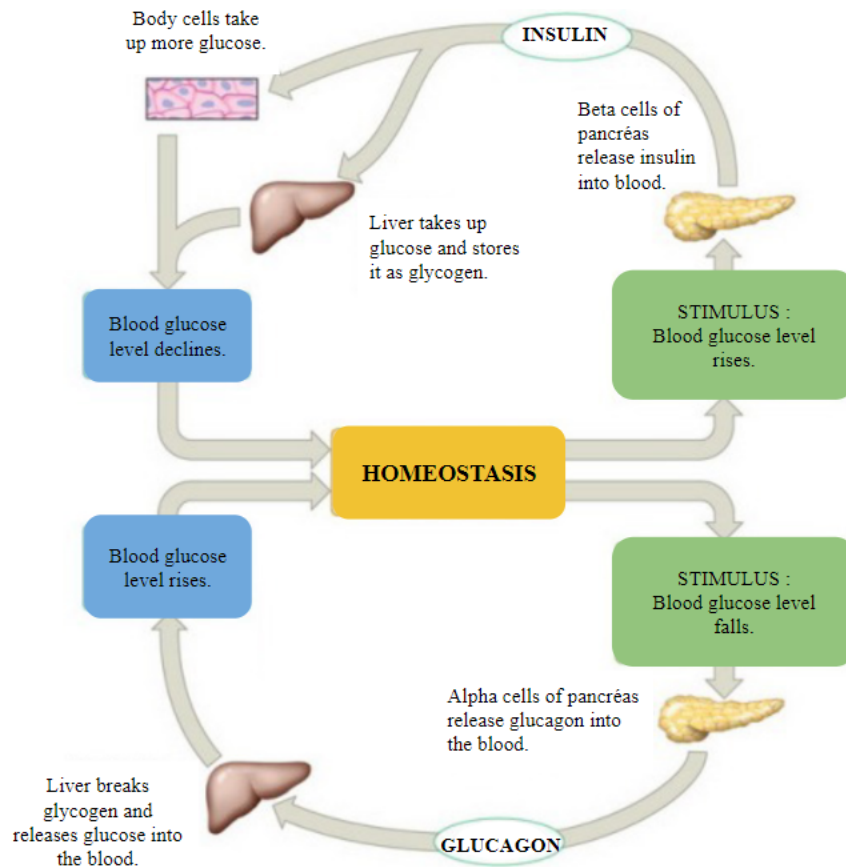


Figure 2.4 :
Normal glucose regulation (inspired from [4]).

However, insulin sensitivity is a broad notion and can cover several phenomena [33]. Indeed, it represents either the ability of the cells to respond to this hormone, either the capacity of beta cells to produce insulin when glucose concentration increases or it may even features the insulin faculty to stop the liver glucose production. When insulin sensitivity is measured through mathematical models and experiments, it is often a combination of these three concepts. Because of the different definitions of this concept, it is important to know which ones are being assessed during insulin sensitivity testing. Figure 2.5 summarises the different notions behind the insulin sensitivity term.

2.5 Diabetes

Diabetes is a disease characterised by hyperglycaemia due to insufficient insulin, (near) complete insulin loss, and/or insulin resistance. Causes of this illness are multiple and diabetes is thus distinguished by types [4].

First, one can mention the case where hyperglycaemia is due to inadequate glucose utilisation, assimilation or storage. People affected by this type of diabetes thus have elevated blood glucose levels. It is related to an improper insulin synthesis or action. Diabetes can be divided into two distinct subcategories : type 1 and type 2.

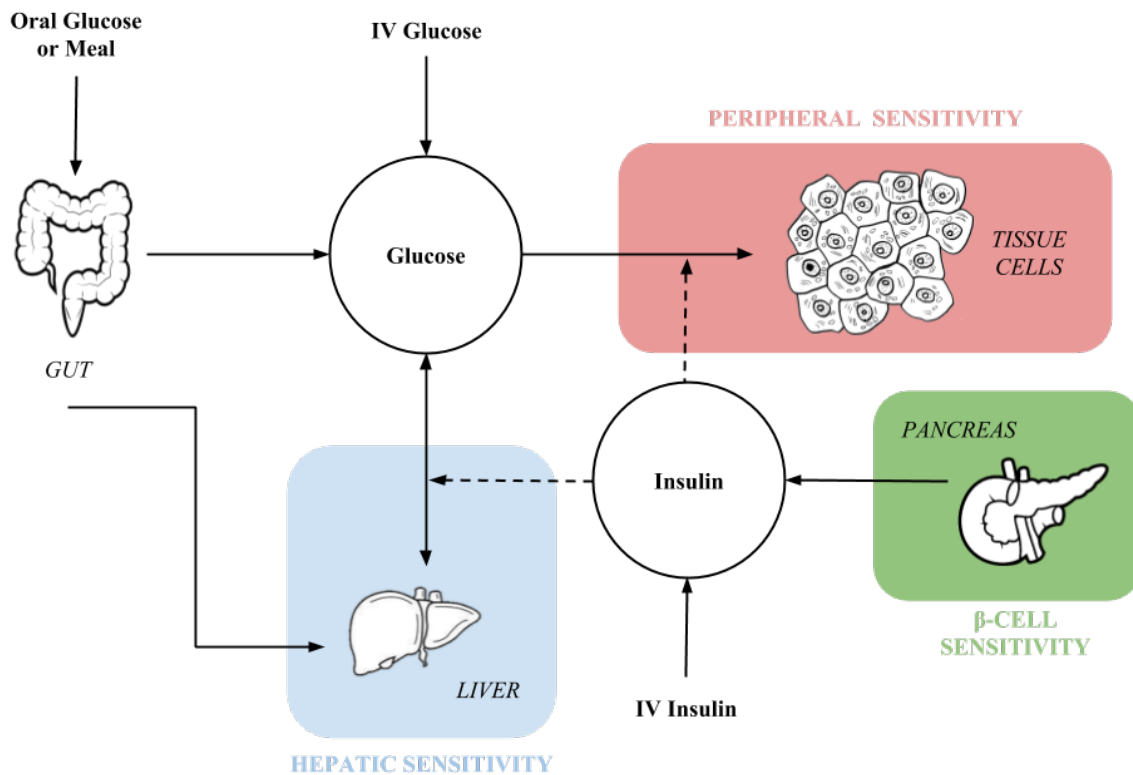


Figure 2.5 :
Different types of insulin sensitivity (inspired from [33]).

Type 1 diabetes, also called juvenile or insulin-dependent diabetes, is described by a destruction (more often immune) of pancreatic beta cells responsible of insulin production. In Type 1 Diabetes (T1D), all insulin must be given exogenously. In contrast, type 2 diabetes, also known as mature onset or non-insulin dependent diabetes, is characterised by a dysfunction of insulin target cells. In Type 2 Diabetes (T2D), despite insulin production, glucose is not able to enter cells, preventing uptake and causing hyperglycaemia. In T2D, insulin production may, at least initially, be normal or elevated, yet the individual has hyperglycaemia. Thus, T1D is a disease of loss of insulin production, while T2D is a disease of poor insulin action [4].

In either case, hyperglycaemia harms health and it is important to manage repeated hyperglycemia at the risk of developing heart attacks, blindness, cerebrovascular accidents and much more [19, 20]. Treatments differ according to the type of diabetes. People affected by T1D are required to take insulin injections. Unfortunately, insulin injections need to be correctly regulated at the risk of facing major hypoglycaemia. For T2D, individuals must improve their quality of life, but eventually may require drug therapy and/or insulin injections.

One can also mention gestational diabetes, which may be considered as a form of T2D. Indeed, during the pregnancy, placental hormones conduct cells to resist the insulin action. This form of T2D is thus transient, but increases risk to the infant [34].

2.5.1 Type 1 diabetes (T1D)

As mentioned, T1D is linked to a loss of insulin secretion capability, typically due to an auto-immune disorder. Because of this insulin deficiency, T1D individuals must take several insulin injections per day to control glucose. This disease appears during childhood or puberty, but rarely later. Type 1 diabetes is not the most common form comprising only 10 % of diabetic individuals [35].

2.5.2 Type 2 diabetes (T2D)

T2D is caused by an (increasing) inability of target cells to respond to insulin, and thus glucose remains in the blood instead of entering inside the cells, leading to hyperglycaemia. These cells are actually resistant or insensitive to insulin.

However, this disease is more incremental in its appearance and evolution. Because the cells are not able to take up glucose, they do not have enough energy to achieve their functions and can thus die. Therefore, they send signals to the pancreas to release more insulin. Since the cells can not fully respond to this hormone, the pancreas produces more and more and eventually becomes exhausted [5].

A progressive decrease of insulin creates a continued increase in demand for insulin. All these different stages actually describe the pathogenesis of this disease (Figure 2.6). First, one can talk about pre-diabetes, in comparison with Normal Glucose Tolerance (NGT). Eventually, T2D is diagnosed by hyperglycaemia. After the pancreas becomes exhausted, there is little difference between T1D and T2D [5].

Different terms, such as Impaired Glucose Tolerance (IGT) and Impaired Fasting Glucose (IFG), can be used to reference the pre-diabetic stage [36]. However, small distinctions between these notions have to be highlighted. They both indicate metabolic abnormalities before diabetes, but they come from different contexts.

The Impaired Glucose Tolerance (IGT) is diagnosed during an Oral Glucose Tolerance Test (OGTT). Blood samples are collected during this diagnostic test and a patient is categorised as IGT regarding the resulting blood glucose concentration. On the other hand, the Impaired Fasting Glucose (IFG) is linked to the Fasting Glucose Test (FGT). According to this criteria, if the blood glucose level after at least 8 hours fasting is above 7 mmol/L, the patient is IFG [36]. Impaired Glucose Tolerance (IGT) is nonetheless more used to denote pre-diabetes because of its better accuracy as pre-diabetes indicator and its parallel with Normal Glucose Tolerance (NGT).

2.6 Diagnosis

This section reviews the techniques used to predict and diagnose diabetes and its early stages. First, simple methods only based on blood sample analysis are explained. They can just diagnose pre-diabetes and diabetes when they are well underway (Figure 2.6). The damage is often irreversible at this point. Second, methods assessing insulin

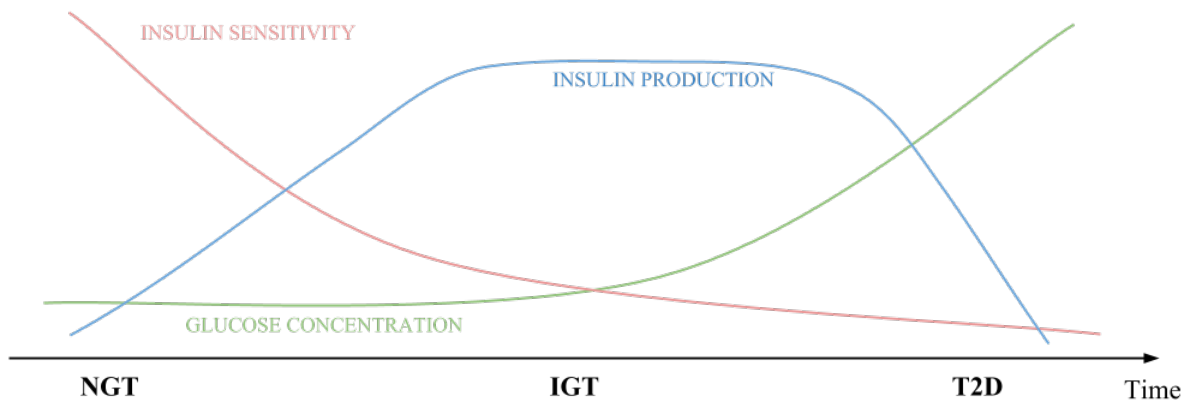


Figure 2.6 :

Pathogenesis of type 2 diabetes (inspired from [8]).

secretion and sensitivity are addressed. Indeed, these two factors are very good predictors of diabetes development [37]. For example, a decrease in insulin sensitivity can occur long before the final stage of the disease (Figure 2.6), as an increased insulin secretion. Its discovery can thus lead to a diabetes prediction or diagnosis when it is still possible to avoid its expansion and irrevocable complications.

2.6.1 Diabetes testing

The Fasting Glucose Test (FGT), the Oral Glucose Tolerance Test (OGTT), and the HbA_{1c} test are explained. Their relative benefits and drawbacks are also described. All utilise only Blood Glucose (BG) measurements.

▷ FPG / FGT

The easiest assay used to screen pre-diabetes and diabetes is the Fasting Glucose Test (FGT), also known as the Fasting Plasma Glucose (FPG) test. After at least eight hours of fasting, a blood sample is collected and the level of sugar in the blood is assessed. Regarding the BG concentration obtained, the patient can be diagnosed either as normal, pre-diabetic or diabetic.

A blood sugar level below 5.4 mmol/L indicates a normal state. In contrast, pre-diabetes and Impaired Fasting Glucose (IFG) are defined by a concentration between 5.5 mmol/L and 6.9 mmol/L. Blood sugar levels larger than 7 mmol/L diagnose diabetes [38]. These different thresholds are summarised in Table 2.1.

However, this test has proved to be inaccurate and has to be performed at least 2 times to avoid false positives [38]. In addition, this test only provides relevant results once endogenous insulin production is already enhanced or plateaued (Figure 2.6). Thus, it does not easily detect the Impaired Fasting Glucose (IFG) state, or only in its latest stages. Indeed, the sensitivity of this test is very low [40]. Poor compliance with fasting before the blood sample can also lead to false results [39]. However, the duration and the stress for the patient and the medical staff are minimal.

Table 2.1 :
Threshold values for the fasting blood sugar level [38].

Stages	Fasting Blood Glucose Level [mmol/L]
No Diabetes	$BGL \leq 5.4$
Impaired Fasting Glucose	$5.5 \leq BGL \leq 6.9$
Diabetes	$7 \leq BGL$

▷ **OGTT**

The Oral Glucose Tolerance Test (OGTT) is another test used to diagnose pre-diabetes and diabetes [41]. It belongs to the Glucose Tolerance Test (GTT) category, during which a glucose dose is given to the patient and blood samples are collected. Regarding the results of the blood tests, assumptions about the sugar metabolism of the patient and thus his/her diabetic state can be made. The patient must fast at least 8 hours prior to the test. The amount of glucose, its administration route, the number of samples and the separation between them may vary from one Glucose Tolerance Test (GTT) to another [42].

Specifically, for an Oral Glucose Tolerance Test (OGTT), the glucose is orally administered through a drink with glucose content. According to the operator, the dose, as well as the number of blood samples and the sampling protocol are different. The most common OGTT is the 75 g 2-hour trial. It requires an oral administration of 75 grams of glucose and the extraction of one blood sample 120 minutes after the beginning of the test.

A blood glucose level below 7.8 mmol/L after an oral glucose dose of 75 grams and 120 minutes indicates no diabetes. Impaired Glucose Tolerance (IGT) is defined by a concentration between 7.9 mmol/L and 11 mmol/L. T2D patients are diagnosed with a blood glucose level larger than 11.1 mmol/L [6]. Table 2.2 presents all these thresholds.

Table 2.2 :
Threshold values for the 75 g 2-hour Oral Glucose Tolerance Test [6].

Stages	Blood Glucose Level [mmol/L]
No Diabetes	$BGL \leq 7.8$
Impaired Glucose Tolerance	$7.9 \leq BGL \leq 11$
Diabetes	$11.1 \leq BGL$

Glucose absorption leads to the increase of the Blood Glucose (BG) and its uptake to the reduction in BG. Regarding diabetic status of the patient, different situations can be considered. Normal patients regulate their glycaemia and it drops to a normal level after 120 minutes. The final BGL in this case may be slightly higher than at the beginning of the test. Regarding patients with IGT, they start the test with the same fasting glycaemia as normal individuals, but their BGL is higher after 120 minutes. At the beginning, T2D individuals have a highr fasting level. Besides a small glycaemia decrease, it remains significantly elevated after 120 minutes. Figure 2.7 summarises these different cases.

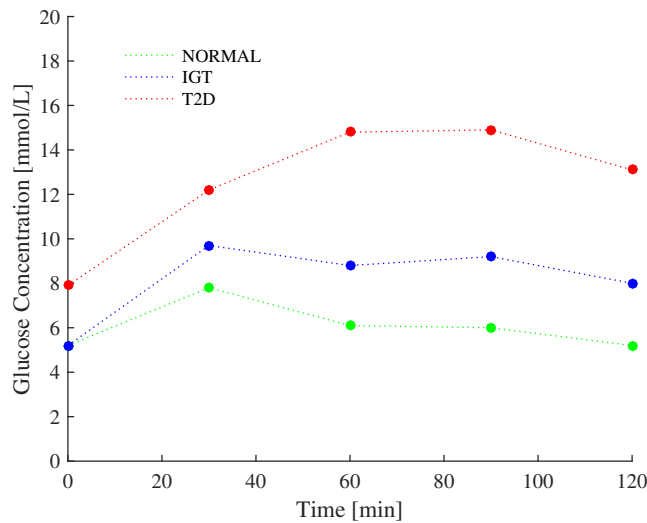


Figure 2.7 :

Evolution of Blood Glucose Level (BGL) during a 75 g 2-hour OGTT (inspired from [43]).

In terms of OGTT strengths, it is simple and minimally invasive compared to intravenous tests. The oral absorption of glucose matches the physiological situation. In addition, this test correctly assesses Impaired Glucose Tolerance (IGT). The World Health Organisation (WHO) considers the OGTT as the test of choice to detect IGT [6]. However, earlier diagnosis and diabetes prevention before irreversible pancreatic damage cannot be achieved with this test. Its standardisation is also needed. Indeed, different protocols are still used between institutions [42]. Thus, comparison of results can not be achieved.

If more blood samples are collected and if they are tested both for glucose and insulin, insulin sensitivity can be deduced [44]. Nonetheless, these metrics are not entirely accurate because gut absorption is not accurately known, and other variables may not be known. Thus, the OGTT is thus more used for assessing diabetes than for estimating insulin sensitivity.

Figure 2.8 highlights the T2D pathogenesis features measured with an Oral Glucose Tolerance Test (OGTT). In a 75 g 2-hour OGTT, the glucose concentration after 120 minutes is measured. However, insulin production and insulin sensitivity (dashed lines) are not measured or known.

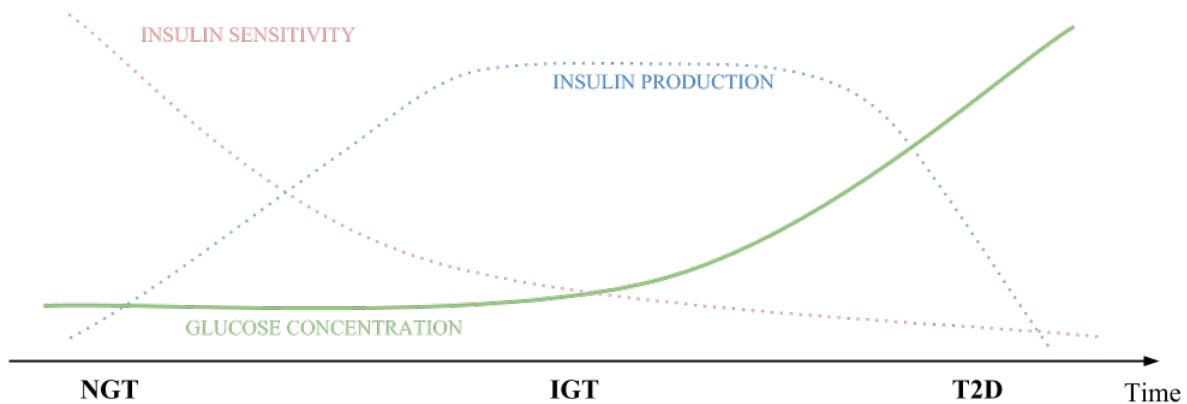


Figure 2.8 :

T2D pathogenesis features measured with the 75 g 2-hour OGTT (inspired from [8]).

▷ **HbA_{1c}**

The glycated or glycosylated haemoglobin (HbA_{1c}) test is an alternative assay to identify diabetes and to monitor the glycaemic control of already diagnosed patients [45, 46]. Specifically, the glycation can be defined as the non-enzymatic mediated formation of covalent bonds between sugar molecules and protein or lipid molecules. The most common form of haemoglobin (HbA) is composed of two α and two β chains. The glucose fixation can occur at different positions in the sequence of amino acids. The HbA_{1c} refers to haemoglobin for which the glycation reaction has taken place at the level of the N-terminal valine of one of the beta chains [47]. By quantifying the proportion of this glycated haemoglobin compared to the normal haemoglobin, the average blood sugar exposure can be assessed.

The more frequent and greater the glucose present in the blood, the more bonds are formed and the higher the HbA_{1c} concentration. Glycated haemoglobin is thus a good marker of average blood sugar levels over time and diabetic state. Although the previous units were percentages, they have been changed and the new ones are mmol/mol (mmol of glycated haemoglobin per mol of total haemoglobin). As indicated by the NZSSD (New Zealand Society for the Study of Diabetes), a normal value for HbA_{1c} is below 40 mmol/mol [50]. Patients with pre-diabetes are characterised by an amount between 41 mmol/mol and 49 mmol/mol. Higher values indicate diabetes. All these cut-off points are gathered in Table 2.3.

The advantage of this method is the provision of what is essentially a three month average blood glucose value, rather than a brief snapshot in time, as with the OGTT. In particular, haemoglobin has a lifetime of approximately three months and the glycated state is irreversible. HbA_{1c} is thus not impacted by short or daily fluctuations. Moreover, this test does not require a fasted state and blood samples can be taken at any time of the day. These features provide convenience. This test can also monitor diabetic state over time and thus predict some potential complications.

Table 2.3 :

Important values of HbA_{1c} according the New Zealand Society for the Study of Diabetes (NZSSD) [50].

Stages	HbA _{1c} [mmol/mol]
No Diabetes	$\text{HbA}_{1c} \leq 40$
Impaired Fasting Glucose	$41 \leq \text{HbA}_{1c} \leq 49$
Diabetes	$50 \leq \text{HbA}_{1c}$

However, as with the fasting plasma glucose test, the impaired fasting glucose (IFG) state is not easily detected and an OGTT is needed [48]. Importantly, IFG is the most interesting to detect in order to provide early detection of emerging diabetes and avoid irreversible complications. In addition, this test is relatively more expensive [49]. Moreover, problems linked to haemoglobin, such as anaemia, can interfere with the results, providing false negatives. Although the intra-patient repeatability is high, the inter-patient values show dissimilarities [49]. Compared to Fasting Plasma Glucose (FPG), the test sensitivity is just a bit lower, but specificity is much higher. Lastly, this method absolutely needs standardisation [49]. The cut-off point for HbA_{1c} in pre-diabetes and diabetes diagnosis, as well as the methodology used to measure this glycated haemoglobin proportion, are widely debated in the scientific world and no consensus has been found [49].

In view of the explanations about the different diabetes tests, one important problem can be highlighted. These tests are only able to correctly diagnose diabetes and pre-diabetes in their latest stages. They are not accurate for determining IGT, except the OGTT, and that case has low sensitivity. However, prevention before irreversible pancreatic damages cannot be achieved with this oral assay because IGT is only diagnosed when it is already well progressed. These diabetes tests are often used to confirm the suspicion of diabetes, but are not at all predictors of the disease.

Other types of test must thus be elaborated. They measure insulin secretion or sensitivity, which are good predictors of diabetes development because these two factors are already damaged long before the disease reaches its final stages (see Figure 2.6) [5].

2.6.2 Insulin secretion or sensitivity testing

Most of the time, the different symptoms of type 2 diabetes only become visible when the disease is already in an advanced state. To avoid irreversible damage and complications, early detection is essential. Methods to screen good predictors of this disease development, such as insulin secretion and sensitivity, have thus been created.

First, the glucose clamp techniques are explained. Then, the IntraVenous Glucose Tolerance Test (IVGTT), the first model-based assay, is described. A specific modification of this test is illustrated. Finally, less invasive techniques, such as the Dynamic Insulin Secretion and Sensitivity Test (DISST) and the quick Dynamic Insulin Sensitivity Test (DISTq), are explained.

▷ **Clamp**

The glucose clamp technique is the best known method to assess insulin secretion and sensitivity [8]. First, the hyperglycaemic clamp technique evaluates insulin secretion capacity and β cell sensitivity to glucose. Second, the Hyperinsulinaemic-Euglycaemic Clamp (HEC) technique is used to measure the peripheral insulin sensitivity [51, 52, 53]. In both cases, the glucose concentration is held (or clamped) to a specific level [52].

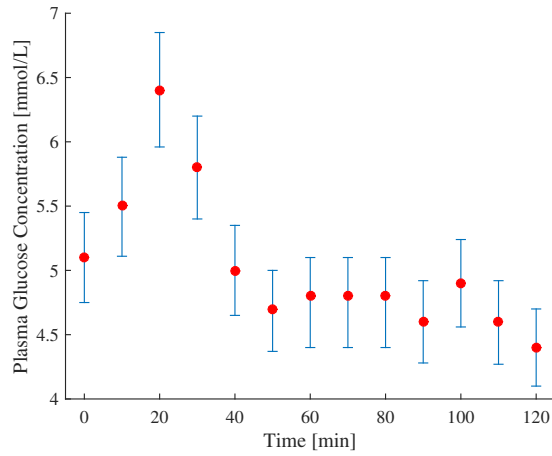
Hyperglycaemic clamp technique [52, 53]

During the hyperglycaemic clamp, the blood glucose concentration is raised to 125 mg/dL (6.938 mmol/L) or more, which is above its basal level. BG is maintained at this hyperglycaemic plateau. This threshold is achieved with a continuous, but adjustable glucose infusion. Each time the Blood Glucose Level (BGL) differs from this high concentration, the infusion is modified to hold the hyperglycaemic state. The added amount of infused glucose, needed to maintain this high BG level, is related to the endogenous insulin secretion, and changes of infused glucose are proportional to variations in endogenous insulin production. Conclusions about pancreatic secretion rate of insulin can consequently be drawn.

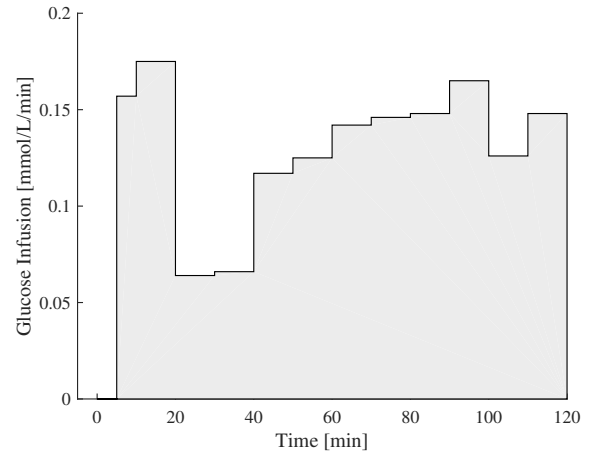
Because of the constant hyperglycaemic state, the β cell sensitivity to glucose levels is highlighted. Information about this specific sensitivity can thus be deduced from this test. Glucose metabolism after a hyperglycaemic stimulus can also be analysed.

Hyperinsulinaemic-Euglycaemic Clamp (HEC) technique

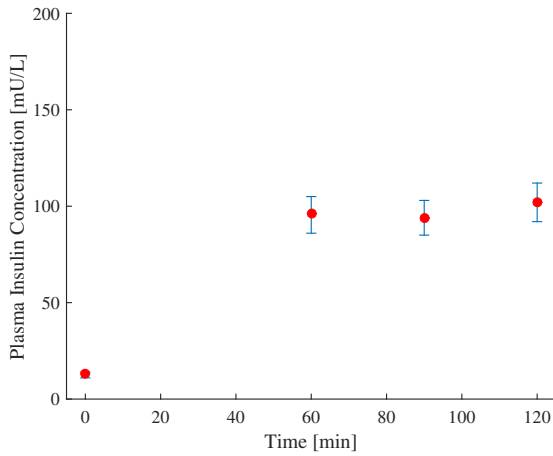
The Hyperinsulinaemic-Euglycaemic Clamp (HEC) technique is the reference test for assessing tissue insulin sensitivity and thus the very early pre-diabetic stages [8]. Both glucose and insulin infusions are needed during this test. The insulin infusion is continuous, relatively large (2 - 6 U/hr) and leads to a hyper-physiological plasma insulin concentration (\pm 150 mU/L). A variable glucose infusion is administered to maintain blood glucose concentration constant at the basal level (4 - 5 mmol/L). Blood samples are collected and assessed for BG every 5 - 10 minutes to hold this fixed level [44, 8, 52]. The glucose infusion is particularly controlled and modified during the first hour. Thereafter, a steady state is achieved and the glucose infusion is almost constant [8]. However, it can sometimes take 2 or 3 hours to reach steady state [44]. Figure 2.9 illustrates an example of the glucose and insulin concentrations (Figures 2.9a and 2.9c), as well as their infusion profiles (Figures 2.9b and 2.9d) [44].



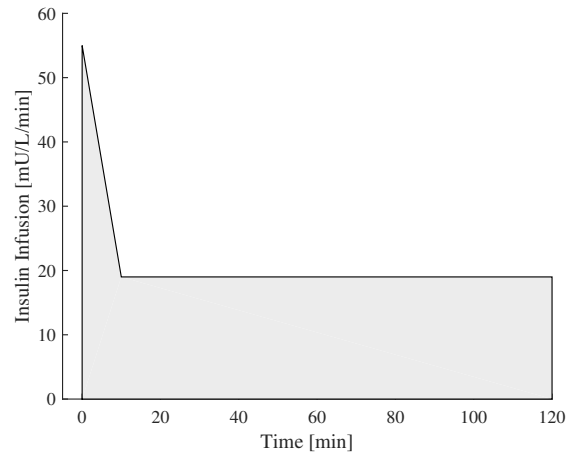
(a) *Glucose concentration.*



(b) *Glucose infusion.*



(c) *Insulin concentration.*



(d) *Insulin infusion.*

Figure 2.9 :

Example of HEC protocol (inspired from [44]).

Because of the hyperinsulaemic state, pancreatic insulin secretion is largely to completely suppressed, hepatic glucose uptake is saturated, and Endogenous Glucose Production (EGP) is practically suppressed [44]. The glucose infusion rate is thus equal to the tissue glucose uptake and conclusions about tissue insulin sensitivity can be made from this rate and the insulin given [51, 52]. Elevated levels of the glucose infusion rate indicate high insulin sensitivity. On the contrary, low levels stand for high insulin resistance [52].

Specifically, the HEC technique defines the Insulin Sensitivity Index (ISI) as the mean glucose infusion rate at steady state (M) divided by the mean plasma insulin concentration at steady state (I) [44]:

$$ISI = \frac{M}{I} \quad (2.1)$$

The clamping, achieved during the HEC technique, enables a very good control and repeatability of the assay. However, it is difficult to compare results with different insulin infusion rates. This test can take a very long time because of the steady state needed. Sometimes, this equilibrium state is not reached and results are thus not guaranteed. A lot of blood samples are collected throughout the duration of the test. Medical staff and specific equipment are required. The non-physiological nature of the experiment is also an important drawback. Finally, not all glucose uptakes are mediated by insulin (e.g. brain and CNS).

The HEC method remains the gold standard technique to assess the insulin sensitivity, despite its cost and intensity. However, it does not provide information about pancreatic insulin secretion. Figure 2.12 highlights the T2D pathogenesis features measured with a Hyperinsulinaemic-Euglycaemic Clamp (HEC) where the insulin production and glucose concentration lines are dashed because they are not assessed in this test.

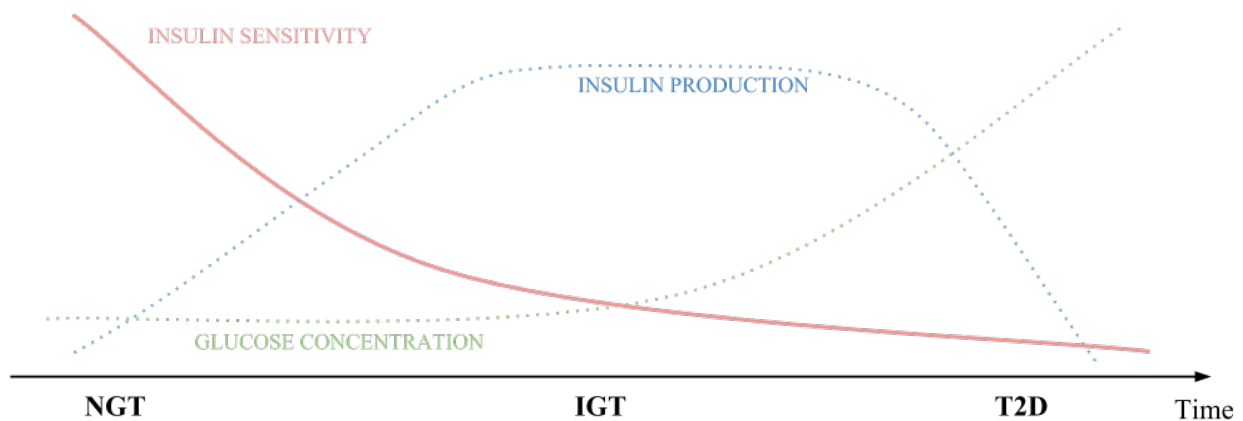


Figure 2.10 :
T2D pathogenesis features measured with the HEC (inspired from [8]).

▷ IVGTT

IVGTT stands for IntraVenous Glucose Tolerance Test. As its name suggests, glucose is injected intravenously during this assay. During the IVGTT duration, several blood samples are collected and it is the reason why this test is also called the Frequently Sampled IVGTT (FS-IVGTT) [8]. It can refer to different particular assays. First, the direct assessment test determines the diabetic status of a patient. Second, the semi-direct or Minimal Model (MM) based assessment test computes its insulin sensitivity .

Direct assessment

After a short IV glucose infusion, several blood samples are collected, providing the temporal evolution of the glucose concentration throughout the duration of the test. By assessing the decay rate, K_G , of the glucose concentration curve after the glucose infusion, information about glucose tolerance or metabolism and thus about

diabetic condition can be provided. By using the half time, $t_{\frac{1}{2}}$, which is the time needed to halve the glucose concentration, the decay rate, K_G , can be easily computed [44] :

$$K_G = \frac{\ln 2}{t_{\frac{1}{2}}} \quad (2.2)$$

Even though insulin sensitivity can be inferred from this index, it is better to use the subsequently described semi-direct method to calculate it with an IVGTT.

Semi-direct assessment (Minimal Model (MM) based assessment) [54]

For the semi-direct assessment, the same IVGTT protocol is used, but a mathematical model is added to deduce insulin sensitivity. The Minimal Model (MM) of Bergman mathematically represents the physiological kinetics of glucose and insulin during an IVGTT. Information about glucose metabolism can be deduce from parametric identification, by fitting the model parameters and the IVGTT data. The IVGTT protocol consists of a glucose intravenous injection, proportional to the patient weight. Then, blood is frequently collected during at least 3 hours. About 22 samples are assessed, both for glucose and insulin. At the beginning, blood samples are extracted very close to each others (2 - 3 minutes). The time of sampling is reduced in frequency after the first hour (15 - 20 minutes).

The minimal model of Bergman is divided in two main compartments, glucose and interstitial insulin. In addition, it brings to light the relations between these two compartments and important organs, as well as the chemical and kinetic properties of the system. Specifically, the glucose can be supplied by either exogenous injections or either by the transformation of glycogen in the liver. On the other hand, it can be reduced by entering the peripheral tissues. The glucose can also be transformed into glycogen and be stored in the liver. The hepatic equilibrium between glucose and glycogen introduces the notion of Net Hepatic Glucose Balance (NHGB).

Regarding the remote (interstitial) insulin, it can be defined as the insulin in the interstitial fluid. It is the most important type of insulin to consider in this case because of its direct interaction with the tissue cells. It enters from the plasma insulin, which is produced by the pancreas, and also decomposed after a certain time due to action at the cells. The two compartments interplay, where the remote insulin affects the transformation of the glycogen into glucose and helps the cells to ingest the glucose. The minimal model is shown in Figure 2.11.

The model of Bergman is described by the following equations and initial conditions :

$$\dot{Q}(t) = NHGB(t) - Rd(t) \quad , \quad Q(0) = Q_b + D \quad (2.3)$$

$$\dot{I}'(t) = -k_3 \cdot I'(t) + k_2 \cdot [I(t) - I_b] \quad , \quad I'(0) = 0 \quad (2.4)$$

$$G(t) = \frac{Q(t)}{V} \quad (2.5)$$

Where Q represents the glucose mass, Q_b its basal value, I' the remote insulin concentration, $NHGB(t)$ the Net Hepatic Glucose Balance, $R_d(t)$ the plasma glucose rate of disappearance, I the plasma insulin concentration, I_b its basal value, D the glucose dose (the exogenous glucose injections), k_i the rate constants, G the glucose concentration and V the volume in which the glucose is distributed. It is essential to notice that some notions are formulated as mass concept and other as concentration ones. Mass conservation is not necessary guaranteed.

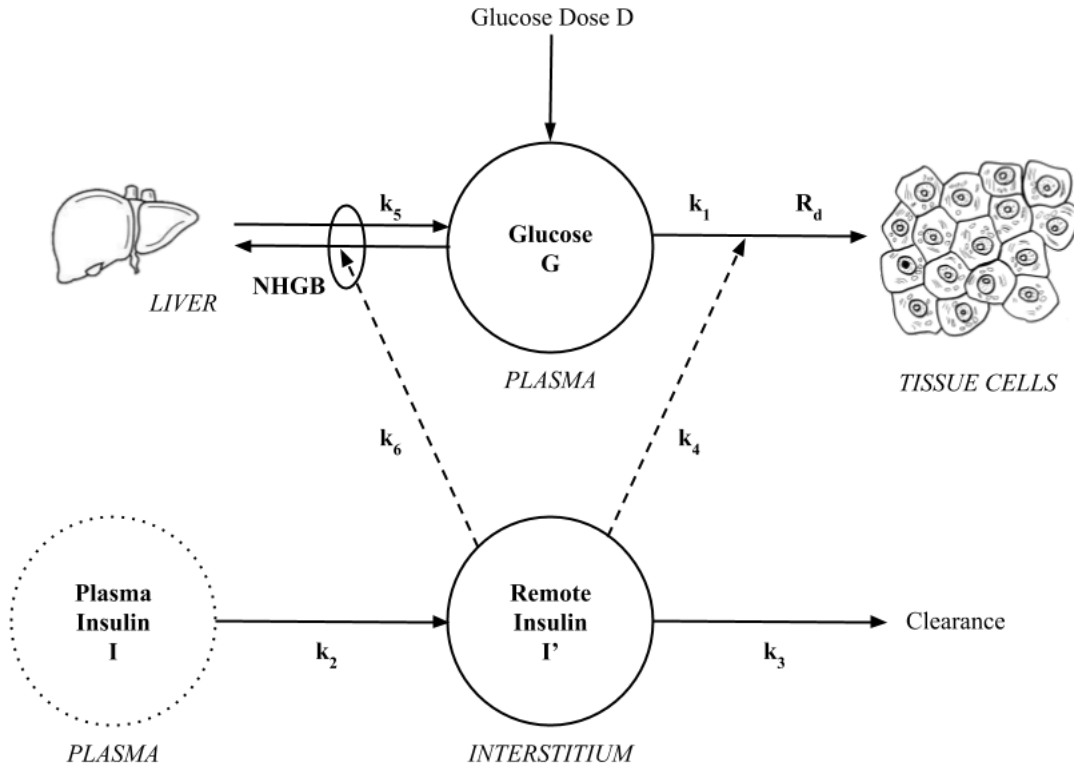


Figure 2.11 :

Schematic representation of Bergman Minimal Model (MM) (inspired from [54]).

Because of its dependency with glucose and remote insulin, the $NHGB(t)$ decreases with increase in glucose and insulin concentrations. Indeed, when there is lot of blood glucose, the liver has to transform it into glycogen instead of driving the reverse operation (glycogenolysis). Moreover, when the blood glucose concentration is high, insulin is produced and inhibits the glycogenolysis. The balance can be thus written like :

$$NHGB(t) = NHGB_0 - [k_5 + k_6 \cdot I'(t)] \cdot Q(t) \quad (2.6)$$

Where $NHGB_0$ stands for the net endogenous glucose balance at zero glucose.

The disappearance rate of glucose can also be redrafted by considering its control by glucose and insulin. The higher the glucose and thus the higher the insulin concentration, the higher the rate of disappearance. It can be rewritten as :

$$Rd(t) = Rd_0 + [k_1 + k_4 \cdot I'(t)] \cdot Q(t) \quad (2.7)$$

Where Rd_0 represents the glucose disappearance rate at zero glucose.

Equation 2.3 can thus be overwritten as :

$$\dot{Q}(t) = -[(k_5 + k_1) - (k_6 + k_4) \cdot I'(t)] \cdot Q(t) + (NHGB_0 - Rd_0) \quad (2.8)$$

One can notice that $NHGB_0 - Rd_0$ can be expressed as $(k_1 + k_5)Q_b$ because they are all basal notions. It gives :

$$\dot{Q}(t) = -[(k_5 + k_1) - (k_6 + k_4) \cdot I'(t)] \cdot Q(t) + (k_1 + k_5) \cdot Q_b \quad (2.9)$$

Because a lot of parameters have to be identified, reparametrisation has been carried out with :

$$X(t) = (k_4 + k_6) \cdot I'(t) \quad (2.10)$$

$$p_1 = k_1 + k_5 \quad (2.11)$$

$$p_2 = k_3 \quad (2.12)$$

$$p_3 = k_2 \cdot (k_4 + k_6) \quad (2.13)$$

Where $X(t)$ is called the remote insulin effectiveness and p_i are rate constants.

The reparametrised model can be written as :

$$\dot{Q}(t) = -[p_1 + X(t)] \cdot Q(t) + p_1 \cdot Q_b \quad , \quad Q(0) = Q_b + D \quad (2.14)$$

$$\dot{X}(t) = -p_2 \cdot X(t) + p_3 \cdot [I(t) - I_b] \quad , \quad X(0) = 0 \quad (2.15)$$

$$G(t) = \frac{Q(t)}{V} \quad (2.16)$$

The glucose effectiveness is the ability the glucose has to enhance the glucose absorption by the cells and to inhibit the hepatic endogenous glucose production. It is derived with the following equation :

$$S_G = - \left. \frac{\partial \dot{Q}}{\partial Q} \right|_{SS} = p_1 \quad (2.17)$$

Insulin sensitivity is the body response to insulin and is thus the ability the insulin has to improve the glucose effectiveness. It can be derived as :

$$S_I = - \left. \frac{\partial S_G}{\partial I} \right|_{SS} = \frac{p_3}{p_2} = \frac{k_2 \cdot (k_4 + k_6)}{k_3} \quad (2.18)$$

One understands that insulin sensitivity (S_I) increases with the rise of insulin input and with the reaction speed enhancement of the glucose intake by the tissues and of the conversion of glucose into glycogen. On the contrary, it falls down when insulin is cleared.

The glucose effectiveness and the insulin sensitivity can be deduced from these equations and with the collected IVGTT data. These measurements enable the parameter identification and the insulin sensitivity is a particular combination of these parameters.

The IVGTT protocol, combined with the Minimal Model (MM) of Bergman, is therefore interesting regarding the insulin sensitivity computation and it enables to identify diabetes or other steps of this disease, like glucose intolerance or pre-diabetes. On the other hand, the model is overly simplified compared to physiological reality. For example, no difference is made between dependent and independent-glucose uptakes [8, 44]. However, even with this poor representation, over-parametrisation occurs [55, 56]. In addition, even if it is less invasive than clamp procedures, the protocol of the IVGTT is very invasive because of the high number of blood samples required. This test is thus only used in research studies and is not extended to larger screening. Another problem is the decrease of accuracy for low insulin sensitivity [8], while pre-diabetic and diabetic patients have such high insulin resistance. To improve this precision, insulin signal has to be enhanced and protocol modifications are thus suggested, such as an insulin injection 20 minutes after the glucose input. This modification is called the Insulin Modified IVGTT (IM-IVGTT).

Figure 2.12 highlights the T2D pathogenesis features measured with an IVGTT. Indeed, the glucose concentration (green solid line) is measured during the test. High insulin sensitivities can be assessed. In contrast, insulin production (blue dashed line) is not quantified during this test.

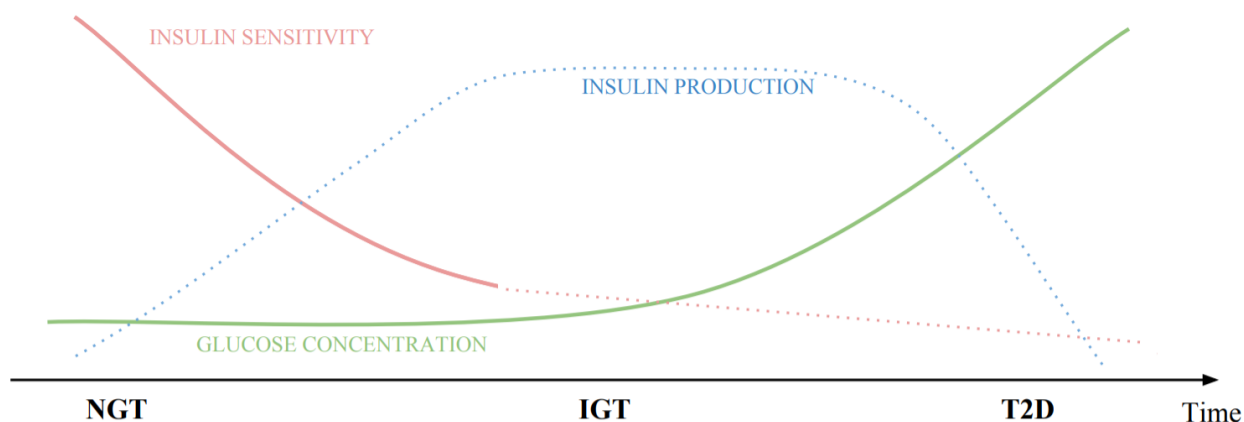


Figure 2.12 :

T2D pathogenesis features measured with the model-based IVGTT (inspired from [8]).

▷ IM-IVGTT

The IM-IVGTT stands for Insulin Modified IntraVenous Glucose Tolerance Test. The protocol is similar to a normal IVGTT, apart from an insulin injection 20 minutes after the glucose intake. It provides an improved insulin signal and thus a potentially parameter identification. However, it still suffers poor identifiability [55, 56], especially at low insulin sensitivity. Its results are thus not always accurate and repeatable. Figure 2.13 illustrates an example of glucose and insulin concentrations and sampling during an IM-IVGTT.

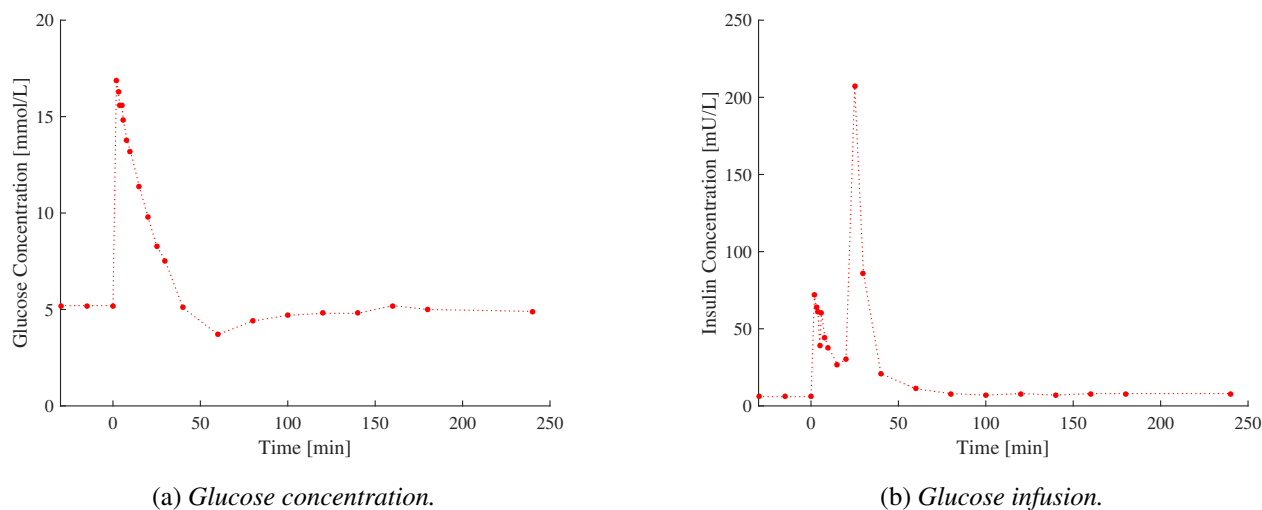


Figure 2.13 :

Example of IM-IVGTT data (inspired from [44]).

▷ DISST

The Dynamic Insulin Secretion and Sensitivity Test (DISST) is another model-based assay, assessing insulin secretion and sensitivity. It was created as an alternative to more tedious and intense tests, such as HEC and IVGTT.

Specifically, this assay could be described as a low dose and infrequently sampled Insulin Modified IntraVenous Glucose Tolerance Test (IM-IVGTT) [8, 9, 10].

The DISST protocol consist of blood samplings at $t = 0, 5, 10, 15, 20, 25, 30, 35, 40$ and 50 minutes. Overnight fasting is required prior the starting of the test. A glucose bolus is injected after 5 minutes, directly after the blood extraction. Then, an insulin injection is administered after the $t = 15$ minute sample. Several glucose and insulin doses can be considered. The high dose consists of 20 grams of dextrose and 2 units of insulin. The medium dose is defined by 10 grams of dextrose and 1 unit of insulin. The low dose is 5 grams of dextrose and 0.5 unit of insulin.

The model linked to the DISST is quite different from the IVGTT. It considers and models the C-peptide action in addition to the glucose and insulin ones, as well as structurally enforcing mass conservation. A two compartments design is used to model C-peptide dynamics, differentiating the plasma and the interstitial compartments. Interactions between these two compartments exist and only plasma C-peptides are cleared by kidneys. Regarding insulin, a distinction between plasma and interstitial insulin is also made. The plasma insulin is produced by the pancreas, but hepatic extraction is assumed before it reaches the plasma compartment. Exogenous injection directly accesses and increases the plasma compartment. Plasma insulin is degraded by the kidneys and the liver. The interactions between the plasma and interstitial insulin are also considered. Regarding the interstitial insulin, it can be cleared by the cells and influences the glucose uptake through insulin sensitivity (S_I). Glucose is either produced endogenously by the liver or comes from an exogenous input. It is degraded either by non-insulin mediated uptake, or by insulin-dependent uptake. Because of the fast interaction between plasma and interstitial glucose, only one glucose compartment is assumed. The model used in the DISST is represented in Figure 2.14.

The model is described by the following equations :

$$\dot{G}(t) = -p_G \cdot (G(t) - G_B) - S_I \cdot G(t) \cdot Q(t) + \frac{P(t)}{V_G} + EGP(t) \quad (2.19)$$

$$\dot{I}(t) = -n_K \cdot I(t) - n_L \cdot \frac{I(t)}{1 + \alpha_I \cdot I(t)} - \frac{n_I}{V_Q} \cdot (I(t) - Q(t)) + \frac{u_{ex}}{V_P} + (1 - x_L) \cdot \frac{u_{en}}{V_P} \quad (2.20)$$

$$\dot{Q}(t) = \frac{n_I}{V_Q} \cdot (I(t) - Q(t)) - n_C \cdot Q(t) \quad (2.21)$$

$$\dot{C}(t) = k_2 \cdot Y(t) - (k_1 + k_3) \cdot C(t) + u_{en}(t) \quad (2.22)$$

$$\dot{Y}(t) = k_1 \cdot C(t) - k_2 \cdot Y(t) \quad (2.23)$$

Where $G(t)$ stands for the plasma glucose concentration, $I(t)$ the plasma insulin concentration, $Q(t)$ the interstitial insulin concentration, $C(t)$ the plasma C-peptide concentration, and $Y(t)$ the interstitial C-peptide concentration.

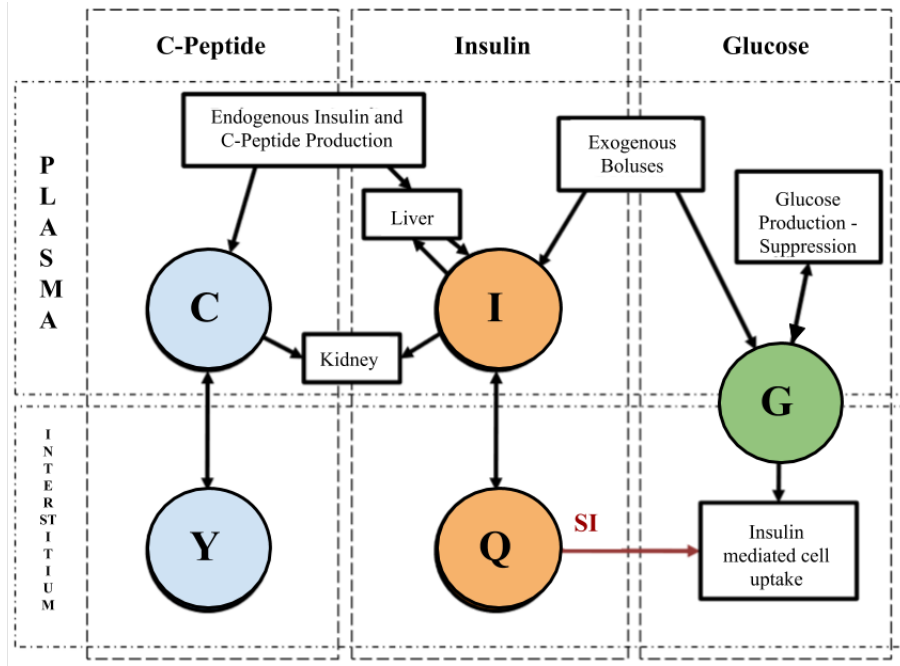


Figure 2.14 :

Glucose and insulin model of the DISST protocol (inspired from [8]).

Then, p_G is the non-dependent insulin uptake rate, G_B the basal glucose concentration, S_I the insulin sensitivity, $P(t)$ the exogenous glucose input, V_G the glucose distribution volume, $EGP(t)$ the Endogenous Glucose Production, n_K the renal insulin clearance rate, n_L the hepatic insulin clearance rate, α_I the hepatic insulin clearance saturation n_I the diffusion constant for insulin transport between plasma and interstitium, V_Q the interstitial volume, u_{ex} th exogenous insulin input into plasma, V_P the plasma volume, x_L the fractional first pass hepatic extraction of pancreatic insulin, n_C the tissue cell insulin clearance, k_1 and k_2 the transport rates between C-peptide compartments and k_3 renal C-peptide clearance rate.

Almost all the parameters are fixed, functions of individual characteristics or *a priori* defined [8]. Insulin sensitivity, S_I , and endogenous insulin production, u_{en} , can be deduced from parameter identification, by fitting the model parameters and the DISST data.

Because of the short duration of the assay, the cost of the test is also reduced. In addition to assessing the insulin sensitivity, the DISST enables to get some information about the endogenous insulin production, as opposed to other tests in which only one of these notions is derived. Importantly, endogenous insulin production is another important factor to diagnose type 2 diabetes. However, this time saving is related to the complexification of the model. The protocol is low-intense and thus less invasive, allowing large scale screening. It has been proven that the DISST is very accurate to determine low insulin sensitivity [8, 9, 10].

▷ DISTq

The DISTq (quick Dynamic Insulin Sensitivity Test) is a subset of the DISST [8, 57, 58]. This assay exactly follows the same protocol than the DISST, except for the insulin and C-peptide part. Even if their analysis is interesting regarding the endogenous insulin secretion, the investigation of these samples is costly and time-consuming. By eliminating the insulin and C-peptide assays, it provides a real time, highly accurate insulin sensitivity. Indeed, the parametric identification can directly be performed with the available data acquired during the test (glucose data) and with population-based assumptions on insulin profile. This test is short, cheap, scalable to population screening and with a very good resolution compared to the HEC [8]. Finally, if blood samples are saved, they may be assessed for insulin and/or C-peptide later to improve resolution in selected subjects [57]. The mathematical derivations are nonetheless complex.

2.7 Summary

This chapter first aims at reminding or explaining physiological basis around diabetes. Especially, the notion of insulin sensitivity is addressed. Pathogenesis of type 2 diabetes includes insulin resistance, or low insulin sensitivity, describing the impaired capacity of the body to regulate glucose. This insulin resistance develops long before the final state of the disease. By assessing insulin sensitivity, the diagnosis of pre-diabetes is thus possible years before type 2 diabetes eventuates.

Second, methods to assess diabetes or its early stages are reviewed. On one hand, diabetes testings only detect the disease on the basis of late-appearing symptoms, particularly rising glucose levels, when it is already in a critical, near diabetes situation, or later. On the other hand, insulin sensitivity tests are either low resolution, and/or costly, invasive, time-consuming, and not adapted for a large population screening. The Dynamic Insulin Sensitivity and Secretion Test (DISST) is short, low-cost and accurate. However, it is still invasive.

Because there is a need for even easier and less invasive insulin sensitivity tests, this research project proposes an new version of the DISST, with an oral glucose ingestion and a subcutaneous insulin injection.

Chapter 3

The SC-OG-ICING-2 model

In this third chapter, the model used in this thesis is fully defined, developed, and discussed. This model is a simple description of glucose and insulin kinetics which will be validated during the new protocol developed by Lui Pearson at the University of Canterbury. Both the combined model and protocol aim at assessing insulin sensitivity in a physiologically realistic manner.

The model comprises three sub-models. First, the interactions between insulin and glucose, as well as their appearance and degradation, are depicted by a glycaemic control model, the second version of the Intensive Control Insulin-Nutrition-Glucose (ICING-2) model [59]. The ICING-2 equations are largely based on the DISST model [8, 9, 10]. The second sub-model represents glucose absorption after oral ingestion. This gastrointestinal model was created by Dalla Man et al. [66]. Third, the model of Wong et al. is also incorporated [33, 67, 68], capturing insulin absorption and appearance after a subcutaneous injection. Because of its features, this overall system model can be named the SubCutaneous Oral Glucose Intensive Control Insulin-Nutrition-Glucose 2 (SC-OG-ICING-2) model. All the parameter values of this integrated model come from the papers and theses of Dalla Man et al. [66], Wong et al. [33, 67, 68], Lotz et al. [44, 69], Docherty et al. [8, 9, 10] and Pretty et al. [59, 60].

The entire model is represented in Figure 3.1.

3.1 Sub-model 1 : Glycaemic control model

The first sub-model describes internal glucose and insulin dynamics, their interactions, as well as their formation, apparition and degradation. It is the second version of the Intensive Control Insulin-Nutrition-Glucose (ICING-2) model. The first version was created by Lin et al. within the framework of Intensive Insulin Therapy (ITT) and Tight Glycaemic Control (TGC) in intensive care unit [61, 62, 60, 32, 63, 64, 65]. It is strongly based on the DISST equations (Equations 2.19 to 2.23). However, it considers the saturation of insulin receptors and the Central Nervous System (CNS) as a separate entity. It also assumes endogenous insulin production depends on insulin concentration. Endogenous Glucose Production (EGP) is fixed as a constant [59, 60, 65]. The second ver-

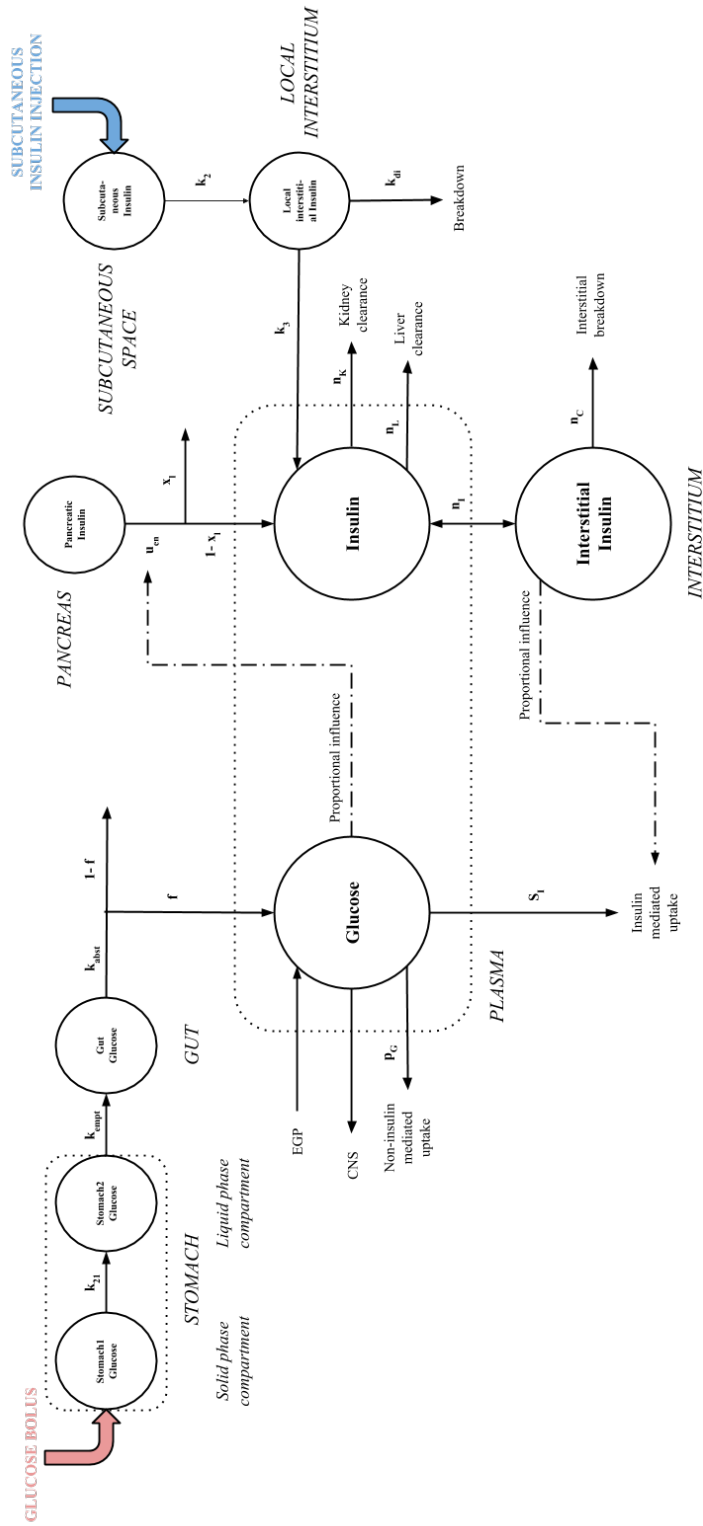


Figure 3.1 :
SC-OG-ICING-2 model overview.

sion of the ICING model was proposed by Pretty et al. [59, 60]. The primary difference with the previous version is the glucose-dependency of the pancreatic insulin secretion. One can notice C-peptide kinetics are not considered.

As with the DISST model, the ICING-2 model incorporates a distinction between plasma and interstitial insulin. Plasma insulin is produced by the pancreas, according to glucose concentration. Hepatic first pass extraction is considered before insulin reaches the plasma compartment. This model also deals with exogenous insulin, directly adding to plasma valve. Plasma insulin is degraded by the kidneys and the liver. The interactions between the two compartments are also considered. Interstitial insulin is cleared by the cells, via insulin sensitivity, where it influences cellular glucose uptake. Glucose can be produced endogenously by the liver. The exogenous glucose (e.g. glucose dose or meal) is also considered as it appears in plasma. Insulin-mediated and insulin-independent glucose uptake are included via insulin sensitivity, S_I , and p_G (insulin-independent glucose uptake rate). This specific model is presented in Figure 3.2.

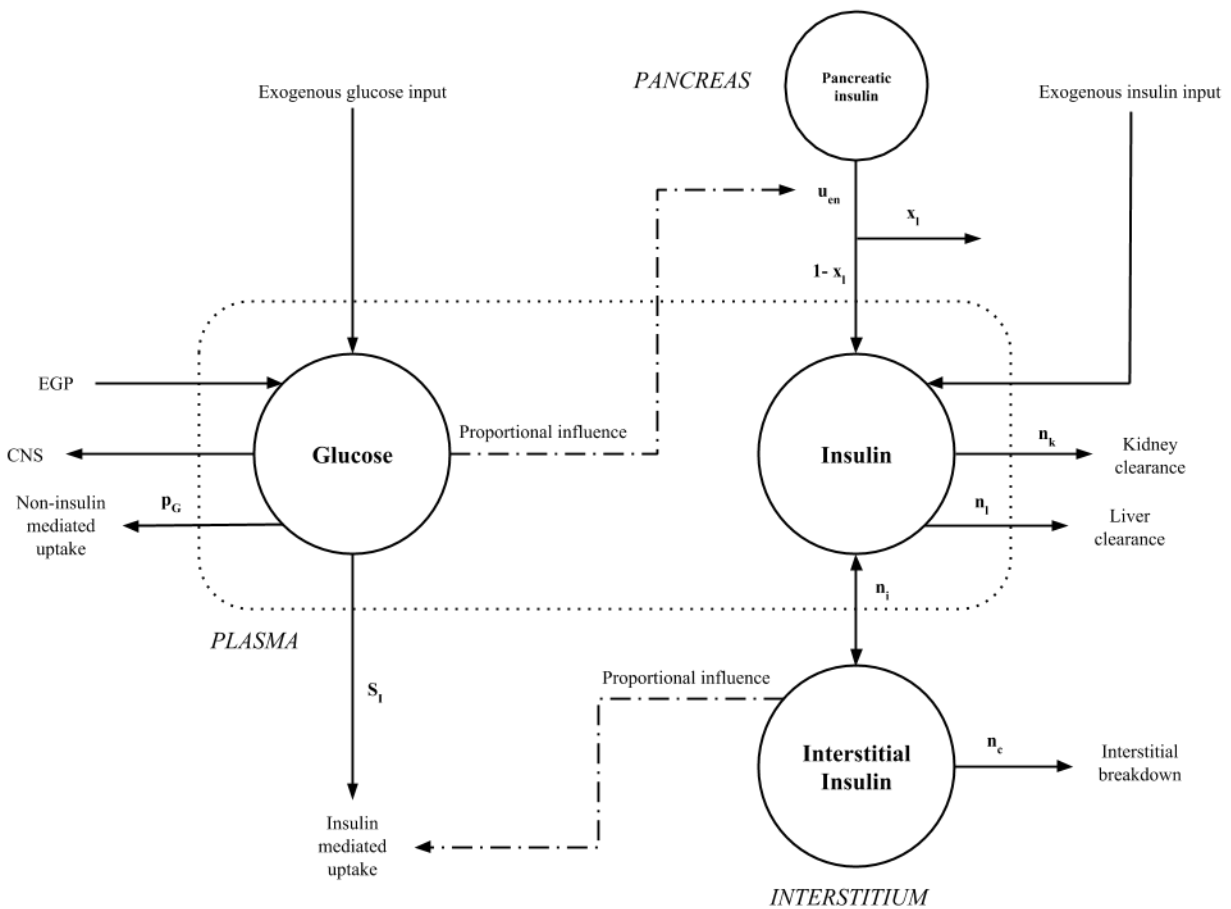


Figure 3.2 :
Glycaemic control model (inspired from [37]).

The ICING-2 model is described by the following equations :

$$\dot{G}(t) = -p_G \cdot (G(t) - G_{fast}) - S_I \cdot G(t) \cdot \frac{Q(t)}{1 + \alpha_G \cdot Q(t)} + \frac{P(t) + EGP - CNS}{V_G} \quad (3.1)$$

$$\dot{I}(t) = -n_K \cdot I(t) - n_L \cdot \frac{I(t)}{1 + \alpha_I \cdot I(t)} - n_I \cdot (I(t) - Q(t)) + \frac{u_{ex}(t) + (1 - x_L) \cdot u_{en}(G)}{V_I} \quad (3.2)$$

$$\dot{Q} = n_I \cdot (I(t) - Q(t)) - n_C \cdot \frac{Q(t)}{1 + \alpha_G \cdot Q(t)} \quad (3.3)$$

Where $G(t)$, $I(t)$ and $Q(t)$ respectively represent the glucose concentration, the plasma insulin concentration, and the interstitial insulin concentration. Concerning the glucose Equation 3.1, p_G is the insulin-independent glucose uptake rate, G_f the fasting blood sugar level, S_I the insulin sensitivity, α_G the insulin binding saturation parameter, $P(t)$ the exogenous glucose inflow rate, EGP the Endogenous Glucose Production rate, CNS the Central Nervous System glucose uptake rate, and V_G the plasma glucose distribution volume. Regarding the plasma insulin Equation 3.2, n_K is the kidney clearance rate, n_L the hepatic clearance rate, α_I the hepatic clearance saturation parameter, n_I the diffusion rate between the plasma and the interstitium, $u_{ex}(t)$ the exogenous insulin input rate, x_L the fractional first pass of hepatic insulin extraction, $u_{en}(G)$ the endogenous pancreatic insulin rate, and V_I the insulin distribution volume. Finally, for the interstitial insulin equation 3.3, n_C is the cellular clearance rate.

This model assumes endogenous insulin production by the pancreas is a function of glucose concentration. This dependency is defined :

$$u_{en}(G) = \begin{cases} u_{min} & \text{if } G(t) < G_{fast} \\ f(G) = k_{sec} \cdot G(t) + k_{off} & \text{otherwise} \\ u_{max} & \text{if } f(G) \geq u_{max} \end{cases} \quad (3.4)$$

Where u_{min} and u_{max} are respectively the minimum and the maximum endogenous pancreatic insulin secretion rate, k_{sec} the glucose sensitivity of this secretion rate, and k_{off} the secretion offset. The shape of the endogenous pancreatic insulin secretion rate is presented in Figure 3.3.

The ICING-2 model variables in Equations 3.1 to 3.3, as well as their initial value and their units, are gathered in Table 3.1. The initial value of plasma glucose concentration is the fasting level, typically 4.8 mmol.L^{-1} . Initial values of plasma and interstitial insulin were assessed by making vary these values and with a steady state assumption, and thus set to 13.4 mU.L^{-1} and 7.4 mU.L^{-1} . A summary of all parameters used in the ICING-2 model, as well as their value and their units, can be found in Table 3.2.

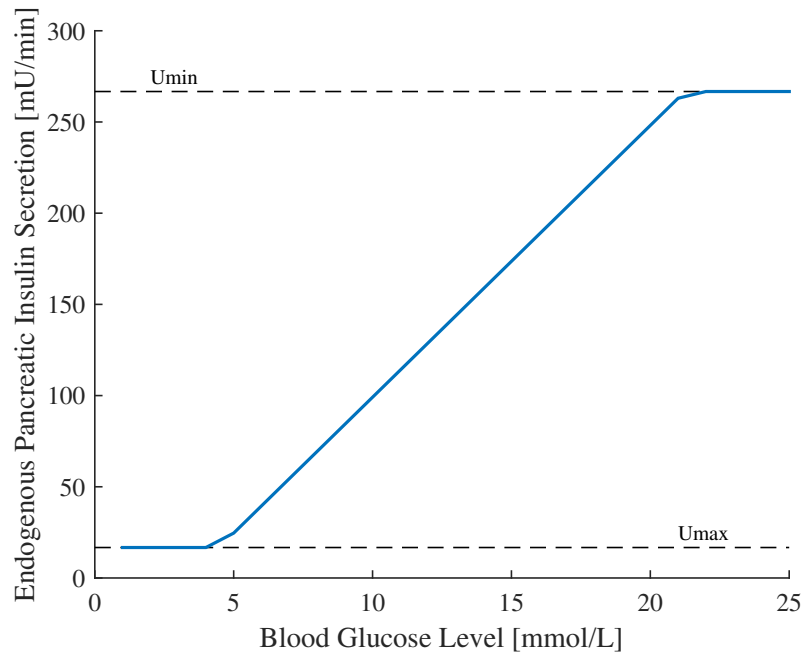


Figure 3.3 :

Shape of the endogenous pancreatic insulin secretion rate
 ($u_{min} = 16.7$, $u_{max} = 267$, $k_{sec} = 14.9$ and $k_{off} = -49.9$).

Table 3.1 :

Summary of the variables used in the ICING-2 model.

Variable	Signification	Initial value	Units
G	Blood glucose concentration	4.8	mmol.L^{-1}
I	Plasma insulin concentration	13.4185	mU.L^{-1}
Q	Interstitial insulin concentration	7.4255	mU.L^{-1}

Table 3.2 :
Summary of the parameters used in the ICING-2 model.

Parameter	Signification	Value	Units
p_G	Insulin-independent glucose uptake rate	0.04	min^{-1}
G_{fast}	Fasting blood glucose level	4.8	mmol.L^{-1}
S_I	Insulin sensitivity	10.8×10^{-4}	$\text{L} \cdot (\text{mU} \cdot \text{min})^{-1}$
α_G	Insulin binding saturation parameter	0.0154	$\text{L} \cdot \text{mU}^{-1}$
P	Exogenous glucose inflow rate	see Section 3.2	$\text{mmol} \cdot \text{min}^{-1}$
EGP	Endogenous Glucose Production rate	0.96	$\text{mmol} \cdot \text{min}^{-1}$
CNS	Central Nervous System glucose uptake rate	0.3	$\text{mmol} \cdot \text{min}^{-1}$
V_G	Plasma glucose distribution volume	12.2	L
n_K	Kidney clearance rate of plasma insulin	0.06	min^{-1}
n_L	Liver clearance rate of plasma insulin	0.0324	min^{-1}
α_I	Hepatic clearance saturation parameter	0.0017	$\text{L} \cdot \text{mU}^{-1}$
n_I	Insulin diffusion rate	0.006	min^{-1}
x_L	Fractional first pass of hepatic insulin extraction	0.67	-
u_{en}	Endogenous pancreatic insulin rate	$f(G)$	$\text{mU} \cdot \text{min}^{-1}$
u_{ex}	Exogenous insulin input rate	see Section 3.3	$\text{mU} \cdot \text{min}^{-1}$
V_I	Plasma and interstitial insulin distribution volume	4	L
n_C	Cellular insulin clearance rate from interstitium	0.032	min^{-1}
u_{min}	Minimum endogenous pancreatic insulin secretion rate	16.7	$\text{mU} \cdot \text{min}^{-1}$
u_{max}	Maximum endogenous pancreatic insulin secretion rate	267	$\text{mU} \cdot \text{min}^{-1}$
k_{sec}	Glucose sensitivity of the endogenous pancreatic insulin secretion rate	14.9	$(\text{mU} \cdot \text{L}) \cdot (\text{mmol} \cdot \text{min})^{-1}$
k_{off}	Endogenous pancreatic insulin secretion offset	-49.9	$\text{mU} \cdot \text{min}^{-1}$

3.2 Sub-model 2 : Gastrointestinal model

The second sub-model represents glucose absorption after a meal or oral glucose. The gastrointestinal model of Dalla Man et al. is non-linear, based on 3 main compartments and yields the appearance glucose rate in plasma [66]. The first two compartments stand for stomach glucose, respectively the solid and liquid phases. The third represents glucose passing through the intestines, namely the gut glucose, and into plasma. The model is shown in Figure 3.4.

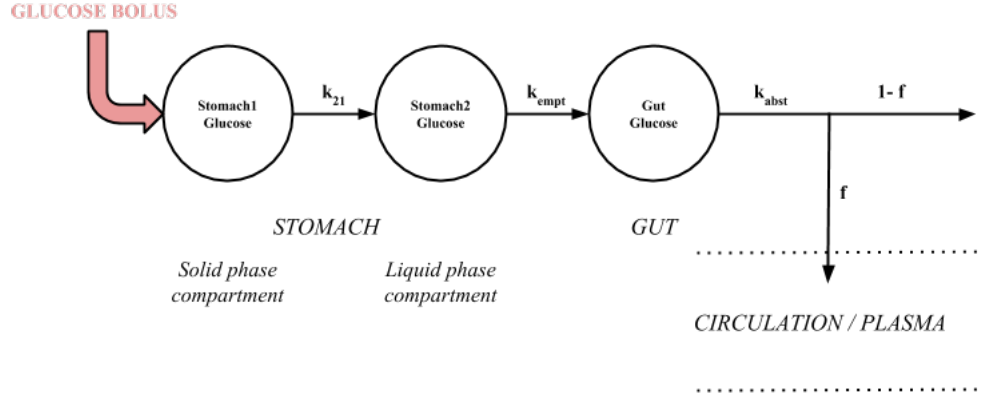


Figure 3.4 :
Gastrointestinal model [66].

The different equations of this gastrointestinal model are defined :

$$\dot{g}_{sto1}(t) = -k_{21} \cdot g_{sto1}(t) + D \cdot \delta(t) \quad (3.5)$$

$$\dot{g}_{sto2}(t) = -k_{empt}(g_{sto}) \cdot g_{sto2}(t) + k_{21} \cdot g_{sto1}(t) \quad (3.6)$$

$$\dot{g}_{gut} = -k_{abs} \cdot g_{gut}(t) + k_{empt}(g_{sto}) \cdot g_{sto2}(t) \quad (3.7)$$

$$Ra(t) = f \cdot k_{abs} \cdot g_{gut}(t) \quad (3.8)$$

Where D represents the amount of ingested glucose, g_{sto1} the amount of glucose in the solid stomach compartment, g_{sto2} the amount of glucose in the liquid stomach compartment, g_{gut} the amount of glucose in the gut, k_{21} the rate of grinding, $\delta(t)$ the impulse function, $k_{empt}(g_{sto})$ the rate of gastric emptying relied on the amount of glucose in the stomach, k_{abs} the rate constant of intestinal absorption, f the fraction of the intestinal absorption that appears in the plasma, and Ra the rate of appearance in plasma of ingested glucose. The amount of glucose in the different compartments and the rate of appearance can be expressed in mass or molar notions. Even though Dalla Man et al. used mass quantities for parameter identification, molar quantities are used in this model for consistency in units.

The rate of gastric emptying $k_{empt}(g_{sto})$ depends on the total quantity of glucose in the stomach and thus has a particular form that can be observed in Figure 3.5 and is specified by :

$$k_{empt}(g_{sto}) = k_{min} + \frac{k_{max} - k_{min}}{2} \cdot \{ \tanh[\alpha \cdot (g_{sto} - b \cdot D)] - \tanh[\beta \cdot (g_{sto} - c \cdot D)] + 2 \} \quad (3.9)$$

$$g_{sto}(t) = g_{sto1}(t) + g_{sto2}(t) \quad (3.10)$$

$$\alpha = \frac{5}{2 \cdot D \cdot (1 - b)} \quad (3.11)$$

$$\beta = \frac{5}{2 \cdot D \cdot c} \quad (3.12)$$

Where k_{min} and k_{max} represent respectively the minimum and maximum possible rates of gastric emptying, g_{sto} the total amount of glucose in the stomach (the sum of the first two compartments), b the percentage of the bolus D for which k_{empt} decreases at $\frac{k_{min}+k_{max}}{2}$, c the percentage of the dose D for which k_{empt} increases at $\frac{k_{min}+k_{max}}{2}$, α the decreasing rate from k_{max} to k_{min} , and β the recovering rate from k_{min} to k_{max} . The rate is maximum for zero stomach glucose or at the beginning of the experiment. The parameters α and β are constrained by these previous observations and are defined by Equations 3.11 and 3.12. The liquid gastric emptying, $k_{empt}(g_{sto})$, leads to the non-linearity of this sub-model.

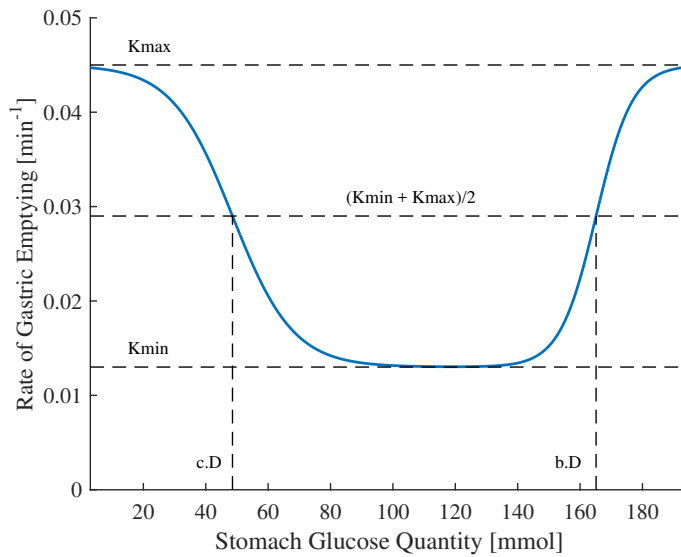


Figure 3.5 :

The rate of gastric emptying regarding to the total amount of glucose in the stomach
 ($k_{min} = 0.013$, $k_{max} = 0.045$, $b = 0.85$ and $c = 0.25$).

A summary of all the parameters, their value, and their units can be found in Table 3.3. The rate of grinding, k_{21} , is fixed to 1 given the liquid, dilute nature of the oral glucose. The intestinal absorption fraction, f , is set to 0.8. The other values have been determined through parameter identification [66]. These parameters have been identified through data obtained in Oral Glucose Tolerance Test (OGTT) [66]. Table 3.4 shows the variables, their units, and their initial value. In this study, the injected dose of glucose is 35 g : this is then the initial value of g_{sto1} .

Table 3.3 :
Summary of the parameters used in the gastrointestinal model.

Parameter	Signification	Value	Units
k_{21}	Rate of grinding	1	min^{-1}
k_{empt}	Rate of gastric emptying	$f(g_{sto})$	min^{-1}
k_{abs}	Rate constant of intestinal absorption	0.205	min^{-1}
f	Intestinal absorption fraction	0.8	-
k_{min}	Minimum rate of gastric emptying	0.013	min^{-1}
k_{max}	Maximum rate of gastric emptying	0.043	min^{-1}
b	"Intersection point"	0.85	-
c	"Intersection point"	0.25	-

Table 3.4 :
Summary of the variables used in the gastrointestinal model.

Variable	Signification	Initial Value	Units
g_{sto1}	Amount of stomach glucose in the solid compartment	35	g (mmol)
g_{sto2}	Amount of stomach glucose in the liquid compartment	0	g (mmol)
g_{gut}	Amount of gut glucose	0	g (mmol)
Ra	Plasma rate of appearance of ingested glucose	0	$\text{g}\cdot\text{min}^{-1}$ (mmol.min ⁻¹)

Unlike linear and simplistic previous gastrointestinal models based only on easily obtained plasma concentrations, this model relies on recent available data from multiple tracers and accurate protocols [66]. This approach and added data allow parameter's identification by focusing precisely on the gastrointestinal system and not on the whole body. The model of Dalla Man et al. [66] is thus suitable for incorporation in a whole-body model and in the research proposed in this thesis.

3.3 Sub-model 3 : Subcutaneous insulin injection model

In order to mathematically represent subcutaneous injection of insulin, the compartmental model of Wong et al. is used [33, 67, 68]. Originally, this model was created to describe pharmacokinetics of all types of subcutaneously injected insulin, from fast- and short-acting prandial insulin (MI and RI) to intermediate- and long-acting insulin types (such as NPH, lente, ultralente and insulin glargine). However, because this project only requires very rapid-acting Monomeric Insulin (MI), the model is considerably simplified.

Injected insulin appears first in a subcutaneous depot space, which is the first compartment. It then crosses a second compartment, the local depot interstitium. This local depot interstitium is different from the global interstitium used in ICING-2 model (see Section 3.1). After that, insulin is either degraded, or passes into the plasma. The model is presented in Figure 3.6.

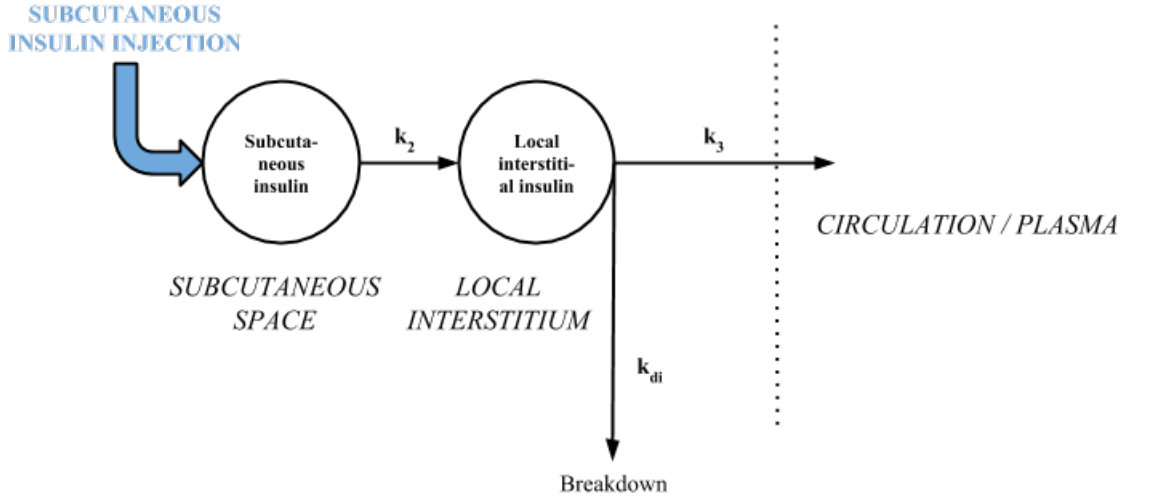


Figure 3.6 :

Subcutaneous insulin injection model for very rapid-acting insulin [33, ?, ?].

The equations for this model are defined :

$$\dot{I}_{sc}(t) = -k_2 \cdot I_{sc}(t) + \delta(t - T) \cdot I_{bolus} \quad (3.13)$$

$$\dot{Q}_{local}(t) = -k_3 \cdot Q_{local}(t) + k_2 \cdot I_{sc}(t) - k_{di} \cdot Q_{local}(t) \quad (3.14)$$

Where I_{sc} represents the amount of insulin in the local subcutaneous depot space, Q_{local} the amount of insulin in this local interstitium depot, which is different from the global body interstitial space considered in the ICING-2 model, I_{bolus} the amount of injected insulin, k_2 the transport rate defining the diffusion from the subcutaneous space into the local interstitium, k_3 the interstitium insulin transport rate into plasma, k_{di} the rate of loss from interstitium, δ the impulse function, and T the insulin injection time after the commencement of the test.

A summary of all the parameters, their value, and their units can be found in Table 3.5. Most of these values have been identified in Wong et al. [33, 67, 68]. In this research, the insulin will be injected 15 minutes after the beginning of the test, so $T = 15$ min. In this test, 2 U are administrated, yielding $I_{bolus} = 2000$ mU. Table 3.6 gathers the model variables, their units and their initial value.

Table 3.5 :
Summary of the parameters used in the subcutaneous insulin injection model.

Parameter	Signification	Value	Units
k_2	Transport rate into interstitium	0.0104	min^{-1}
k_3	Interstitial insulin transport rate into plasma	0.06	min^{-1}
k_{di}	Rate of loss from interstitium	0.0029	min^{-1}
I_{bolus}	Amount of injected insulin	2000	mU
T	Time delay	15	min

Table 3.6 :
Summary of the variables used in the subcutaneous insulin injection model.

Variable	Signification	Initial Value	Units
I_{sc}	Amount of insulin in the subcutaneous space	2000	mU
Q_{local}	Amount of insulin a local interstitium	0	mU

3.4 Summary

The clinical protocol used to assess insulin sensitivity requires an oral glucose bolus and a subcutaneous insulin injection. The protocol-related model thus considers these two particular aspects, as well as internal glucose and insulin dynamics. For oral glucose absorption, the gastrointestinal model of Dalla Man et al. is used [66]. The model by Wong et al. [33, 67, 68] is applied for modelling the appearance kinetics of the subcutaneous insulin injection [33]. The glucose-insulin interactions, as well as their formation and degradation, are modelled by the second version of the Intensive Control Insulin-Nutrition-Glucose (ICING-2) model [59]. These three sub-models are combined together to form the overall SubCutaneous Oral Glucose Intensive Control Insulin-Nutrition-GLucose 2 (SC-OG-ICING-2) model represent changes of glucose and insulin concentrations during the suggested protocol. A big summary of the overall model equations, parameter and variable values is in Appendices.

Chapter 4

Single parameter sensitivity analysis

The SC-OG-INCING-2 model is the foundation element of a clinical trial to validate this model, as well as as accurately assess metabolic status using subcutaneous insulin and oral glucose. It is expected to correctly describe the glucose and insulin kinetics and dynamics. Insulin sensitivity and secretion can only be directly assessed using a clinical protocol, data, and an accurate model. A sensitivity analysis is thus performed to demonstrate the robustness of the model, as well as the potential accuracy of this new kind of Dynamic Insulin Sensitivity and Secretion Test (DISST). This *in-silico* investigation also provides a means to discover any model and protocol weaknesses.

This chapter presents a single parameter sensitivity analysis, where the effects of model parameters on model outcomes are analysed individually. Not all parameters are investigated. Parameters are varied considering realistic physiological ranges. The combined influence of several parameters is studied in Chapter 5, based on results in this chapter.

4.1 Parameters of interest

As discussed in Chapter 3, the model is comprised of three physiological sub-models. The first sub-model is the glycaemic control model and it mathematically represents internal glucose and insulin dynamics. The second one models the glucose absorption after an oral ingestion, while the third sub-model reflects the subcutaneous injection of insulin. Each dynamic system exerts an overall effect or sensitivity of response on the complete system.

The glycaemic control model (ICING-2) is strongly inspired from the DISST model. Both have been validated in several studies [8, 59, 9, 10, 60, 62, 63, 64, 65]. Thus, the impact of specific parameters in the glucose and insulin dynamics description, is not considered in this thesis, and is taken for granted. However, considering the role of insulin sensitivity (S_I) and secretion (u_{en}) in this work, their incidence is analysed. In addition, the most important difference between ICING-2 and DISST model is the glucose-dependency of modelled endogenous pancreatic insulin secretion. Investigation of the parameters included in this glucose-dependency is thus very significant.

Regarding the other two sub-models, they can be considered as inputs interfering with an already well-validated model. Indeed, orally absorbed glucose and its modifications in the gastrointestinal tract, represented by the second sub-model, can be seen as the exogenous glucose inflow in the glycaemic control model. This sub-model is described by Equations 3.5 to 3.12, involving the parameters k_{21} , $k_{empt}(k_{min}, k_{max}, b, c)$, k_{abs} , and f . Equally, subcutaneously injected insulin and its appearance in plasma, depicted by the third sub-model, can be considered as the exogenous insulin input in the glycaemic control model. This sub-model is described by Equations 3.13 and 3.14, involving the parameters k_2 and k_3 . Hence, the influence of all the parameters involved in these two models is investigated.

In summary, the glycaemic control model is the central part of the system model and is both well-validated and taken for granted. In contrast, all inputs of this validated sub-model, namely oral glucose ingestion and subcutaneous insulin injection, and their resultant appearance, are investigated. The influence of glucose-dependent endogenous pancreatic insulin secretion is not neglected and can also be considered as an input of the central part. The impact of insulin sensitivity is also analysed. The single parameter sensitivity analysis thus only deals with the following parameters :

- S_I
- **"Input 1"** : $k_{21}, k_{empt}(k_{min}, k_{max}, b, c), k_{abs}, f$
- **"Input 2"** : k_2, k_3, k_{di}
- **"Input 3"** : $u_{en}(u_{min}, u_{max}, k_{sec}, k_{off})$

Figure 4.2 schematically explains the selection of the parameters of interest.

4.2 Physiological ranges

To examine the effect of parameters of interest on the model, their values are modified and the resulting model-based influence of these modifications is analysed and plotted. One parameter at a time is changed with all others hold fixed. However, these parameters represent real and physiological phenomena. Thus, their value can only be changed in a well-defined range around their mean or initially imposed value. Ranges of variations are defined in two specific ways, depending on whether the thesis or article, in which parameter value is referenced, also provides its standard deviation (s.d.).

If standard deviation of a parameter is given, its variation range is defined as 2 standard deviations above and below its mean. It is also assumed that the parameter values are normally distributed. Thus, 95.45 % of the possible physiological values belong to this range of variation. Figure 5.2 reminds the shape of a normal distribution, as well as the relationship with its standard deviation.

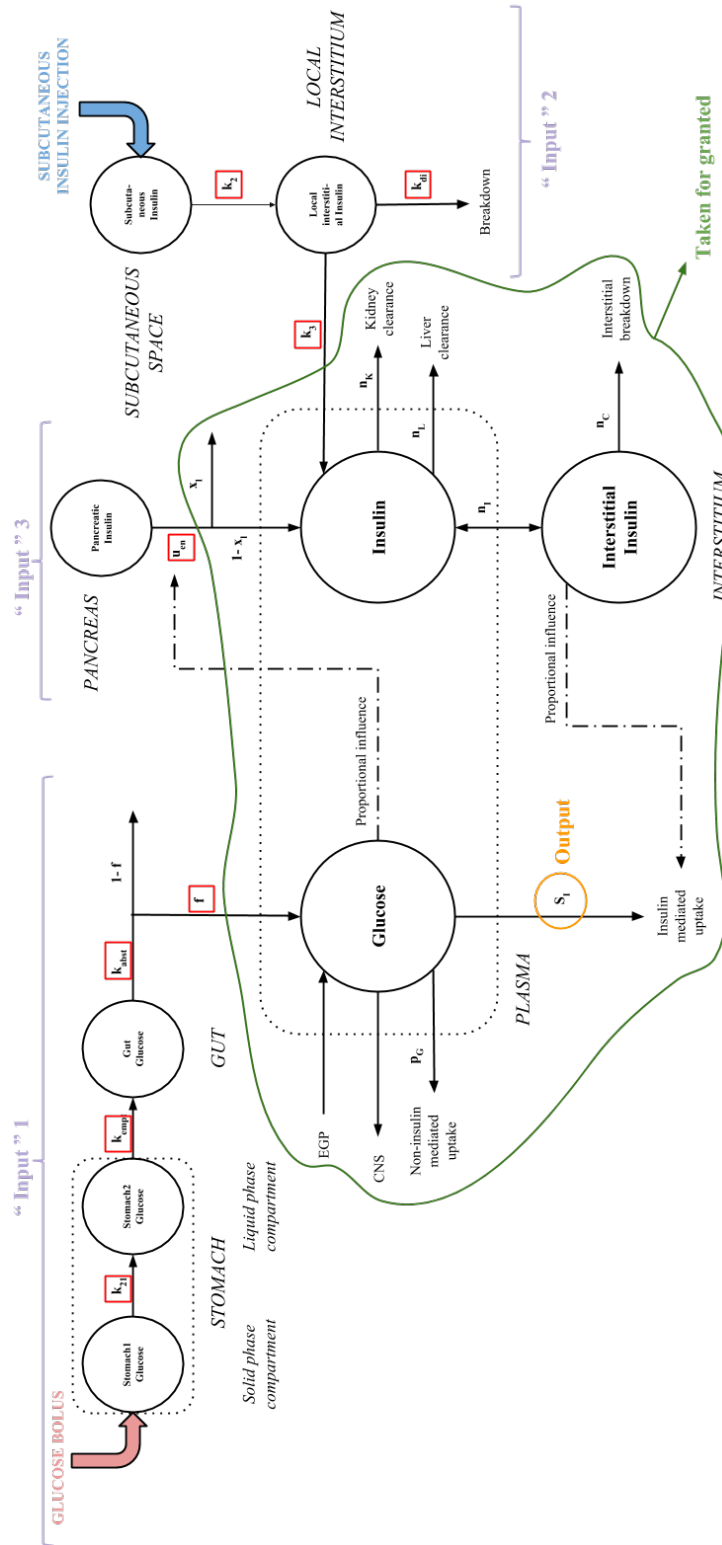


Figure 4.1 :
 Selection of the parameters of interest for single parameter sensitivity analysis.

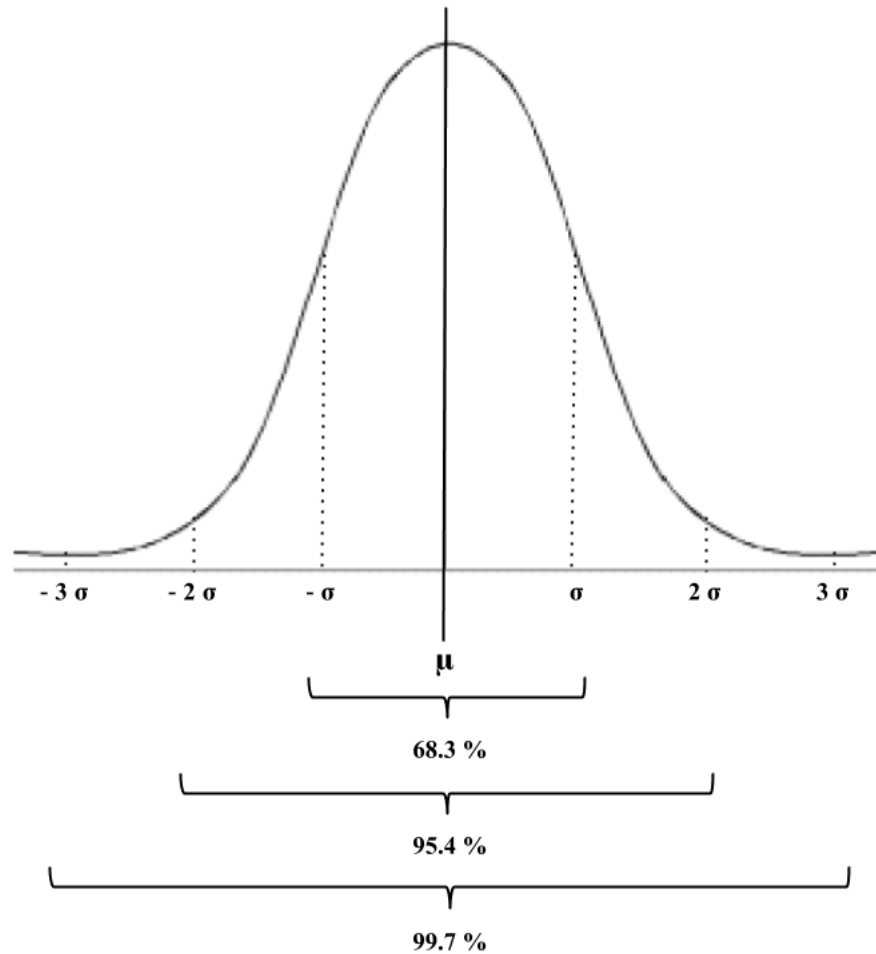


Figure 4.2 :

Shape of a normal distribution, as well as the relationship with its standard deviation.

In contrast, if standard deviation is not provided or known from other sources, the variation range of the parameter is specified as the average value plus or minus 25 % of this mean value and the distribution is assumed to be normal.

The special case of insulin sensitivity has to be noted. This parameter is linked to diabetic status and does not vary around a mean value, but evolves over a range. Non-diabetic individuals have an insulin sensitivity around $0.00108 \text{ L} \cdot (\text{mU}/\text{min})^{-1}$ in the model used [9]. This value is thus considered as the mean or middle value and is used as the normal insulin sensitivity in all simulations. However, some individuals have a much higher insulin sensitivity, reaching sometimes $0.0018 \text{ L} \cdot (\text{mU}/\text{min})^{-1}$ [44, 10]. This value is considered as the upper limit. In contrast, diabetic individuals have a very low insulin sensitivity, around $0.00025 \text{ L} \cdot (\text{mU}/\text{min})^{-1}$ (lower limit) [44, 10]. Impaired Glucose Tolerance (IGT) and its progressive state is characterised by two specific insulin sensitivities, specifically $0.0005 \text{ L} \cdot (\text{mU}/\text{min})^{-1}$ and $0.00083 \text{ L} \cdot (\text{mU}/\text{min})^{-1}$.

Table 4.1 summarises parameters of interest. It also provides lower and upper limits, as well as how they have been calculated, or gathered by reference.

Table 4.1 :
Variation ranges of the parameters of interest.

Parameter	Mean	Lower Bound	Upper Bound	Method
S_I	0.00108	0.00025	0.0018	Fixed [8, 9]
k_{min}	0.013	0.009	0.017	± 2 s.d. [66]
k_{max}	0.045	0.037	0.053	± 2 s.d. [66]
b	0.85	0.81	0.89	± 2 s.d. [66]
c	0.25	0.19	0.31	± 2 s.d. [66]
k_{abs}	0.205	0.161	0.249	± 2 s.d. [66]
f	0.8	0.6	1	± 25 %
k_2	0.0104	0.0076	0.0132	± 2 s.d. [33, 67, 68]
k_3	0.0613	0.0131	0.1095	± 2 s.d. [33, 67, 68]
k_{di}	0.0029	0.0022	0.0036	± 25 %
u_{min}	16.7	12.525	20.875	± 25 %
u_{max}	266.7	200.025	333.375	± 25 %
k_{sec}	14.9	11.175	18.625	± 25 %
k_{off}	- 49.9	- 62.375	- 37.425	± 25 %

4.3 Results and Discussion

Before performing the single parameter sensitivity analysis, the clinical trial protocol must be described. It first consist of an oral ingestion of 35 grams of glucose at the test beginning. Fifteen minutes later, it is followed by a subcutaneous injection of 2 units of insulin.

To carry out the single parameter sensitivity analysis and thus to plot simulated BG evolution, some existing MATLAB codes were adapted. This MATLAB code solves the differential equations of the model. Thus, it includes these mathematical equations, as well as initial values of the different variables (see Tables 3.1, 3.4 and 3.6) and typically used parameter mean values (see Table 3.2, 3.3 and 3.5).

Figure 4.3 presents BG evolution generated by the model equations. Parameter values can be found in Tables 3.2, 3.3 and 3.5. Virtual patient mass is set to 75 kg and simulation duration is 150 minutes, even though the

proposed clinical trial lasts 120 minutes. The two vertical lines indicate the theoretical end of the clinical trial and the simulation end. Limits of low and high BGL are indicated in this Figure. For hyperglycaemic thresholds, two dashed lines at 8.0 mmol/L and 10.0 mmol/L are plotted. The two pink rectangles indicate hypoglycaemia. The lightest one imposes a light hypoglycaemic limit at 4.0 mmol/L and the darkest one sets this limit at 3.5 mmol/L. BG in one of these two rectangles should be avoided. More or less restrictive limitations of BG have been considered because of the different tendencies worldwide. However, these limits represent current consensus on light and mild hypoglycaemia.

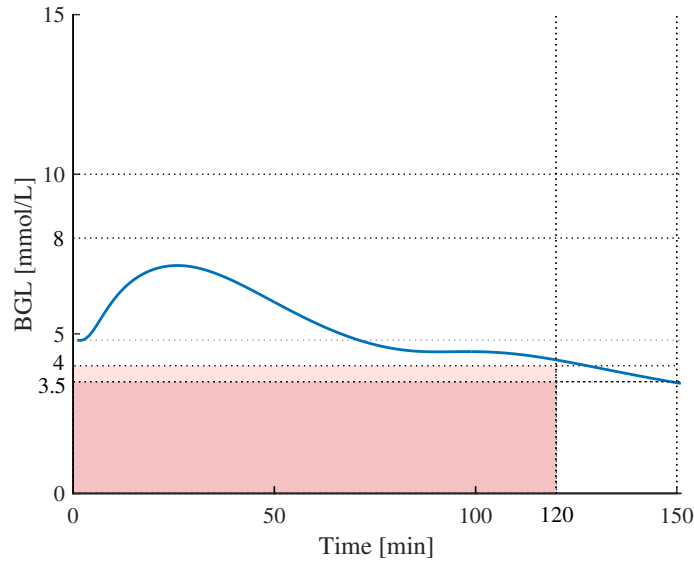


Figure 4.3 :

BG evolution, for $S_I = 0.00108 \text{ L} \cdot (\text{mU} \cdot \text{min})^{-1}$, an oral 35 g glucose dose, a subcutaneous 2 U insulin bolus and with mean parameter values.

The influence of the parameters of interest on BG evolution (Figure 4.3) is analysed in this chapter. The values of these parameters are individually changed to its lower and upper limit (see Table 4.1). The resulting shifts in BG evolution are presented and discussed, where a larger shift indicates greater sensitivity to this parameter.

▷ Insulin sensitivity S_I

Figure 4.4 represents BG evolution according to different values of insulin sensitivity (S_I), specifically 0.00025, 0.0005, 0.00083, 0.00108 and 0.0018 $\text{L} \cdot (\text{mU} \cdot \text{min})^{-1}$. The value of $S_I = 0.0005 \text{ L} \cdot (\text{mU} \cdot \text{min})^{-1}$ represents pre-diabetes, and $S_I = 0.00083 \text{ L} \cdot (\text{mU} \cdot \text{min})^{-1}$ is an intermediate value between low and normal insulin sensitivities [9, 44, 10]. All other parameters remain unchanged.

As expected, high insulin sensitivity ($0.0018 \text{ L} \cdot (\text{mU} \cdot \text{min})^{-1}$) leads to a lower BG evolution and mild hypoglycaemia within 120 minutes. Because of this high insulin sensitivity, it takes less insulin to remove glucose, and thus a fixed insulin dose leads to greater glucose removal. In contrast, the lowest insulin sensitivities lead to hy-

perglycaemia above normal. For $S_I = 0.00025 \text{ L} \cdot (\text{mUmin})^{-1}$, a sustained hyperglycaemic situation is achieved as expected for a S_I value of a T2D individual. In this case, there is too little insulin to remove glucose given the low sensitivity. Note that extreme situations are only considered before 120 minutes, because the test stops at this time with a snack not modelled here.

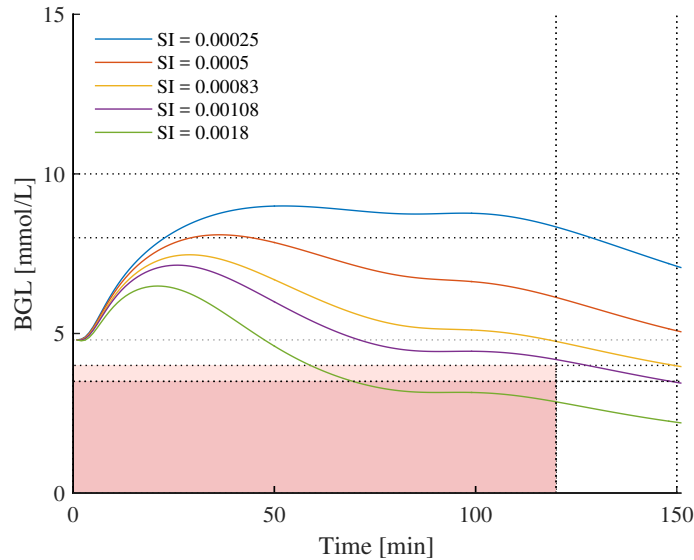


Figure 4.4 :

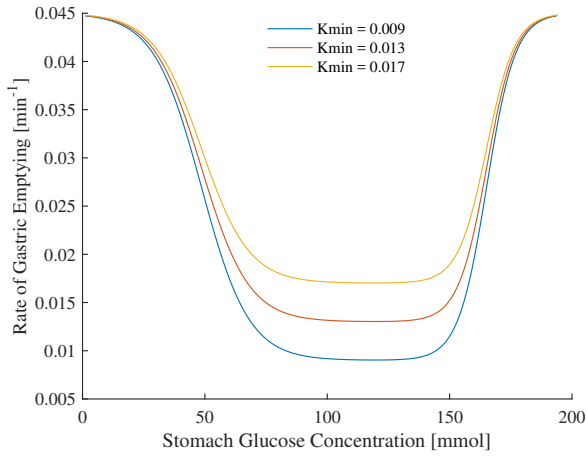
BG evolution according to different values of S_I .

▷ **Minimum rate of gastric emptying k_{min}**

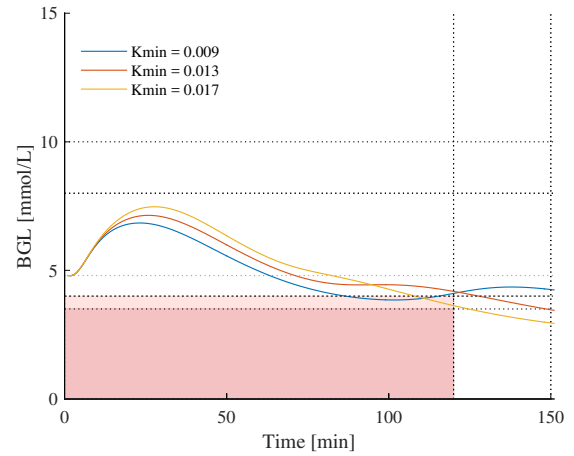
The rate of gastric emptying, k_{empt} , is a function of several parameters, including k_{min} (see Equation 3.9). Figure 4.5a represents the shape of this gastric emptying rate, according to different imposed minimum rates (0.009, 0.013 and 0.017 min^{-1}). Figure 4.5b reflects evolution of BG according to these values of k_{min} with all other parameters unchanged.

Considering the "u-shape" of k_{empt} , a change of k_{min} leads to a vertical displacement of the horizontal plateau (Figure 4.5b). An upward displacement for the largest minimum rate and a downward displacement for the smallest minimum rate are observed. Overall, the BG evolutions do not change in any clinically significant fashion.

An increase of k_{min} causes a rise of the BG peak, occurring at the beginning of the simulation (Figure 4.5b). Stomach glucose reaches the gut faster, and thus the circulation level rises faster. There is thus a larger quantity of glucose in the plasma before insulin is injected. The opposite conclusion is drawn for smallest minimum rate. At the end of the test ($\simeq 110 \text{ min}$), BGL evolution with the smallest k_{min} crosses the one with the largest k_{min} . Indeed, for $k_{min} = 0.009 \text{ min}^{-1}$, some glucose still reaches the plasma compartment after the insulin action peak, increasing overall BG, which is not possible for $k_{min} = 0.017 \text{ min}^{-1}$ because no more gut glucose is available to enter from the oral glucose load.



(a) Shape of k_{empt} according to different values of the parameter k_{min} .



(b) BG evolution according to different values of the parameter k_{min} .

Figure 4.5 :

Influence of the parameter k_{min} on BG evolution and on shape of k_{empt} , for $S_I = 0.00108 \text{ L} \cdot (\text{mU} \cdot \text{min})^{-1}$.

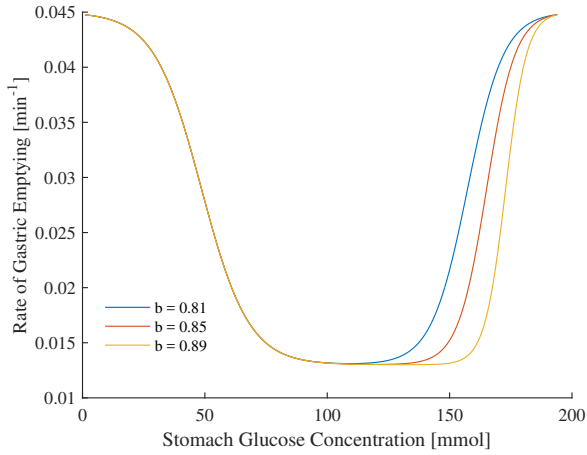
▷ **Maximum rate of gastric emptying k_{max}**

Regarding Equation 3.9, gastric emptying rate also depends on its maximum rate, k_{max} . Even if changes of k_{max} influence the shape of k_{empt} , it has almost no impact on BG evolution. Indeed, the absorbed glucose only follows this kinetics in two particular cases (e.g. $q_{sto} = D$ and $q_{sto} = 0$), which is not enough to affect overall BG evolution. In contrast, stomach glucose often has the minimum dynamics because of k_{empt} and its resulting inverted "plateau-shape". Graphical representations of k_{empt} shape and BG evolution according to different values of k_{max} are in the Appendices.

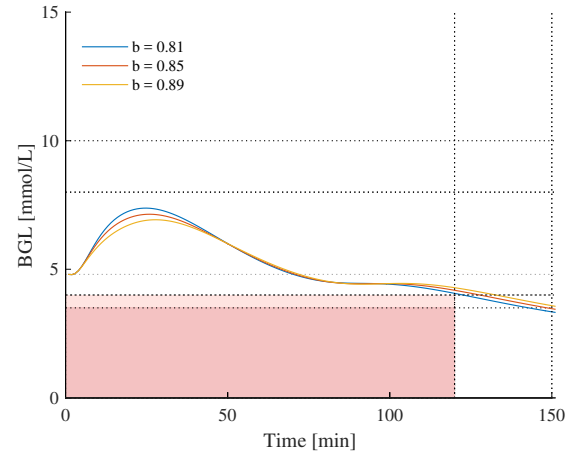
▷ **"Intersection point" b**

Influence of the parameter b , which is involved in the rate of gastric emptying k_{empt} (Equation 3.9), is analysed through Figure 4.6a and Figure 4.6b. Figure 4.6a presents the shape of k_{empt} according to different values of b (0.81, 0.85 and 0.85). Figure 4.6b reflects resulting BG evolution in function of these changes in b . All other parameters remain unchanged. As with k_{min} , the overall impact is small.

Parameter b is the percentage of the bolus glucose dose D for which k_{empt} begins to decrease. It is thus expected that the right side of k_{empt} curve is horizontally displaced (Figure 4.6a). A right horizontal shift for $b = 0.89$ is observed, where a left one occurs for $b = 0.81$. In contrast, regarding BG evolution, changes in b lead to a vertical displacement of the glucose peak at the beginning of the simulation. For the smallest b , glucose peak is higher because gastric emptying rate remains elevated for longer. The opposite conclusion is drawn for the largest b .



(a) Shape of k_{empt} according to different values of the parameter b .



(b) BG evolution according to different values of the parameter b .

Figure 4.6 :

Influence of the parameter b on BG evolution and on shape of k_{empt} , for $S_I = 0.00108 L.(mU.min)^{-1}$.

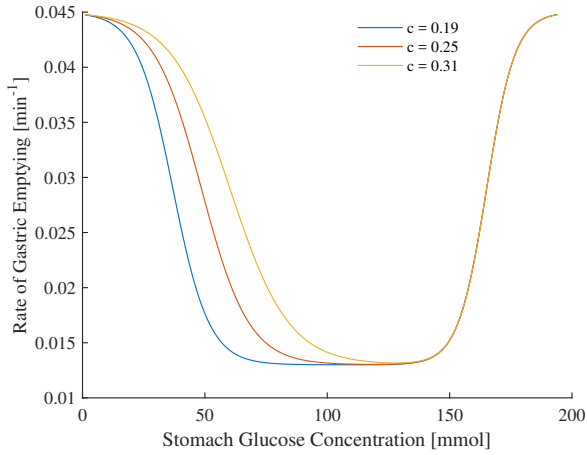
▷ **"Intersection point" c**

Figure 4.7a illustrates the shape of gastric emptying rate, k_{empt} , according to different values of the parameter c (0.19, 0.25 and 0.31). Given Equation 3.9, k_{empt} also depends on c . Figure 4.7b represents BGL evolution according to the same changes of c . All other parameters remain unchanged.

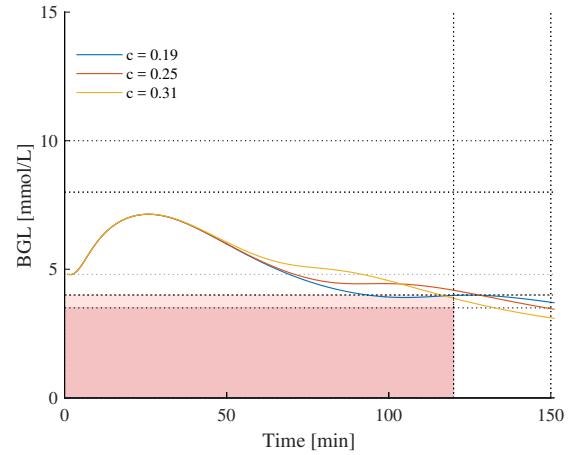
Parameter c stands for the percentage of glucose dose, D , for which k_{empt} begins to increase again. According to the value of c , a horizontal shift of the left part of the k_{empt} curve is expected and observed (Figure 4.7a). The smallest value ($c = 0.19$) leads to a left displacement, where the largest one ($c = 0.31$) operates a right displacement. About BG evolution, some differences in the middle of the simulation are observed for various c values (Figure 4.7b). For $c = 0.31$, the rate of gastric emptying begins to increase again for higher stomach glucose concentrations. This leads to the rise of BG in the middle of the simulation, in comparison with BG evolution for which c is imposed to 0.19. Again, changes are not clinically significant and sensitivity is thus low.

▷ **Rate constant of intestinal absorption k_{abs}**

The rate constant of intestinal absorption, k_{abs} , characterises glucose transition between the gut and the circulation. Changes of this parameter have almost no effect on BG evolution. Graphical BG evolution according to different values of k_{abs} can thus be found in the Appendices.



(a) Shape of k_{empt} according to different values of the parameter c .



(b) BG evolution according to different values of the parameter c .

Figure 4.7 :

Influence of the parameter c on BG evolution and on shape of k_{empt} , for $S_I = 0.00108 L.(mU.min)^{-1}$.

▷ Intestinal absorption fraction f

Figure 4.8 brings to light the influence of intestinal absorption fraction, f , on BGL evolution. Intestinal absorption fraction represents the fraction of gut glucose reaching the circulation. Three different values of f are considered : 0.6, 0.8 and 0.95. Even if the calculated upper limit of this parameter is equal to 1.0 (see Table 4.1), imposing $f = 1.0$ questions the overall utility of this parameter. All other parameters remain unchanged.

Reasonably, when f changes, BGL evolution is totally shifted (Figure 4.8). For $f = 0.95$, more gut glucose reaches the circulation, leading to an upper displacement of BGL evolution. In contrast, when less gut glucose arrives in the circulation ($f = 0.6$), the curve is shifted downwards. All these results are as expected, and variability is low and not really clinically significant.

▷ Transport rate into interstitium k_2

The impact of the transport rate of subcutaneously injected insulin into local interstitium is also analysed. Figure 2 represents BGL evolution according to different values of this parameter (0.0076, 0.0104 and 0.0132 min^{-1}). All other parameters remain unchanged. Sensitivity is very low and no clinically significant shift is observed.

The larger the transport rate k_2 , the faster the injected insulin transport between subcutaneous depot and local interstitium compartment, and thus the faster it arrives in the plasma to act on BG. For $k_2 = 0.0132 \text{ min}^{-1}$, BG evolution is thus locally shifted downwards, where the curve moves upwards for the largest value of k_2 . These changes can only occur after the insulin injection time, as expected.

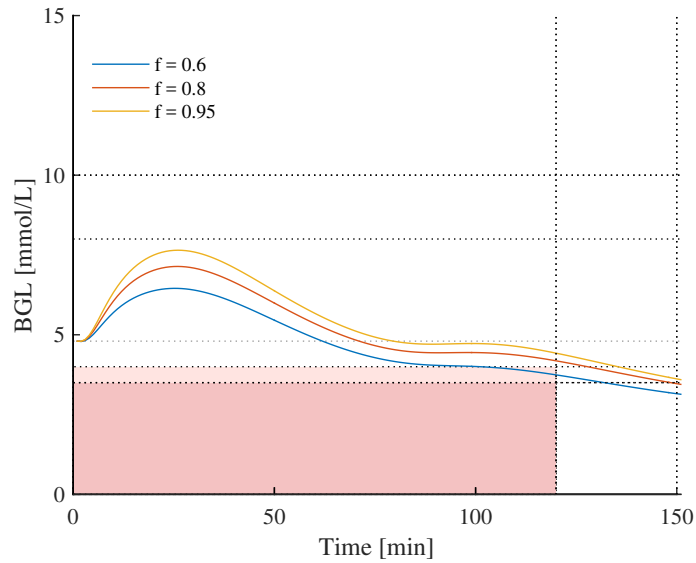


Figure 4.8 :

BG evolution according to different values of the parameter f , for $S_I = 0.00108 L.(mU.min)^{-1}$.

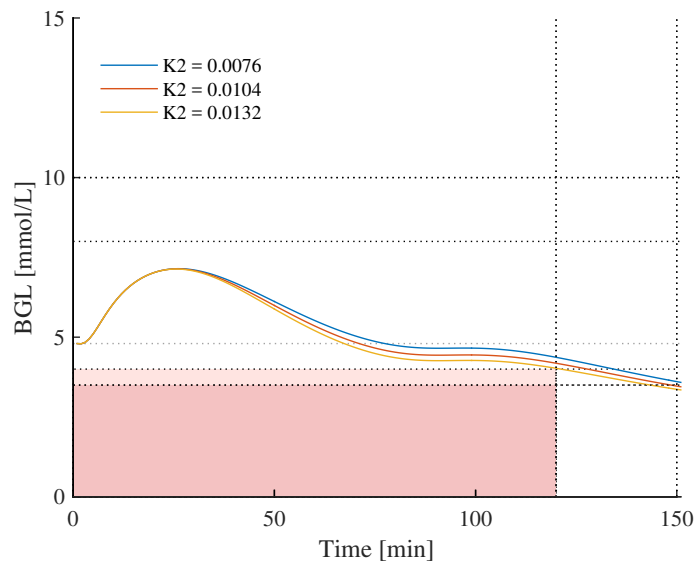


Figure 4.9 :

BG evolution according to different values of the parameter k_2 , for $S_I = 0.00108 L.(mU.min)^{-1}$.

▷ **Interstitial insulin transport rate into plasma k_3**

The interstitium transport rate of subcutaneously injected insulin between the local interstitium and the plasma, k_3 , is also considered. Three values of this parameter are considered : 0.0131, 0.0613 an 0.1095 min^{-1} . Figure 4.10 represents the influence of k_3 on BGL evolution. All other parameters remain unchanged.

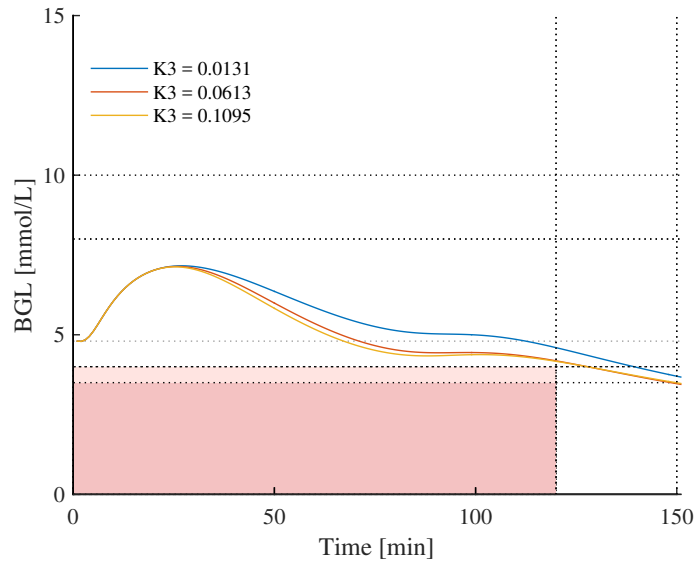


Figure 4.10 :

BG evolution according to different values of the parameter k_3 , for $S_I = 0.00108 \text{ L} \cdot (\text{mU} \cdot \text{min})^{-1}$.

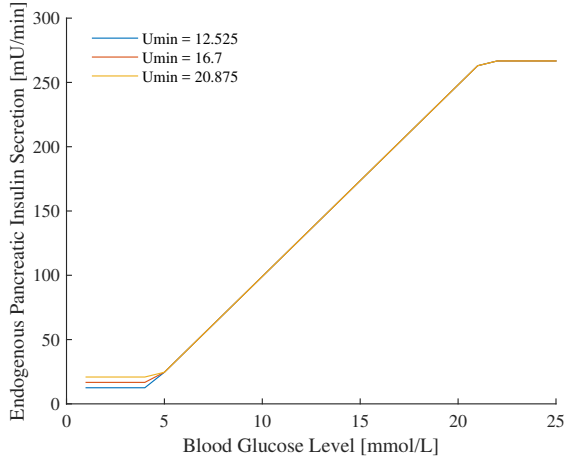
The impact of k_3 on BG evolution is quite similar to the one of k_2 . An increase of the interstitium insulin transport rate into plasma ($k_3 = 0.1095 \text{ min}^{-1}$) leads to faster insulin action on blood glucose and thus a faster decrease of BG. In contrast, a local vertical displacement of BG is observed for a decrease of k_3 . However, for the same deviation with respect to the mean, a diminution of k_3 appears to have a greater effect on BG evolution. Again, these changes only occur after the insulin injection. Overall, sensitivity is moderate.

▷ **Rate of loss from the local interstitium k_{di}**

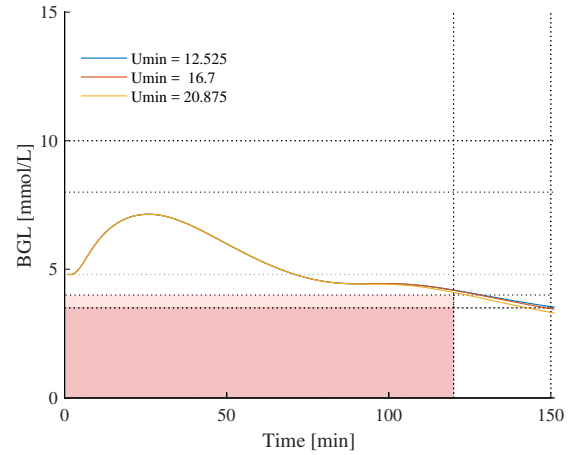
In the local interstitium, subcutaneously injected insulin is either degraded, or reaches the blood circulation. This degradation is characterised by the rate of loss from interstitium, k_{di} . However, this parameter does not influence BG evolution significantly because of its relatively very low value compared to the injected insulin transport rate from the local interstitium into plasma, k_3 . Most of injected insulin reaches the plasma before being cleared in the local interstitium. Graphical BG evolution according to different values of k_{di} can be found in the Appendices.

▷ **Minimum endogenous pancreatic insulin secretion rate u_{min}**

According to Equation 3.4, endogenous pancreatic insulin secretion rate, u_{en} , is a function of its minimum rate, u_{min} . Figure 4.11a illustrates the shape of u_{en} according to different values of u_{min} (12.525, 16.7 and 20.875 $\text{mU} \cdot \text{min}^{-1}$). Figure 4.11b represent the impact of these changes on BGL evolution. All other parameters remain unchanged. There is virtually no change as BG is very rarely below 5.0 mmol/L in these tests, so the value of u_{min} is never active.



(a) Shape of u_{en} according to different values of the parameter u_{min} .



(b) BG evolution according to different values of the parameter u_{min} .

Figure 4.11 :

Influence of the parameter u_{min} on BG evolution and on shape of u_{en} , for for $S_I = 0.00108 L.(mU.min)^{-1}$.

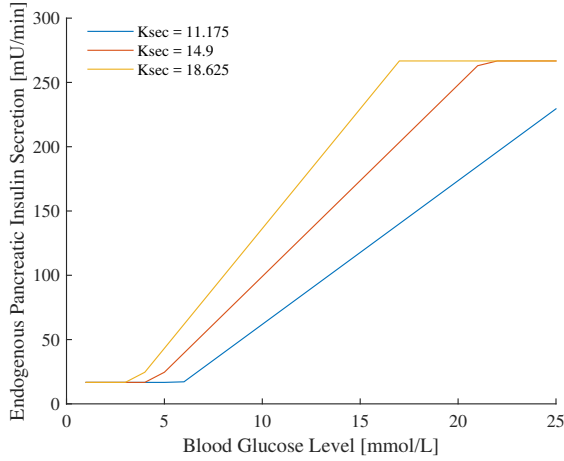
▷ **Maximum endogenous pancreatic insulin secretion rate u_{max}**

Endogenous pancreatic insulin secretion rate, u_{en} , also depends on its maximum rate, u_{max} (Equation 3.4). However, this parameter does not influence at all BG evolution. This maximum rate is only achieved for very high glucose concentrations (BG > 20.0 mmol/L), which are not encountered in this project. The shape of u_{en} according to different values of u_{max} , as well as influence of these variations on BG evolution, can be found in the Appendices.

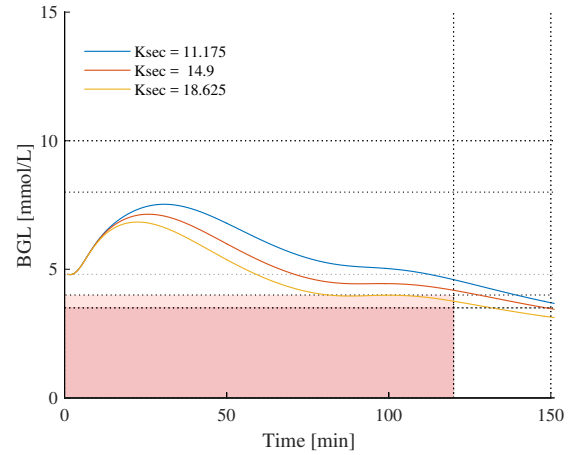
▷ **Glucose sensitivity of the endogenous pancreatic insulin secretion rate k_{sec}**

An important feature of the model used in this project is the glucose-dependent endogenous pancreatic insulin secretion rate. The parameter k_{sec} reflects this pancreatic glucose sensitivity. Figure 4.12a represents the shape of the secretion rate, u_{en} , according to different values of k_{sec} (11.1751, 14.9 and 18.625 (mU.L).(mmol.min)⁻¹). Figure 4.12b illustrates impact of this parameter on BG evolution. All other parameters remain unchanged.

First, the change of this pancreatic glucose sensitivity has an impact on the slope of u_{en} (Figure 4.12a). The larger this parameter, the larger the secretion of insulin for the same blood glucose concentration. Second, k_{sec} strongly impacts BG evolution (Figure 4.12b). If pancreatic glucose sensitivity is smaller ($k_{sec} = 11.1751$ (mU.L).(mmol.min)⁻¹), endogenous pancreatic insulin secretion rate is less affected by blood glucose concentration. Thus, endogenous insulin is less able to regulate BG, leading to a local upward shift of the BG curve ($k_{sec} = 14.9$ (mU.L).(mmol.min)⁻¹). For $k_{sec} = 18.625$ (mU.L).(mmol.min)⁻¹, the inverse situation applies. There is thus a high and clinically relevant sensitivity to this parameter.



(a) Shape of u_{en} according to different values of the parameter k_{sec} .



(b) BG evolution according to different values of the parameter k_{sec} .

Figure 4.12 :

Influence of the parameter k_{sec} on BG evolution and on shape of u_{en} , for $S_I = 0.00108 \text{ L} \cdot (\text{mU} \cdot \text{min})^{-1}$.

▷ **Endogenous pancreatic insulin secretion offset k_{off}**

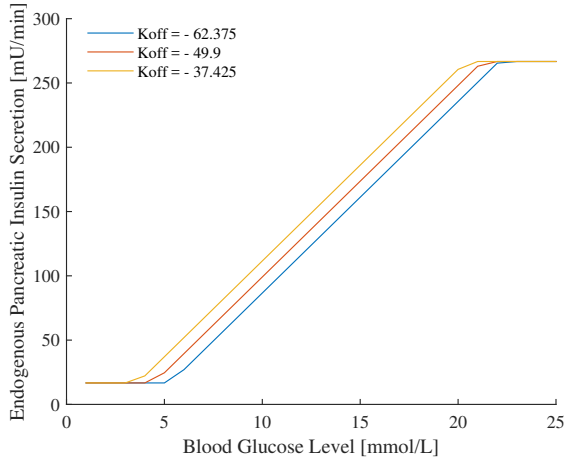
Endogenous pancreatic insulin secretion rate also depends on the parameter k_{off} (Equation 3.4). It is the endogenous pancreatic insulin secretion offset. The influence of this parameter is analysed. Figure 4.13a represents the shape of endogenous pancreatic insulin secretion rate according to different values of k_{off} (- 62.375, - 49.9 and - 37.425 $\text{mU} \cdot \text{min}^{-1}$). Figure 4.13b illustrates the influence of k_{off} on BGL evolution. All other parameters remain unchanged.

This offset horizontally displaces the curve of u_{en} (Figure 4.13a). If endogenous pancreatic insulin secretion rate was not defined by this kind of step function, k_{off} would be the Y-axis intersection of the middle sub-function (Equation 3.4). The shift of the curve is thus easily understood. This parameter influences BG evolution moderately. For the same blood glucose concentration, less insulin is produced for $k_{off} = - 62.375 \text{ mU} \cdot \text{min}^{-1}$, leading to an upward displacement of the BG in this case. The inverse situation is observed for $k_{off} = - 37.475 \text{ mU} \cdot \text{min}^{-1}$.

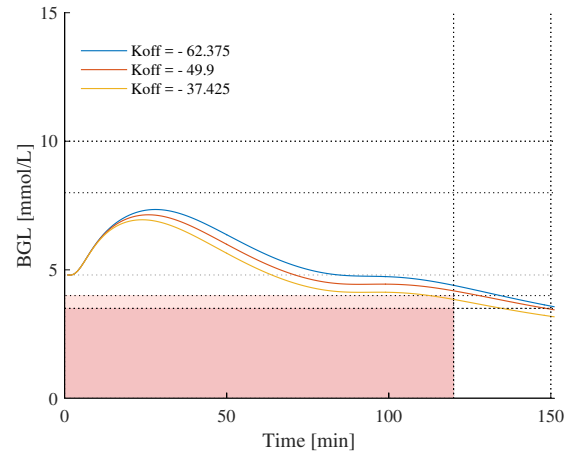
4.4 Summary

In this chapter, a single parameter sensitivity analysis has been performed to assess the strength of the model used in this project and determine which parameters are the most crucial to accuracy in prediction. Equally, inter-subject variability in sensitive parameters is likely to be unavoidable. Thus, understanding the impact of this variability will allow better understanding of the resulting test's variability and potential errors.

First, parameters of interest have been identified. Second, their physiological variation ranges have been calculated. Then, model has been simulated *in silico* for the lower, upper and mean value of the parameters of interest. BG evolutions have been plotted and analysed. The parameters with the biggest influence are S_I , k_{min} , c , f , k_2 , k_3 , k_{sec} and k_{off} . No non-physiological behaviours were observed and changes of parameter always lead to a coherent modification of BG evolution. This analysis allows assessment of the overall reliability of SC-OG-ICING-2 model. However, multiple parameter influence has to be investigated to confirm the potential range of the model and thus its potential inter-subject and intra-subject variability.



(a) Shape of u_{en} according to different values of the parameter k_{off} .



(b) BG evolution according to different values of the parameter k_{off} .

Figure 4.13 :

Influence of the parameter k_{off} on BG evolution and on shape of u_{en} , for $S_I = 0.00108 \text{ L} \cdot (\text{mU} \cdot \text{min})^{-1}$.

Chapter 5

Multiple parameter sensitivity analysis

The single parameter sensitivity analysis of Chapter 4 assessed the physiological relevance of the model and identified the most sensitive parameters for inter-patient and intra-patient variability. However, this analysis only considered individual parameter changes. Multiple parameter sensitivity analysis provides a full range of realistic possibilities across these critical parameters.

For this analysis, several parameters are changed simultaneously in a Monte Carlo analysis. Investigation of families of BG enables detection of any model and/or protocol weakness, as well as displaying the possible range of the model and test to ensure safety by design. Indeed, by assuming that each random combination of parameters represents the physiological features of an individual, the inter-patient variability of the model can be assessed. Finally, comparing model-based BG evolutions with an already certified test assessing diabetic status of an individual, the validity of the model can also be reinforced.

5.1 Parameters of interest

Given the single parameter sensitivity analysis of Chapter 4, some parameters have more impacts on BG evolution than others. Specifically, S_I , k_{min} , c , f , k_2 , k_3 , k_{sec} and k_{off} strongly influence this evolution. However, not all of these parameters are used in the multiple parameter sensitivity analysis.

Because of the importance of insulin sensitivity, this parameter is not randomly fixed. Each Monte Carlo simulation case is considered for the same five specific values of insulin sensitivity (S_I) equals to 0.00025, 0.0005, 0.00083, 0.00108 and 0.0018 L.(mU.min)⁻¹. These five values provide a fairly good overview of this parameter from diabetes to very high. Normal insulin sensitivity is fixed at $S_I = 0.00108$ L.(mU.min)⁻¹, as in Chapter 4.

If two influential parameters follow each other in the kinetic chain (see Figure 3.1) or if they are involved in the same physiological phenomenon, only one is considered, as they will trade off and thus only one is necessary. More specifically, because their values are randomly chosen in this multiple parameter sensitivity analysis, impact

of these parameters on BG evolution could be suppressed if two inverse random values are picked up for representing two successive actions. From a physiological point of view, it would be unlikely to have two successive kinetics with totally inverse trend. The more influential parameter between these pairs is chosen based in the analysis in Chapter 4.

The two parameters k_{min} and c are both involved in the gastric emptying rate, k_{empt} . Graphically, the minimum rate, k_{min} , is more influential and is thus chosen for this multiple parameter sensitivity analysis. Next, k_2 and k_3 follow each other in the insulin kinetic chain, and the local interstitium insulin transport rate into plasma, k_3 , is selected. Regarding k_{sec} and k_{off} , they are both linked to endogenous pancreatic insulin secretion rate, u_{en} , and the glucose sensitivity, k_{sec} , is chosen. This decision is graphical, but also logical, as this parameter expresses the glucose-dependency of u_{en} , which is of paramount importance.

The intestinal absorption fraction, f , is also considered. It is not involved in a specific phenomenon or coupled with any other parameters. Moreover, the value of this parameter does not originate from any theses or articles, but is more a coherent and implicit choice, based on its impacts.

In summary, each specific situation is individually analysed for 5 values of S_I and for random values in a physiological range for :

- k_{min}
- f
- k_3
- k_{sec}

5.2 Methodology

To assess the simultaneous influence of several parameters on BG evolution, random combinations of these four parameters are generated. To generate random values, the MATLAB function `randn` is used. The probabilistic distribution of these values is Gaussian. Figures 5.1a, 5.1b, 5.1c and 5.1d are histograms of the values of f , k_{min} , k_3 and k_{sec} , when ($N =$) 10000 values of each are randomly generated for a Monte Carlo analysis from within their physiological range (Table 4.1).

These random combinations of parameters serve two specific goals in a Monte Carlo analysis. First, consolidation of model validity. Second, verification of protocol safety.

Concerning consolidation of the model validity, two specific situations are considered :

- **NORMAL SITUATION** : In the model, glucose dose is maintained at 35 g and 2 U of subcutaneous insulin are injected after 15 minutes. Several parameters are randomly changed at the same time. With several combinations of parameters, a lot of BG evolutions can be generated. Model reliability can be checked. Inter-patient variability and range of the model can also be assessed.
- **COMPARISON WITH AN OGTT** : The protocol for an Oral Glucose Tolerance Test (OGTT) is applied to the model of this study. Glucose dose is fixed to 75 g and there is no insulin injection. If generated BG evolutions are in accordance with expected OGTT results, at each S_I value, model validity is reinforced by reproducing this known case.

Regarding verification of the protocol safety, two other situations are analysed :

- **INFLUENCE OF THE GLUCOSE DOSE** : If hypoglycaemic situations are detected during the simulation of the normal situation, adapting glucose dose reduces these potential risks. However, according to the considered insulin sensitivity, this increase can also lead to greater hyperglycaemia at lower S_I values.
- **INFLUENCE OF THE INSULIN BOLUS** : Subcutaneous injection of insulin is performed with a Needle Free Injection Device (NFID). Fixing the insulin bolus to 0 U, allows examination of the consequences of a malfunction of this instrument.

Each situation is simulated for $N = 10000$ random combinations and at each of the five S_I values. So many combinations allow to describe all possible physiological scenarios and thus reflect all possible cases that could be encountered during the trial. Hence, the resulting 90-95 % will robustly capture all possibilities.

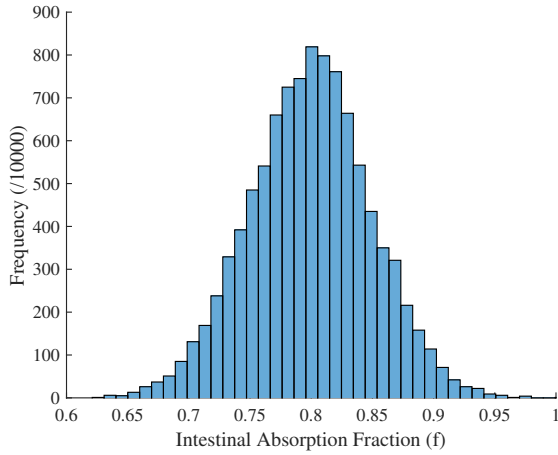
5.3 Results and Discussion

5.3.1 Consolidation of model validity

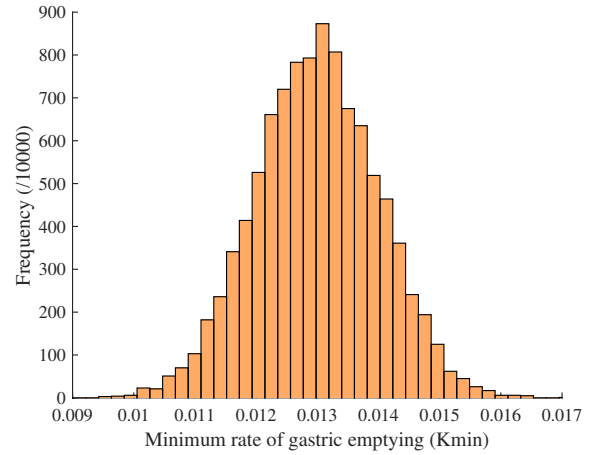
▷ Normal case

Figure 5.2 represents 10000 BG evolutions for each specific value of insulin sensitivity, for a glucose dose of 35 g and 2 U of subcutaneous injected insulin. Respectively, Figure 5.2a stands for $S_I = 0.00025 \text{ L.}(mU.min)^{-1}$, Figure 5.2b for $S_I = 0.0005 \text{ L.}(mU.min)^{-1}$, Figure 5.2c for $S_I = 0.00083 \text{ L.}(mU.min)^{-1}$, Figure 5.2d for $S_I = 0.00108 \text{ L.}(mU.min)^{-1}$ and Figure 5.2e for $S_I = 0.0018 \text{ L.}(mU.min)^{-1}$.

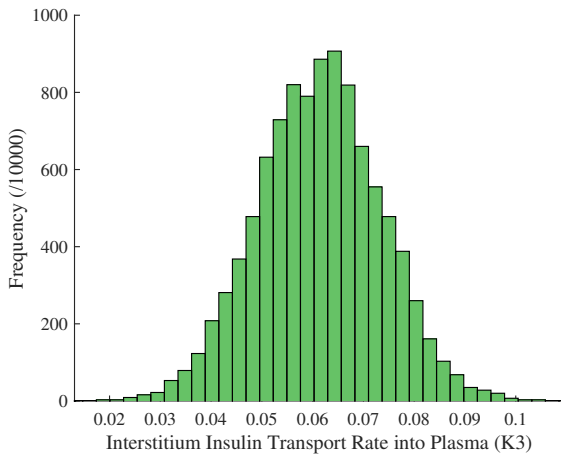
For each S_I value, the solid green line is the BG evolution with the mean parameter values (Table 4.1). Solid yellow lines are the worst upper cases. For each particular insulin sensitivity, it represents the BG evolution with the highest glucose value, corresponding to a specific random combination of parameters. In contrast, solid red lines indicate the worst lower cases which have the earliest hypoglycaemia. They are not necessarily the ones with the



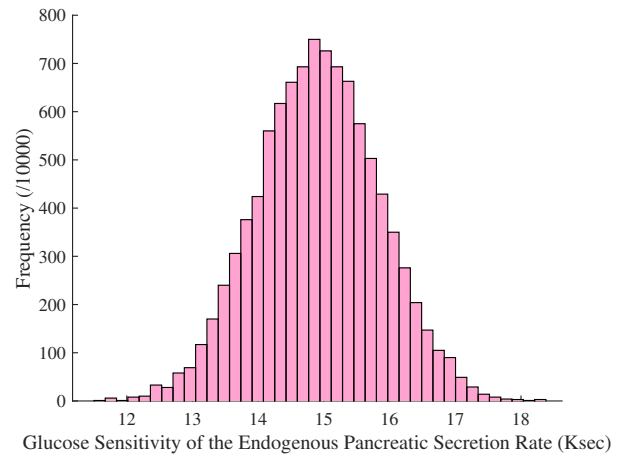
(a) Histogram of f .



(b) Histogram of k_{min} .



(c) Histogram of k_3 .



(d) Histogram of k_{sec} .

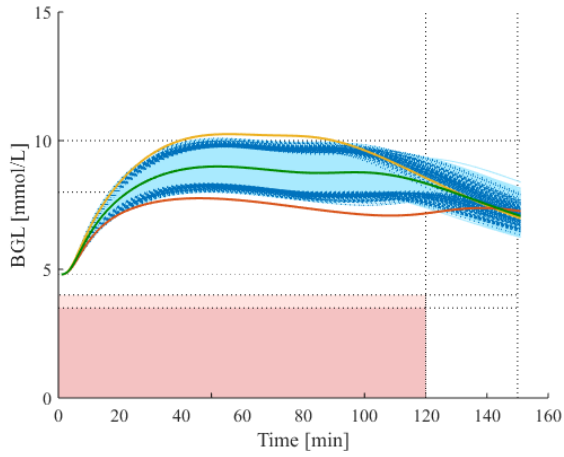
Figure 5.1 :

Histograms of the parameters of interest.

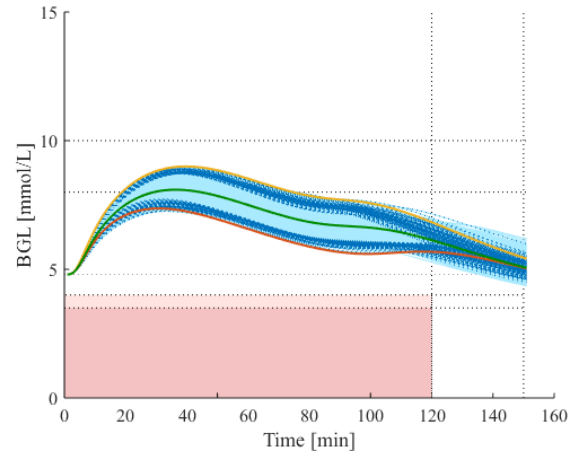
lowest glucose values. Solid light blue lines stand for all 10000 generated BG evolutions. Dashed dark blue lines depict the 100 upper and lower BG evolutions (of 10000). Only the first 120 minutes are considered and analysed.

When insulin sensitivity is very high ($S_I = \mathbf{0.0018} \text{ L} \cdot (\text{mU} \cdot \text{min})^{-1}$), all 10000 BG evolutions reach mild, and thus light, hypoglycaemic situations before 120 minutes (Figure 5.2e). This might or light hypoglycaemia is possible for very insulin-sensitive patients [9, 44, 10]. Changes of protocol could be interesting for such individuals, if they could be identified ahead of time.

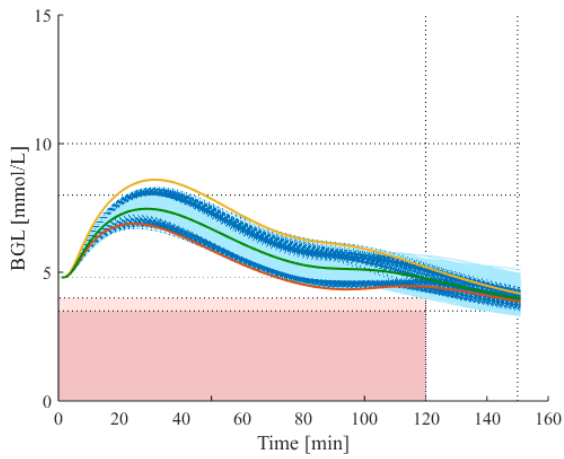
For normal insulin sensitivity ($S_I = \mathbf{0.00108} \text{ L} \cdot (\text{mU} \cdot \text{min})^{-1}$), 2000 (of 10000) curves cross the light hypoglycaemia limit at 4.0 mmol/L (Figure 5.2b). No BG evolution moves beyond the limit of mild hypoglycaemia at 3.5 mmol/L. Equally, only 3 curves are above the first hyperglycaemic threshold (8.0 mmol/L).



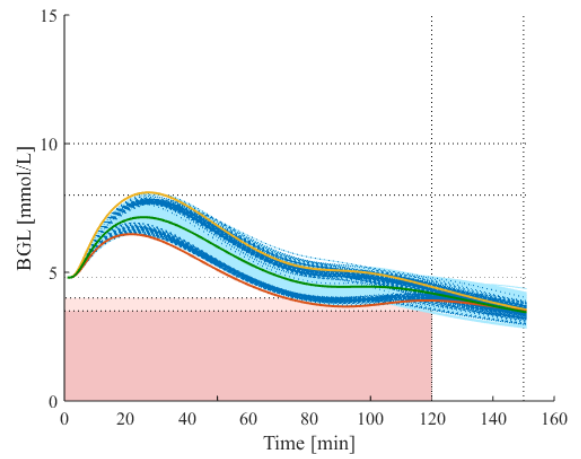
(a) $S_I = 0.00025 \text{ L.}(mU.min)^{-1}$.



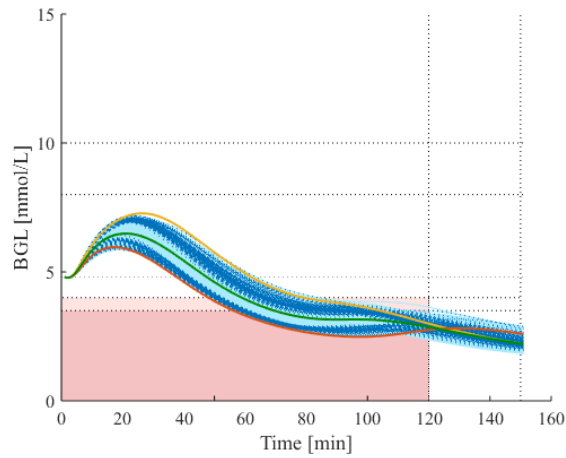
(b) $S_I = 0.0005 \text{ L.}(mU.min)^{-1}$.



(c) $S_I = 0.00083 \text{ L.}(mU.min)^{-1}$.



(d) $S_I = 0.00108 \text{ L.}(mU.min)^{-1}$.



(e) $S_I = 0.0018 \text{ L.}(mU.min)^{-1}$.

Figure 5.2 :

10000 random BG evolutions according to different values of insulin sensitivity, for $D = 35 \text{ g}$ and $I_{bolus} = 2 \text{ U}$
 (green curve : mean parameter BG, yellow curve ; upper BG, red curve : lower BG).

For $S_I = \mathbf{0.00083} \text{ L} \cdot (\text{mU} \cdot \text{min})^{-1}$, no hypoglycaemia happens before 120 minutes. However, about 100 (of 10000) curves move beyond the 8.0 mmol/L limit (Figure 5.2c).

A bit more than 6000 (of 10000) BG evolutions reach the first hyperglycaemic threshold for $S_I = \mathbf{0.0005} \text{ L} \cdot (\text{mU} \cdot \text{min})^{-1}$ (Figure 5.2d). Glucose concentrations slowly decrease and take time to stabilise to a normal glycaemia. This correctly characterises IGT individuals, which are described by such a S_I level.

For $S_I = \mathbf{0.00025} \text{ L} \cdot (\text{mU} \cdot \text{min})^{-1}$, all BG evolutions, except 1, reach the 8.0 mmol/L limit. Moreover, 7 (of 10000) of these curves move beyond the second threshold (10.0 mmol/L). These hyperglycaemic situations remain for almost all of the simulation time and really struggle to correct to normal glycaemia. Hence, diabetic status of this low S_I is well represented by these conclusions.

Table 5.1 summarises all these results. For each specific insulin sensitivity, the number of curves reaching hypoglycaemic and/or hyperglycaemic thresholds are gathered. Figures 5.3a, 5.3b and 5.3c represent respectively the worst upper cases, normal mean cases and worst lower cases of each particular insulin sensitivity.

Table 5.1 :
Proportion of BGL evolutions reaching hypoglycaemic and/or hyperglycaemic thresholds.

Insulin Sensitivity [L.(mU.min) ⁻¹]	Hypoglycaemia		Hyperglycemia	
	≤ 3.5 mmol/L	≤ 4 mmol/L	≥ 8 mmol/L	≥ 10 mmol/L
0.00025	0 %	0 %	99.99 %	0.07 %
0.0005	0 %	0 %	63.9 %	0 %
0.00083	0 %	0 %	1.05 %	0 %
0.00108	0 %	20 %	0.03 %	0 %
0.0018	100 %	100 %	0 %	0 %

All of these simulated BG evolutions enable to provide an overview of the model range. If each BG evolution is linked to the profile of an individual, it also assesses the inter-patient variability. This model range, or inter-patient variability, is quite compressed and do not provide non-physiological situations.

However, a physiological inconsistency can be observed. Indeed, Figures 5.2c, 5.2d and 5.2e indicate no stabilisation of the glycaemia at the end of the simulation but a continuous decrease. Physiologically, BG does not normally continuously decline in this way. Normally, Endogenous Glucose Production (EGP) increases for low BG and it stabilises glycaemia. In this model, EGP is fixed and does not vary according to glucose concentration,

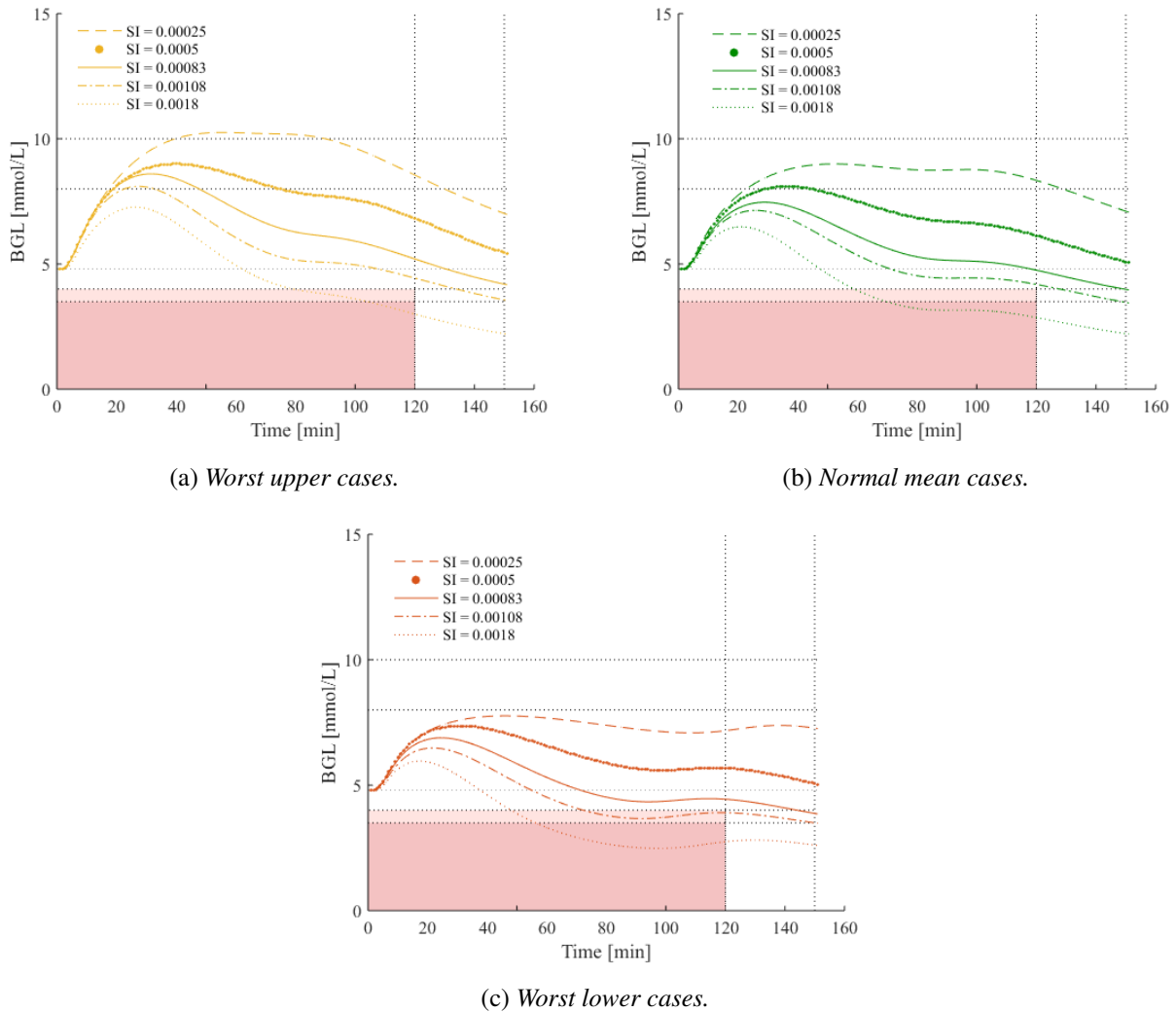


Figure 5.3 :

Worst upper cases, normal fixed cases and worst lower cases for each insulin sensitivity, for $D = 35$ g and $I_{bolus} = 2$ U.

as this response is highly variable, leading to this behaviour. However, it is only observable at the end of the simulations, after the real duration of the clinical trial, after which the participants are given a snack. Thus, because the simulation is only analysed to 120 minutes, it is not a problem in this research.

A small other inconsistency regarding the fasting glucose level can be noticed. In the model, it is fixed to 4.8 mmol/L. However, diabetic individuals have a more elevated basal glucose concentration. In the multiple parameter sensitivity analysis, each time an insulin sensitivity of $0.00025 \text{ L} \cdot (\text{mU} \cdot \text{min})^{-1}$ is considered, it represents a diabetic state. However, the fasting glucose level is not changed. Fasting blood glucose levels should be increased in simulating T2D cases. This is not really dramatic for this study because an increase of this value would lead to an upward shift of BG evolutions, and thus an increase of hyperglycaemic situations. Hypoglycaemia, and not hyperglycaemia, is often highlighted in this study.

▷ Comparison with an OGTT

The reference test for diagnosing diabetes and Impaired Glucose Tolerance (IGT) is the 75 g 2-hour Oral Glucose Tolerance Test (OGTT) (see Section 2.6.1). Although it is only able to assess IGT in its latter stages, it remains the gold standard to diagnose diabetes. To check the reliability of the assay and the model studied in this project, the protocol is adapted to match the OGTT. Glucose dose is changed to 75 g and no insulin is injected. A comparison between the virtually generated results and the OGTT thresholds is performed.

Figure 5.4 represent 10000 BG evolutions for each specific value of insulin sensitivity, for a glucose dose of 75 g and for no injected insulin. Specifically, Figure 5.4a stands for $S_I = 0.00025 \text{ L} \cdot (\text{mU} \cdot \text{min})^{-1}$, Figure 5.4b for $S_I = 0.0005 \text{ L} \cdot (\text{mU} \cdot \text{min})^{-1}$, Figure 5.4c for $S_I = 0.00083 \text{ L} \cdot (\text{mU} \cdot \text{min})^{-1}$, Figure 5.4d for $S_I = 0.00108 \text{ L} \cdot (\text{mU} \cdot \text{min})^{-1}$ and Figure 5.4e for $S_I = 0.0018 \text{ L} \cdot (\text{mU} \cdot \text{min})^{-1}$. Gray dashed lines represent OGTT diagnostic thresholds, specifically 7.8 mmol/L and 11.0 mmol/L (see Section 2.6.1).

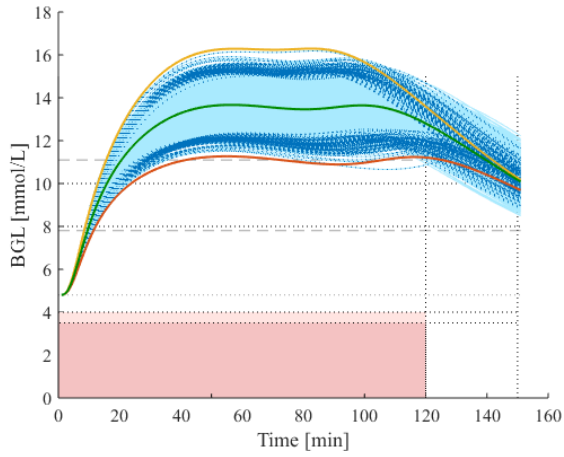
For $S_I = \mathbf{0.00025} \text{ L} \cdot (\text{mU} \cdot \text{min})^{-1}$ and thus for a diabetic state, all BG evolutions are above 11.0 mmol/L at 120 minutes (Figure 5.4a). This result matches OGTT diagnostic thresholds. Hence, the model accurately captures this diagnosis in all Monte Carlo cases.

For a simulation time of 120 minutes and for $S_I = \mathbf{0.0005} \text{ L} \cdot (\text{mU} \cdot \text{min})^{-1}$, all BG evolutions are situated between 7.8 and 11.0 mmol/L (Figure 5.4b). Such an insulin sensitivity reflects IGT diagnostically. It is thus logical that all curves are in the IGT range of the OGTT.

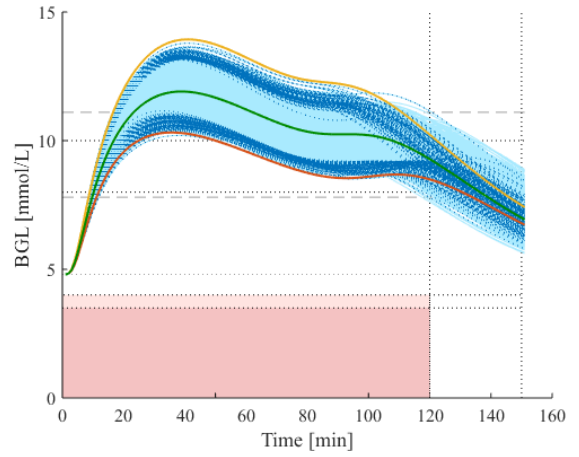
An insulin sensitivity of $\mathbf{0.00083} \text{ L} \cdot (\text{mU} \cdot \text{min})^{-1}$ reflects the early stages of pre-diabetes or lower normal. Figure 5.4c shows some BGL evolutions move above 7.8 mmol/L at 120 minutes, where the others are below this threshold. Moreover, the green normal mean curve is at the level of this limit. These results confirm and match the low accuracy of the OGTT for IGT and, especially, for early stages of IGT. Thus, such individuals are after diagnosed as normal because other of its physiological features enables a sufficient decrease of his glycaemia. One can talk of false negative in this situation.

For $S_I = \mathbf{0.00108} \text{ L} \cdot (\text{mU} \cdot \text{min})^{-1}$, almost all BG evolutions are below 7.8 mmol/L at 120 minutes and, according to OGTT diagnostic thresholds, are thus considered normal. This result is logical because this insulin sensitivity is used to represent healthy individuals. However, about 10 of 10000 (1 in 1000) curves move beyond the limit. One can talk in this case about false positive.

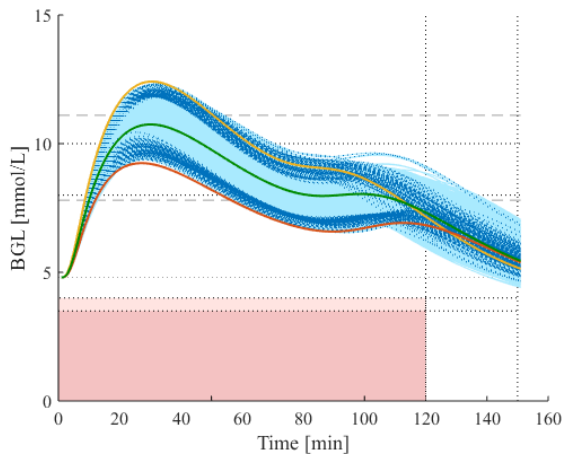
Finally, as expected, after 120 minutes, all BG evolutions generated for an insulin sensitivity of $\mathbf{0.0018} \text{ L} \cdot (\text{mU} \cdot \text{min})^{-1}$ are situated below the 7.8 mmol/L limit and are thus diagnosed as normal.



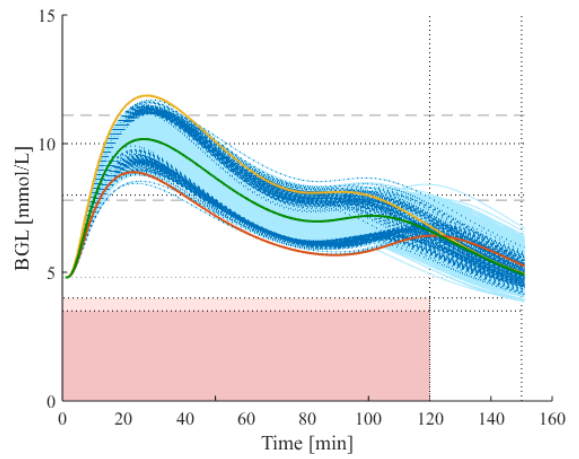
(a) $S_I = 0.00025 \text{ L.}(mU.min)^{-1}$.



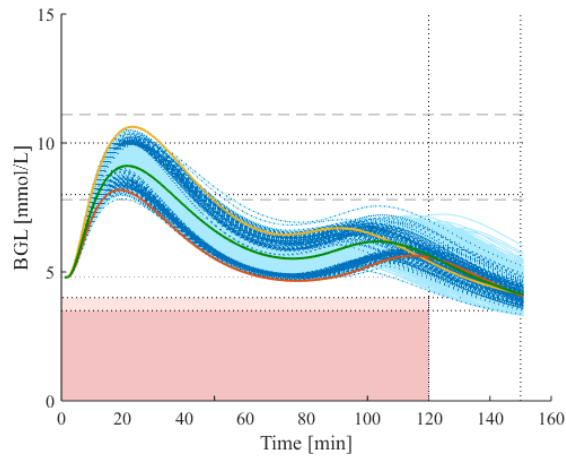
(b) $S_I = 0.0005 \text{ L.}(mU.min)^{-1}$.



(c) $S_I = 0.00083 \text{ L.}(mU.min)^{-1}$.



(d) $S_I = 0.00108 \text{ L.}(mU.min)^{-1}$.



(e) $S_I = 0.0018 \text{ L.}(mU.min)^{-1}$.

Figure 5.4 :

10000 random BG evolutions according to different values of insulin sensitivity, for $D = 75 \text{ g}$ and $I_{bolus} = 0 \text{ U}$
 (green curve : mean parameter BG, yellow curve ; upper BG, red curve : lower BG).

By changing the protocol to match with the one of a 75 g 2-hour OGTT, BG evolutions, the model outcomes coincide with the physiological and diagnostic expectations of this test. This result reinforces the validity of the model.

5.3.2 Verification of protocol safety

▷ Influence of the glucose dose

In this part, the influence of glucose dose is studied. Figure 5.2d shows light or mild hypoglycaemia occurs in every case for very high-insulin sensitive individuals ($S_I = 0.0018 \text{ L} \cdot (\text{mU} \cdot \text{min})^{-1}$). Augmented glucose quantity during the clinical trial seems to be the natural solution to address this problem. However, even if insulin sensitivity is fixed for this multiple parameter sensitivity analysis, it is actually unknown during the clinical trial. Athletic and healthy people may have this kind of high insulin sensitivity [9, 44, 10]. Thus, based on an external opinion, increased glucose quantity could be given to these individuals. However, because of the subjective part of this decision, participants could have a smaller insulin sensitivity than expected. Thus, the impact of such an increase on participants with a normal insulin sensitivity ($S_I = 0.00108 \text{ L} \cdot (\text{mU} \cdot \text{min})^{-1}$) is also analysed to quantify the risk of hyperglycemia.

Glucose dose = 45 g

Figures 5.5a and 5.5b represent BG evolutions with a glucose dose changed to 45 g, respectively for $S_I = 0.0018 \text{ L} \cdot (\text{mU} \cdot \text{min})^{-1}$ and $S_I = 0.00108 \text{ L} \cdot (\text{mU} \cdot \text{min})^{-1}$. This increase of glucose dose leads to an upward shift of all BG evolutions, for both insulin sensitivities. Compared with a glucose dose of 35 g (Figure 5.2e), only about half number of the curves reach the mild hypoglycaemic limit for an insulin sensitivity at $0.0018 \text{ L} \cdot (\text{mU} \cdot \text{min})^{-1}$ (Figure 5.5a). However, this glucose dose is not sufficient to significantly decrease the hypoglycaemic situations. In contrast, 3 (of 10000) BG evolutions move beyond the first hyperglycaemic threshold. For $S_I = 0.00108 \text{ L} \cdot (\text{mU} \cdot \text{min})^{-1}$, no or limited hypoglycaemia is observed (Figure 5.5b), but more hyperglycaemic cases occur.

Glucose dose = 55 g

Figures 5.6a and 5.6b represent BG evolutions with a glucose dose changed to 55 g, respectively for $S_I = 0.0018 \text{ L} \cdot (\text{mU} \cdot \text{min})^{-1}$ and $S_I = 0.00108 \text{ L} \cdot (\text{mU} \cdot \text{min})^{-1}$. For a glucose dose of 55 g and $S_I = 0.0018 \text{ L} \cdot (\text{mU} \cdot \text{min})^{-1}$, only 2800 (of 10000) BG evolutions are situated below the mild hypoglycaemic limit, but all still reach 4.0 mmol/L (Figure 5.6a). This glucose dose is thus not sufficient to significantly decrease the hypoglycaemia encountered during the trial. In contrast, 2500 BG evolutions move beyond 8.0 mmol/L. For $S_I = 0.00108 \text{ L} \cdot (\text{mU} \cdot \text{min})^{-1}$, no hypoglycaemia is observed, where almost all curves reach the hyperglycaemic lower limit of 8.0 mmol/L (Figure 5.6b).

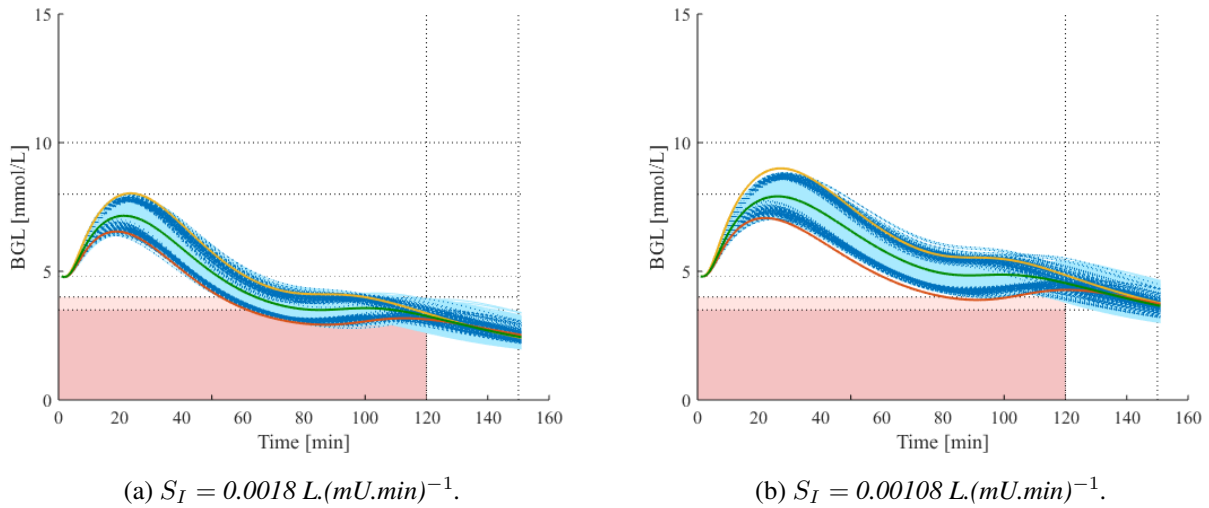


Figure 5.5 :

10000 random BG evolutions according to different values of insulin sensitivity, for $D = 45 \text{ g}$ and $I_{bolus} = 2 \text{ U}$
 (green curve : mean parameter BG, yellow curve ; upper BG, red curve : lower BG).

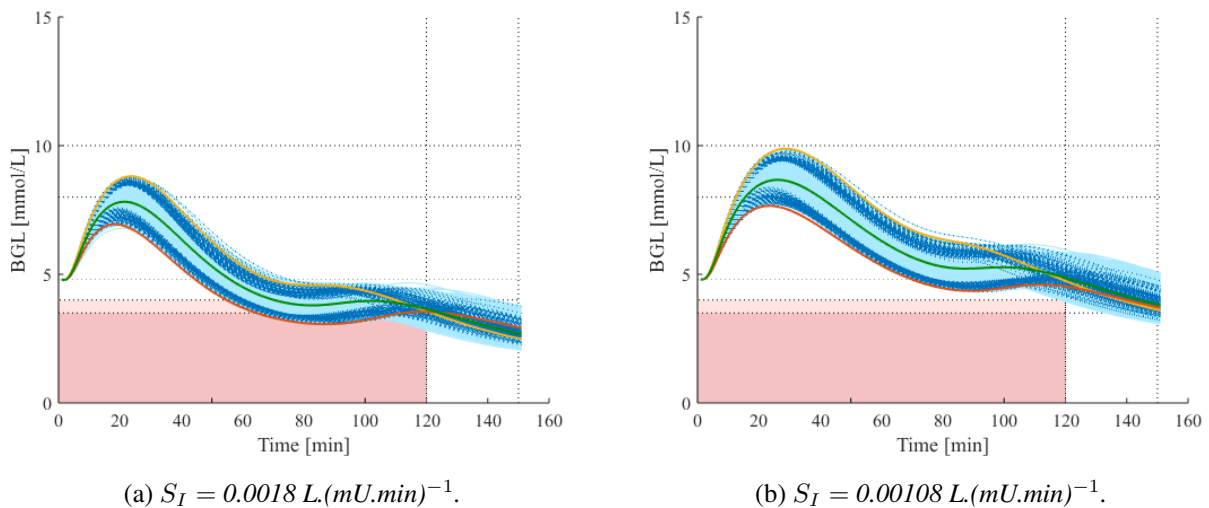


Figure 5.6 :

10000 random BG evolutions according to different values of insulin sensitivity, for $D = 55 \text{ g}$ and $I_{bolus} = 2 \text{ U}$
 (green curve : mean parameter BG, yellow curve ; upper BG, red curve : lower BG).

Glucose dose = 65 g

Figures 5.7a and 5.7b represent BG evolutions with a glucose dose changed to 65 g, respectively for $S_I = 0.0018 \text{ L.}(mU.min)^{-1}$ and $S_I = 0.00108 \text{ L.}(mU.min)^{-1}$. Regarding $S_I = 0.0018 \text{ L.}(mU.min)^{-1}$, the mild hypoglycaemic limit at 3.5 mmol/L is only crossed by about 300 (of 10000) BG evolutions (Figure 5.7a). In contrast, 7100 still cross 4.0 mmol/L. Almost all curves reach the hyperglycaemic threshold of 8.0 mmol/L. This glucose dose could be a good trade-off for potential high insulin-sensitive individuals, if only mild hypoglycaemia is to be avoided. Regarding the effect of this increased dose in participants with normal insulin sensitivity ($S_I = 0.00108 \text{ L.}(mU.min)^{-1}$),

no hypoglycaemia is observed, but all BG evolutions reach hyperglycaemia over 8.0 mmol/L. Some even pass 10.0 mmol/L (Figure 5.7b).

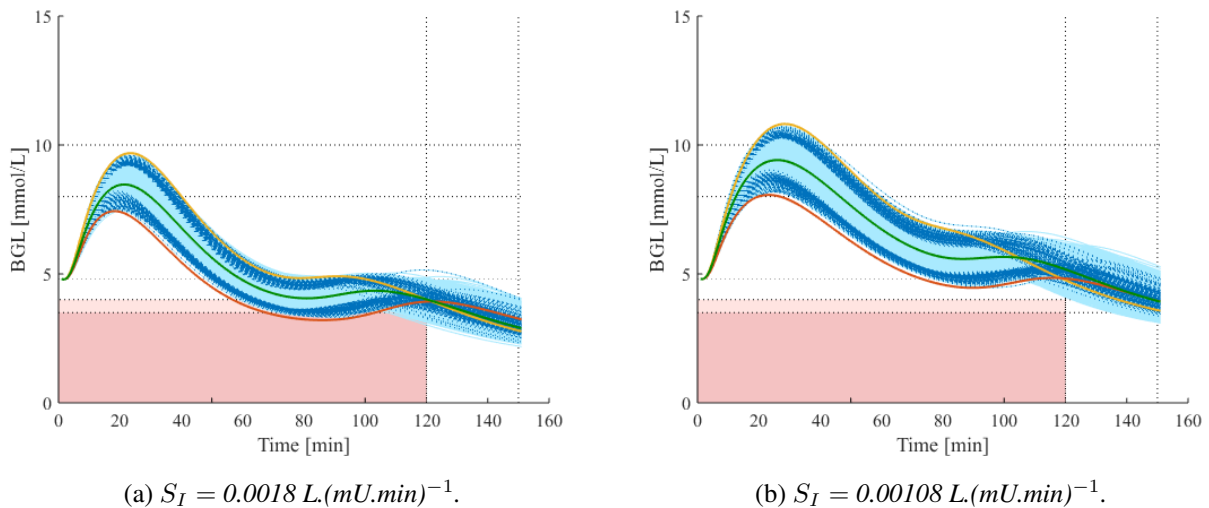


Figure 5.7 :

10000 random BG evolutions according to different values of insulin sensitivity, for $D = 65 \text{ g}$ and $I_{bolus} = 2 \text{ U}$
 (green curve : mean parameter BG, yellow curve ; upper BG, red curve : lower BG).

Glucose dose = 75 g

Figures 5.8a and 5.8b represent BG evolutions with a glucose dose changed to 75 g, respectively for $S_I = 0.0018 \text{ L.}(mU.min)^{-1}$ and $S_I = 0.00108 \text{ L.}(mU.min)^{-1}$. This glucose dose reduces BG evolutions crossing light hypoglycaemia to 2000 (of 10000) for $S_I = 0.0018 \text{ L.}(mU.min)^{-1}$. Only 20 cross 3.5 mmol/L (Figure 5.8a). This glucose quantity could be a good trade-off for potential high insulin-sensitive individuals and if light and mild hypoglycaemia is to be avoided. However, almost all curves reach 8.0 mmol/L and 50 severe hyperglycaemia (> 10.0 mmol/L) are observed. Regarding $S_I = 0.00108 \text{ L.}(mU.min)^{-1}$, more than 6000 curves move beyond 10.0 mmol/L (Figure 5.8b).

Table 5.2 summarises all these results. For $S_I = 0.0018 \text{ L.}(mU.min)^{-1}$ and for $S_I = 0.00108 \text{ L.}(mU.min)^{-1}$, it shows the number of curves reaching hypoglycaemic and/or hyperglycaemic thresholds are gathered. It thus quantifies the trade offs seen with glucose dose size.

▷ Influence of the insulin bolus

During the clinical trial, subcutaneous insulin injection is performed with a needle free injection device. This part examines the consequences of a malfunction of this instrument. The insulin bolus is thus changed to 0 U and glucose bolus remains fixed to 35 g.

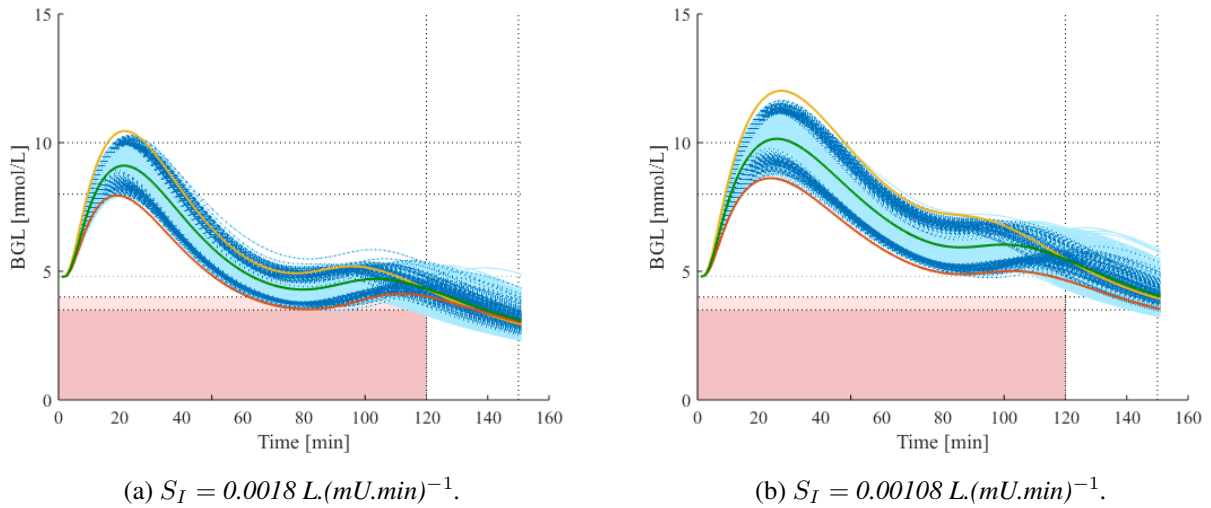


Figure 5.8 :

Change of glucose dose to 75 g for normal ($S_I = 0.0018 \text{ L} \cdot (\text{mU} \cdot \text{min})^{-1}$) and high ($S_I = 0.00108 \text{ L} \cdot (\text{mU} \cdot \text{min})^{-1}$) insulin sensitivities

(green curve : mean parameter BG, yellow curve ; upper BG, red curve : lower BG).

Table 5.2 :

Proportion of hypoglycaemic and hyperglycaemic situations for an increasing dose of glucose and for normal and high insulin sensitivities.

Glucose Dose [g]	Insulin Sensitivity [L.(mU.min) ⁻¹]	Hypoglycaemia		Hyperglycaemia	
		≤ 3.5	≤ 4	≥ 8	≥ 10
45	0.0018	50 %	100 %	0.02 %	0 %
45	0.00108	0 %	0.5 %	37.5 %	0 %
55	0.0018	28 %	98.9 %	25 %	0 %
55	0.00108	0 %	0.02 %	98.7 %	0 %
65	0.0018	3 %	71 %	94 %	0 %
65	0.00108	0 %	0 %	100 %	5.7 %
75	0.0018	2 %	20 %	99.9	0.5 %
75	0.00108	0 %	0 %	100 %	64.5 %

Figure 5.9 represent 10000 BG evolutions for each specific value of insulin sensitivity, for a 35 g glucose dose and for no injected insulin. Specifically, Figure 5.9a stands for $S_I = 0.00025 \text{ L.}(mU.min)^{-1}$, Figure 5.9b for $S_I = 0.0005 \text{ L.}(mU.min)^{-1}$, Figure 5.9c for $S_I = 0.00083 \text{ L.}(mU.min)^{-1}$, Figure 5.9d for $S_I = 0.00108 \text{ L.}(mU.min)^{-1}$ and Figure 5.9e for $S_I = 0.0018 \text{ L.}(mU.min)^{-1}$.

If no insulin is injected, the high glycaemia, consecutive to the glucose dose, is only regulated by endogenous pancreatic insulin. Compared to Figure 5.2, BG evolutions for all specific insulin sensitivities are more elevated after a simulation time of 60 minutes. Hypoglycaemic situations are no longer observed.

For $S_I = \mathbf{0.00025} \text{ L.}(mU.min)^{-1}$, endogenous pancreatic insulin is not able to regulate glycaemia (Figure 5.9a). This insulin sensitivity is linked to diabetic individuals, so a failure of regulation of BG is thus expected. Compared to Figure 5.2a, for which $I_{bolus} = 2 \text{ U}$, BG evolutions have shifted upwards, as expected.

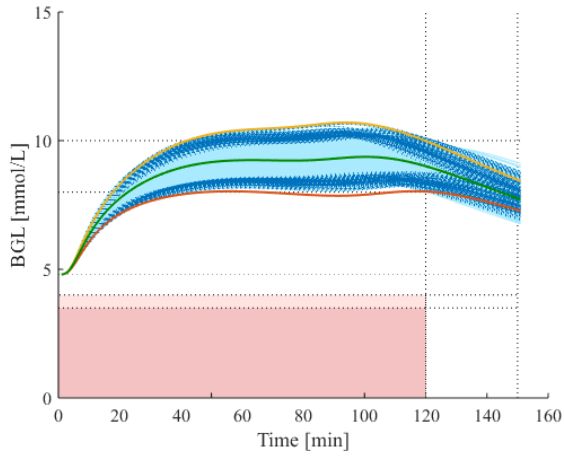
For $S_I = \mathbf{0.0005} \text{ L.}(mU.min)^{-1}$ and for $S_I = \mathbf{0.00083} \text{ L.}(mU.min)^{-1}$, almost half of BG evolutions remain hyperglycaemic(Figures 5.9b and 5.9c). Compared to Figures 5.2b and 5.2c, BG evolutions do not decrease a lot during the simulation time. Subcutaneous injected insulin is needed to obtain such a decrease for these subjects.

For $S_I = \mathbf{0.00108} \text{ L.}(mU.min)^{-1}$ and $S_I = \mathbf{0.0018} \text{ L.}(mU.min)^{-1}$, the conclusions are identical. The lack of subcutaneous injected insulin leads to a smaller decrease of BG evolutions (Figures 5.9d and 5.9e). Compared to Figures 5.2d and 5.2e, upward shifts of BG evolutions are observed. Moreover, no hypoglycaemia is identified. These insulin sensitivities are linked to healthy individuals, so it is thus expected they are able to regulate this glucose dose without added insulin.

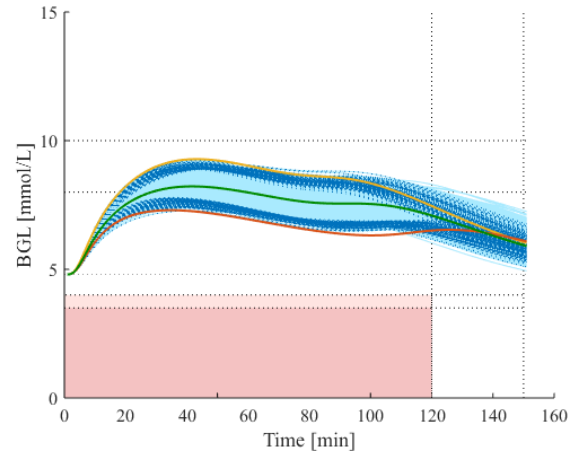
Because less hypoglycemia is observed without subcutaneous injected insulin, why is this protocol not used ? However, the principal objective of this clinical trial is to assess insulin sensitivity, particularly in or near IGT, IFG and pre-diabetes. This parameter precisely defined the influence of insulin on glucose uptake. Graphically, it can be represented by the slope of BG evolutions after the glucose peak. Without subcutaneous injected insulin, this slope does not really emerge for these more insulin resistant subjects and cannot be analysed as well or accurately.

To prove the reliability of the protocol, it would also be interesting to know how long a patient remains in hypoglycaemia before it is detected. During the clinical trial, blood samples are collected at specific times. They are directly assessed for blood glucose concentration using a glucometer. Thus, hypoglycaemia detection at specific monitoring points is possible during the trial. The model and these curves are thus used to determine the mean time between the beginning of hypoglycaemia and possible detection.

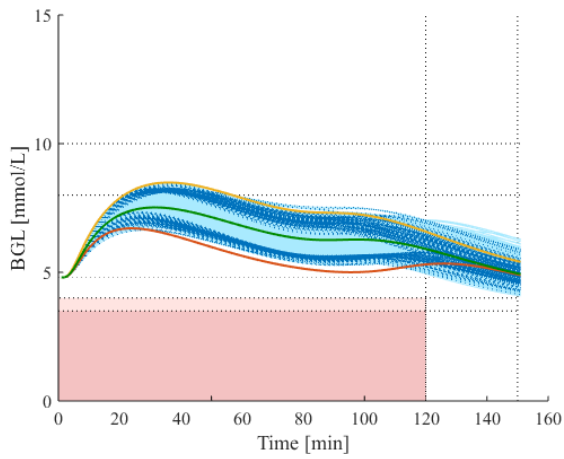
For calculating this mean time value, the worst case regarding hypoglycaemic situations is considered, specifically an insulin sensitivity of $0.0018 \text{ L.}(mU.min)^{-1}$. The protocol considered is the normal one, with a glucose



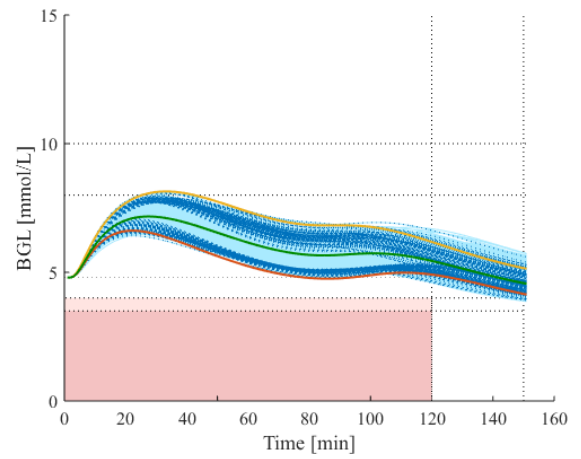
(a) $S_I = 0.00025 \text{ L.}(mU.min)^{-1}$.



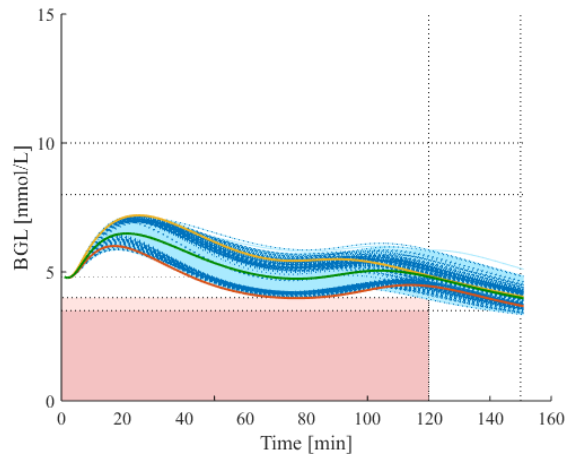
(b) $S_I = 0.0005 \text{ L.}(mU.min)^{-1}$.



(c) $S_I = 0.00083 \text{ L.}(mU.min)^{-1}$.



(d) $S_I = 0.00108 \text{ L.}(mU.min)^{-1}$.



(e) $S_I = 0.0018 \text{ L.}(mU.min)^{-1}$.

Figure 5.9 :

10000 random BG evolutions according to different values of insulin sensitivity, for $D = 35 \text{ g}$ and $I_{bolus} = 0 \text{ U}$
 (green curve : mean parameter BG, yellow curve ; upper BG, red curve : lower BG).

dose of 35 g and 2 U of subcutaneous injected insulin. The 100 lower BG evolutions in Figure 5.2e are presented in Figure 5.10. Green dashed lines are detection times, respectively at $t = 50, 60$ and 70 minutes. Light hypoglycaemia is achieved around 50 minutes. Important detection times are thus 50 and 60 minutes. The mean time before light hypoglycaemic detection is equal to 6.6 minutes. In contrast, mild hypoglycaemia is achieved around 60 minutes. Important detection times are thus 60 and 70 minutes. The mean time before mild hypoglycaemic detection is 3.5 minutes. These limits are both very short and pose no clinical risk.

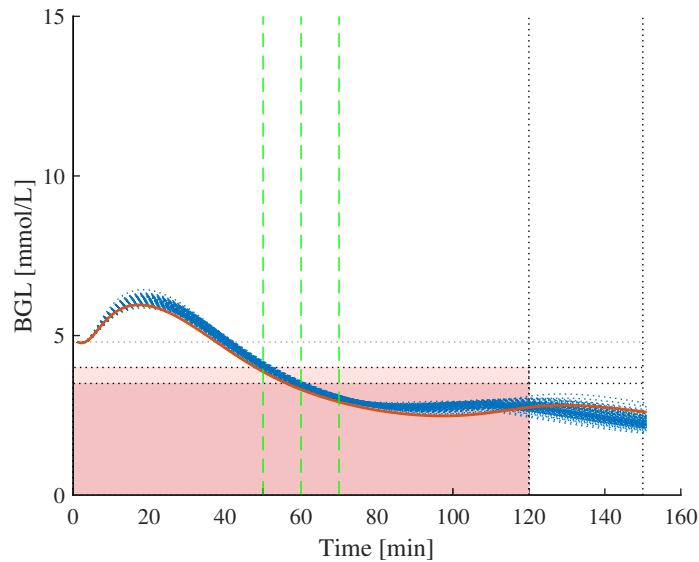


Figure 5.10 :

The 100 lower BG evolution for $S_I = 0.0018 L.(mU.min)^{-1}$, for $D = 35 g$ and $I_{bolus} = 2 U$ (red curve : lower BG).

5.4 Summary

In this chapter, a multiple parameter Monte Carlo sensitivity analysis has been conducted to consolidate the validation of the model, as well as to assess protocol safety. First, the range of the model and the inter-patient variability have been identified. They stand in physiological limitations and do not follow incoherent behaviours. Second, a comparison between model-based BG simulations and an OGTT has been conclusive, assessing the validity of this model. Then, hypoglycaemic situations and their occurrence have been observed. Solutions have been found for repeating hypoglycaemic cases. Changes of protocol have also analysed and its reliability has been assessed.

The model and protocol have now been validated as much as possible *in silico*. The clinical trial can now be performed to determine if the model-based calculated insulin sensitivity is accurate enough and if this new Dynamic Insulin Sensitivity and Secretion Test (DISST) can be applied to a larger population.

Note that all the results generated *in silico* in this research are not fundamental truth because they are intrinsic to the model. Even though they are able to help for the implementation of the experimental part, the clinical trial is needed to confirm these obtained ranges.

Chapter 6

Clinical trial

This chapter describes the clinical trial designed at the University of Canterbury (Christchurch, New Zealand) in order to assess the new developed Dynamic Insulin Sensitivity and Secretion Test (DISST). First, the protocol followed during all this pilot clinical trial is described. Using the outcomes of the multiple parameter sensitivity analysis in Chapter 5, small changes of the initial protocol could be considered in some specific situations and are thus explained. Second, ethics approval is presented. Thereafter, the results of the first patient are discussed. Finally, these results are analysed.

6.1 Protocol

The initial protocol, applied to every patient involved in the study, is detailed. Some potential changes of the protocol and the reasons for these modifications are also presented.

6.1.1 Initial protocol

Before describing all the different steps of the protocol, one can emphasise the similarities between this test and an Oral Glucose Tolerance Test (see Section 2.6.1). More specifically, the participant drinks a glucose solution and blood samples are collected. In contrast, a subcutaneous insulin injection is added and blood samples are collected more frequently, requiring an intravenous (IV) cannula.

This experimental trial first requires the patient fasts at least 10 hours before the test. Age, sex, height, weight and allergies are also recorded. The test begins with the oral intake of 35 g of glucose in solution. For context, a 350 mL can of Coke is composed of the same mass of sugar. The glucose looks like a white powder and comes from the EQUAGOLD[®] company (Figure 6.1a). The glucose is measured using a scale (Figure 6.1b) and is diluted in 200 ml of water.

Fifteen minutes later, 2 units of very rapid-acting insulin are injected in the patient's leg or belly (Figure 6.2). The delivery is made through a needle free injection method. In this kind of device, high pressure is generated and



(a) EQUAGOLD[®] glucose.



(b) Measurement of 35 g of glucose.

Figure 6.1 :
Glucose kit.

propels insulin through the skin at high velocity in an approximately 0.1 μm hole. The insulin diffuses subcutaneously into plasma.

Originally, this Needle Free Injection Technology (NFIT) was developed to administer very viscous liquids [70], which were sometimes impossible or very difficult to inject through normal syringes. By modifying some properties of this device, such as the generated pressure, the depth of injection can be regulated and this technology can be employed for a broad range of drugs. Several companies have marketed needle free injection products, each with specific features in term of infusion depth and medicines, but none have used the electromagnetic technology here.

For this particular trial, the needle free injection device is a prototype developed by Portal Instruments NZ. This product is adapted for less viscous liquid, like insulin. The needle free instrument looks like a pistol and currently requires external power (Figure 6.3). Besides being painless, this sort of device is reusable, can be used at home, and decreases the risk of disease transmission. The injection time is also reduced. This technology is thus highly suitable for the treatment of chronic diseases and improving adherence to injections, as it is also painless.

The drug container of the needle free injection device is filled with a fast-acting, monomeric insulin, from a NovoRapid[®] FlexPen[®] (Roche AG, Denmark [71]). A dilution in a physiological solution has to be carried out before the injection in the container to obtain the required concentration. The container has a capacity of 0.5 mL, which is supplied with a liquid mixture containing 5 units of insulin and saline solution. Only 2 units are injected, the residual is thrown away. Filling is achieved with the aid of an adapter, a needle and a syringe. For the practical

side during the trial, all the equipment related to the insulin and the filling of the needle free injection device are gathered in the same box (Figure 6.4).



Figure 6.2 :
Injection of the insulin in the patient's leg.



Figure 6.3 :
Needle free injection device.



Figure 6.4 :
Insulin box.

Throughout the test duration, the blood glucose level is monitored with finger-prick blood tests. The samples are collected at time points $t = 0, 10, 15, 20, 25, 30, 40, 50, 60, 70, 80, 90, 100$ and 120 minutes. An added fasting sample is taken 30 to 60 minutes prior the starting. A finger-prick blood test consists of a small needle inserted in the fingertip, extracting a small drop of blood. This small amount of blood is then placed on a test strip for an Accu-Check[®] glucometer (Roche AG, Denmark [71]), as shown in Figure 6.5.

In addition to the finger-prick blood tests, other samples are collected through an intravenous (IV) cannula at the wrist. The intravenous cannula is installed by Dr Geoff Shaw. All the material related to this procedure such as needles, catheter, syringes of saline solution, IV film dressing, connector, compresses and alcohol swabs are gathered in the same box (Figure 6.6).



Figure 6.5 :

The Accu-Check[®] monitoring instrument, the test strips and the finger-pricker.

These IV blood samples are taken at time points $t = 0, 20, 40, 50, 60, 90,$ and 120 minutes. For each extraction, 8 mL is removed. In comparison with a standard blood donation for which 470 mL are collected over a period of 15 minutes, only 56 mL over 120 minutes are taken. For each sample, a very small amount of blood is first collected and thrown away to be able to access non-contaminated or non-diluted blood thereafter. Saline solution is injected after the extraction to flush the cannula. The box illustrated in Figure 6.7 groups all the equipment linked to the intravenous blood samples.

Each sample is collected by the doctor and separated in two distinct tubes for glucose, and insulin and C-peptide assays. Finally, no finger-prick blood sample is drawn if an intravenous one is taken at the same time. Instead, a small amount of the intravenous extraction is placed on the Accu-Check[®] strip.



Figure 6.6 :

IV box.



Figure 6.7 :

Box related to intravenous blood samples.

At the end of the test, the intravenous cannula is removed and the patient gets a biscuit and a soft drink to ensure no post-test hypoglycaemia. Some questions about the pain perceived during the insulin injection and the finger-prick are asked to assess relative discomfort, if any. The blood samples are brought to the laboratory (Canterbury Labs, Christchurch) to be tested.

Given the previous explanations, the test lasts less than three hours. If the patient feels uncomfortable, he/she can decide to stop the trial. Some minor risks are involved. First, the intravenous cannula and finger-prick tests can lead to pain, irritation and infection. Second, regarding the injection of insulin, a small risk of hypoglycaemia, as shown in the simulations, has to be considered.

All the data obtained during this study are confidential and saved under a non-identifying number to respect patient confidentiality. Only Lui Pearson and his supervisors have access to the identifying figures. Regarding any published articles, only non-identifying data are used.

A schematic representation of the protocol and the different blood sample times can be found in Figure 6.8.

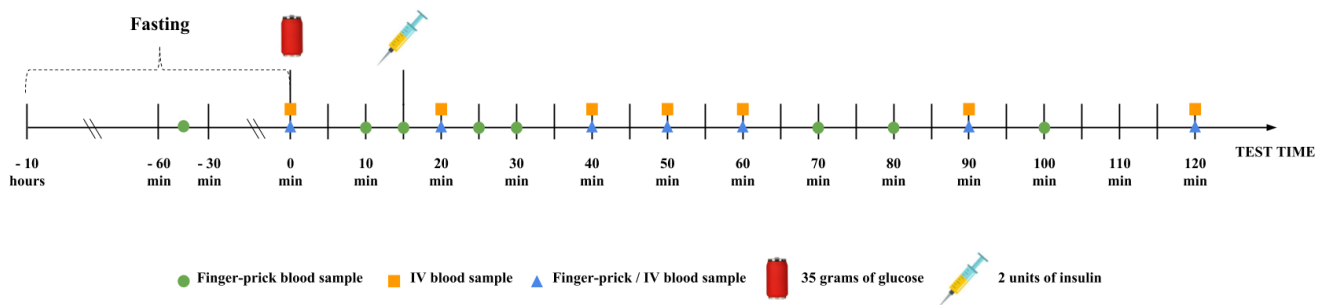


Figure 6.8 :
Trial protocol and timing.

6.1.2 Possible changes

Regarding the multiple parameter sensitivity analysis in Chapter 5, hypoglycaemic situations can occur in every case for very high insulin sensitivity individuals ($S_I = 0.0018 \text{ L} \cdot (\text{mU} \cdot \text{min})^{-1}$), assuming no responsive change in EGP and endogenous insulin secretion. Athletic and healthy people may have such a high model-based insulin sensitivity due to larger than normal non-insulin-mediated glucose uptake. For these patients, it may be interesting to enhance the glucose dose to decrease the potential risk of hypoglycaemia. Indeed, by increasing the glucose dose to 65 g or 75 g, it enables to cancel hypoglycaemic situations for high insulin sensitivity (Chapter 5). However, the decision to increase the dose would be only based on an external opinion and initial experience in pilot trials. The impact of such an increase on participant with a normal insulin sensitivity ($S_I = 0.00108 \text{ L} \cdot (\text{mU} \cdot \text{min})^{-1}$) has thus also been analysed. Results of Chapter 5 shows some risks of hyperglycaemia.

6.2 Ethics approval

Because this trial requires an experimental part on persons, an ethics approval was necessary. The latter has been submitted to the Human Ethics Committee (HEC) of the University of Canterbury in February 2018. First, a questionnaire about the project has to be filled out, and information and consent sheets have to be provided. For more aspects of the procedure that has to be followed, the website of the Human Ethics Committee (<http://www.canterbury.ac.nz/study/ethics/human-ethics-committee/>) can be visited. After some discussion and revision, the trial received final ethics approval April 30, 2018.

6.3 Test results

In addition to the personal data and sensation of the patient, two distinct types of results are presented in this section. First, the blood sugar levels are recorded during all of the test by means of finger-prick samples and the Accu-Check[®] monitoring device. These results are directly available. Second, some blood samples have been collected intravenously. They were brought to the laboratory to obtain glucose, insulin and C-peptide concentrations. These results are thus not directly ready.

▷ Identity sheet of patient

- ID : 1
- AGE : 53 years
- SEX : Male
- WEIGHT : 90 kg
- SIZE : 1.89 m
- ALLERGIES : /

The ID is the number of the test and coincides with the non-identifying data.

▷ Sensations of the patient

- DISCOMFORT OF THE FINGER-PRICK : 3/10
- DISCOMFORT OF THE INSULIN DELIVERY : 0-1/10

According to this patient, the insulin delivery was much less painful than the finger-prick.

▷ **Results of the finger-prick blood samples**

During the trial, blood samples are collected and directly assessed for blood glucose concentration. Two types of data are available. First, finger-prick blood samples are collected and blood glucose concentrations are measured with the Accu-Check[®] monitoring device. In contrast, no finger-prick blood sample is collected when an intravenous one is already extracted. Instead, a small droplet of this sample is placed on the Accu-Check[®] test strip and the measurement is obtained. The directly available results of all these samples are gathered in Table 6.1. Note that some of the finger-prick blood samples have been collected in the finger, and others in the arm.

Table 6.1 :

Directly available results with the Accu-Check[®] monitoring device

(the blood sample in gray (■) has been added in comparison with the normal protocol).

Time [min]	Sample Type	Sample Location	BGL [mmol/L]
- 42	Finger-prick	Finger	4.9
0	IV	IV Installation	4.9
10	Finger-prick	Finger	5.5
15	Finger-prick	Finger	6.8
20	IV	IV Installation	7.5
25	Finger-prick	Finger	7.8
30	Finger-prick	Arm	7.9
40	IV	IV Installation	6.5
50	IV	IV Installation	5.5
60	IV	IV Installation	4.6
70	Finger-prick	Arm	4.8
80	Finger-prick	Arm	4.8
90	IV	IV Installation	3.9
100	Finger-prick	Finger	4.4
100	IV	IV Installation	4.0
120	IV	IV Installation	4.4

Figure 6.9 presents the directly available data. At time $T = 100$ min, both finger-prick and IV blood samples were collected. It was done in addition for comparison between capillary and venous blood. In particular, very close to the skin, capillary blood may contain more interstitial fluid if the finger is squeezed, and this difference can distort the results. The difference is in this case 0.4 mmol/L.

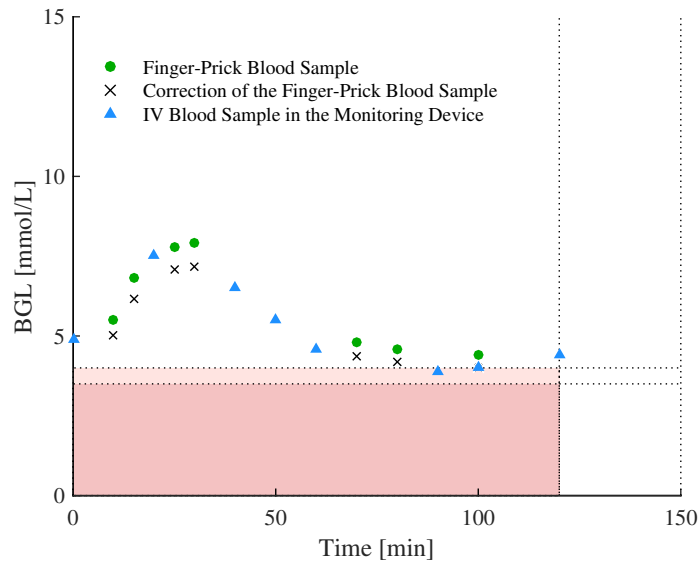


Figure 6.9 :

Finger-prick BG measurements and measurements of BG with IV blood in the monitoring device for Patient 1.

▷ **Results of the IV blood samples**

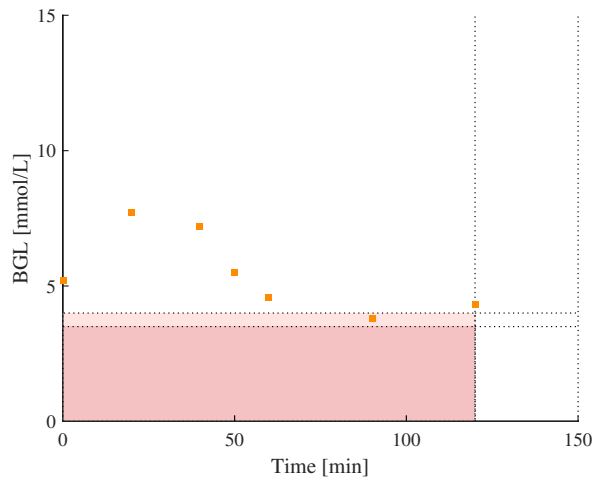
The IV blood samples were brought to the laboratory (Canterbury Labs, Christchurch) and tested for blood glucose, insulin, and C-peptide. Results for blood glucose and C-peptide are presented in Figures 6.10a and 6.10b. Unfortunately, results for insulin are not available to date.

Note that blood samples are collected and assessed with three different ways. First, finger-prick blood samples are extracted and assessed with a monitoring device. Then, the monitoring device also measures the blood glucose concentration of IV samples. These are the directly available data. Third, IV blood samples are collected and brought to a laboratory to assess blood glucose, insulin and C-peptide. These results are not directly available. Incoherence between glucose concentrations originating from different measurements can be observed.

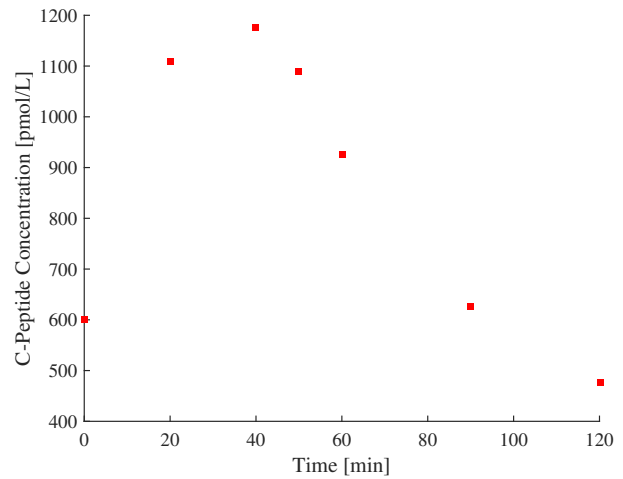
Before analysing the obtained results, a small clarification should be made. During this clinical trial, we faced some problems regarding the subcutaneous insulin injection. Because we were not sure about the first injection, a second one was performed. The individual has thus received between 0.0 and 4.0 U of insulin. Moreover, the time of injections was thus delayed by 3 minutes.

6.4 Analysis

Regarding Figures 6.9 and 6.10a, BG evolutions strongly look like model-based BG evolutions. After a glucose peak, this evolution decreases and finally stabilises. This stabilisation results from Endogenous Glucose Production (EGP), which normally is dependent on blood glucose concentration. In this model, EGP is fixed as a constant.



(a) IV blood glucose results.



(b) IV C-peptide results.

Figure 6.10 :
IV results for Patient 1.

The insulin sensitivity of Patient 1 can be assessed via a parametric identification, by comparing the data obtained during the clinical trial and the model-based BG evolutions. IV results are assumed more accurate than other BG results. Thus, they are used for the parametric identification. Because of the fixed EGP of the model, only the beginning of the model-based BG evolution must match with the clinical data. Thus, only the first five IV blood samples are considered. Weight is fixed to 90 kg in the model. Because of the problem with the insulin injection, the insulin time delay is fixed to 18 min. Insulin sensitivity is made varying between $0.0007 \text{ L} \cdot (\text{mU} \cdot \text{min})^{-1}$ and $0.0015 \text{ L} \cdot (\text{mU} \cdot \text{min})^{-1}$ by steps of $0.00005 \text{ L} \cdot (\text{mU} \cdot \text{min})^{-1}$. Respective model-based BG evolutions are generated. The BG evolution, which is the closest to the first five IV blood samples, is chosen. The insulin sensitivity of this curve is assigned to Patient 1 as a first analysis.

The method of least squares is used to assess the difference between the generated BG evolutions and the first five IV blood samples. The function that quantifies this gap is defined :

$$\phi = (5.2 - BG(0))^2 + (7.7 - BG(20))^2 + (7.2 - BG(40))^2 + (5.5 - BG(50))^2 + (4.6 - BG(60))^2 \quad (6.1)$$

Where 5.2, 7.7, 7.2, 5.5 and 4.6 are the first five results of IV blood samples and $BG(x)$ represents the value for time x of the considered BG evolution.

Because of the problem with the insulin injection, 2 insulin doses are considered, specifically 2 U or 4 U. Figure 6.11a represents the model-based BG evolutions, generated for different insulin sensitivities (defined above) and for $I_{bolus} = 2$ U. The curve, which has the better match with the clinical data, is linked to an insulin sensitivity of $0.0012 \text{ L} \cdot (\text{mU} \cdot \text{min})^{-1}$ and is represented in dark. In contrast, Figure 6.11b represents the model-based BG evolutions, generated for different insulin sensitivities and for $I_{bolus} = 4$ U. The curve, which has the better match with the clinical data, is linked to an insulin sensitivity of $0.0010 \text{ L} \cdot (\text{mU} \cdot \text{min})^{-1}$.

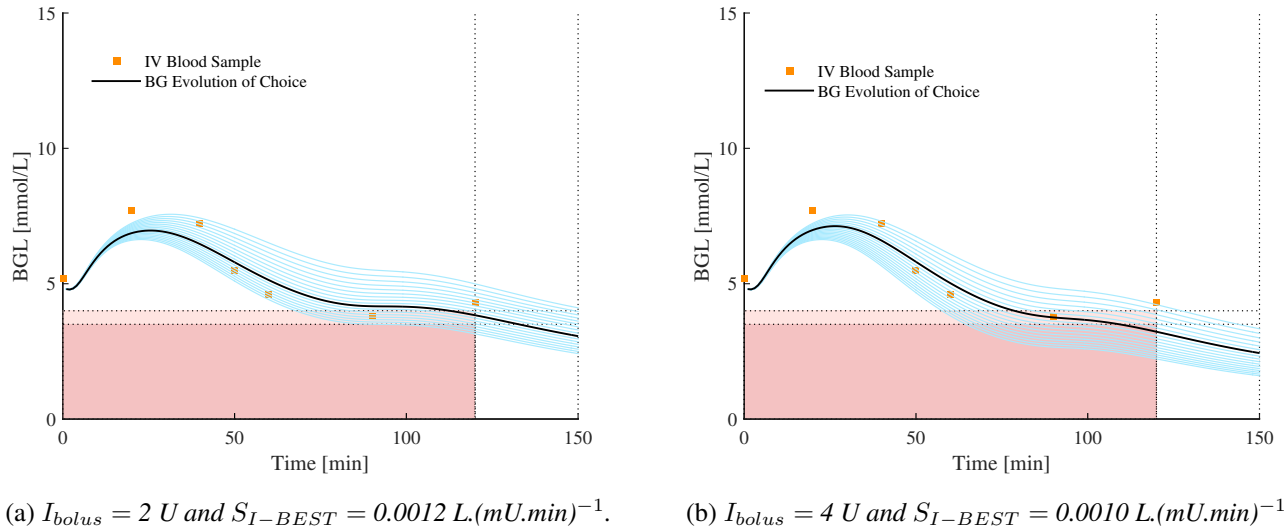


Figure 6.11 :
Parametric identification of Patient 1.

Even though this parametric identification is not perfectly accurate, it provides an idea of the insulin sensitivity of the patient. Indeed, this clinical data was the first one and some small modifications have thus to be provided. Moreover, the hypothesis of a constant EGP leads to some small issues for a consistent parametric identification.

6.5 Summary

In this chapter, the protocol followed during the clinical trial is carefully described. Because the ethical agreement was accepted on time, I have assisted the first one. Its results are provided and analysed. A rapid parametric identification enables to assess an approximation of the insulin sensitivity of the patient. The clinical data also allow to highlight some weaknesses of the model, such as the constant Endogenous Glucose Production (EGP) that does not reflect the physiological situation.

Chapters 4 and 5 have assessed the reliability of the model and protocol. This chapter describes a clinical trial, where these validated model and protocol are used. This clinical trial is in fact the end state and culmination of this

thesis. Indeed, as the experimental part is still in its early days, the aim of this part of the project is more related to a proof of concept of the model, as well as a personal achievement, to see how could the model be useful for real clinical applications.

Chapter 7

Conclusions

7.1 General conclusions

Because of the increasingly ageing population and prevalence of obesity, diabetes has reached epidemic proportions worldwide. The total health expenditures related to this disease and its long-term complications are very high, approaching $\approx 1\%$ of GDP in many countries. Diabetes is thus a major public health problem. Type 2 diabetes is characterised by a resistance to insulin or a decrease of insulin sensitivity. As insulin resistance developed during the pre-diabetic stage, long before the final stage of the disease, its diagnosis is thus possible years before diagnosis of type 2 diabetes. Irreparable damage and cost could thus be prevented or reduced by early diagnosis. However, common current insulin sensitivity tests are either low resolution, and/or costly, invasive, time consuming, and not adapted for economic wide scale screening.

A new model-based insulin sensitivity test is studied in this master thesis. It is a less invasive, new version of the already validated model-based Dynamic Insulin Sensitivity and Secretion Test (DISST). The proposed protocol uses 35 g of oral glucose and 2 units of rapid-acting insulin. The insulin injection is performed subcutaneously with a needle free injection device, 15 minutes after the beginning of the test. The number of blood samples is minimal and some are even extracted with a less invasive finger-prick method than the intravenous route, in preparation for emerging needle free technology. Blood samples are collected over a 2-hour period and are assessed for blood glucose, C-peptide and insulin.

The original DISST model is a glycaemic control model and is thus modified to consider the oral glucose absorption and the subcutaneous insulin injection, applied during this new test. A gastrointestinal glucose sub-model and a subcutaneous insulin delivery sub-model are added. The orally absorbed glucose and its modifications in the gastrointestinal tract can be seen as the exogenous glucose inflow in the glycaemic control model. In contrast, subcutaneously injected insulin and its appearance in plasma can be considered as the exogenous insulin input in the glycaemic control model. In combination, they create a full system model.

Even though the different sub-models have been validated separately, especially the DISST model, the entire system model needs validation. A single sensitivity analysis is thus performed. This *in silico* investigation provides a means to highlight any model weakness, as well as emphasising the critical parameters and/or model assumptions. It can also demonstrate the robustness of the model, as well as the potential accuracy of this new kind of DISST.

In this single parameter sensitivity analysis, effects of model parameters on model outcomes are analysed individually. Parameters with the biggest influence on the model-based BG evolutions are identified, specifically the insulin sensitivity, S_I , the minimum rate of gastric emptying, k_{min} , the intersection point, c , the intestinal absorption fraction, f , the transport rate into the interstitium, k_2 , the interstitium insulin transport rate into the plasma, k_3 , the glucose sensitivity, k_{sec} , and the endogenous pancreatic insulin secretion offset, k_{off} . Parameter changes always lead to a coherent modification of blood glucose evolution. The BG trajectories generated correspond to the expected physiological dynamics after an oral glucose dose and a subcutaneous insulin injection. No non-physiological behaviours are observed, providing further validation. Even though shifts in BG evolutions are observed, most are not clinically significant. This leads to the preliminary assessment of the new model overall reliability.

The results of the single parameter sensitivity analysis are used to perform a multiple parameter Monte Carlo analysis. The different insulin sensitivities considered in this part represent all the stages in the pathogenesis of type 2 diabetes, from Normal Glucose Tolerance (NGT) to severe diabetes, including Impaired Glucose Tolerance (IGT). A much higher insulin sensitivity is also considered to address safety. For each of these insulin sensitivities, four of the previously detected parameters of interest are randomly changed simultaneously to create a range of possible model-based BG evolutions. The potential range of the model, as well as the inter-subject and intra-subject variability, are quantified to ensure robustness and safety. Once again, no non-physiological situation or clinically relevant behaviour is detected and this analysis further consolidates model reliability.

Now that the model is validated *in silico* and shown to follow physiological expectations, it is used to assess protocol safety. This protocol must ensure the security of all the patients who are going to participate to the clinical trial, which is an essential step to confirm the performance of this type of model-based test. The multiple BG evolutions generated, each representing a physiological situation that could be encountered during a clinical trial, are analysed for any potential hypoglycaemia. Increases of the oral glucose dose are performed and shown to reduce the hypoglycaemic situations when high insulin-sensitive individual are considered. A zero subcutaneous insulin injection is then imposed to examine behaviour when a dysfunction of the needle free injection device occurs. Safety issues were observed, but the importance of this injection on trial results is assessed. Indeed, the fundamental decrease of BG evolution due to insulin effects is enhanced with this injection and insulin sensitivities are thus more easily identified.

The model and protocol have thus been validated. A clinical trial thus needs to be performed to assess the performances of this new insulin sensitivity test. The trial received ethics approval during the redaction of this master thesis (April 30, 2018). The first assay is described and all technical details are explained. With the obtained results, a rapid parametric identification is performed to assess insulin sensitivity. However, as those experiments are still in a pilot trial stage, the aim of this part of the project is a proof of concept and a personal achievement. However, the calculated insulin sensitivity is in compliance with the documentation and the external features and physiological data of the patient. This is thus encouraging for the clinical validation of this new test.

7.2 Perspectives and Future work

For the sake of completeness, limitations of the model, as outlined in the specific chapters, should be corrected. First, in the model, the Endogenous Glucose Production (EGP) is fixed as a constant. However, this does not correspond to the physiological situation, where it varies according to the blood glucose concentration. Because of this constant EGP, model-based BG evolutions drop at the end of the simulation. In real life, BG finally stabilises. The single and multiple parameter sensitivity analysis should thus be performed with a fluctuating EGP, in particular if a suitable EGP model can be found. Second, a small limitation concerns the fasting glucose level. In the model, it is fixed to 4.8 mmol/L. However, diabetic individuals have a more elevated basal glucose concentration. In the multiple parameter sensitivity analysis, each time an insulin sensitivity of $0.00025 \text{ L} \cdot (\text{mU} \cdot \text{min})^{-1}$ is considered, it represents a diabetic state. However, the fasting glucose level is not changed. Fasting blood glucose levels should thus also be increased in simulating T2D cases.

After the *in silico* validation of the model and the protocol, the clinical trial is performed to assess the reliability of this new insulin sensitivity testing. The results of this trial would be analysed to measure insulin sensitivity. Accuracy, sensitivity and specificity of this method should then be quantified.

Even if this insulin sensitivity from this test is finally clinically validated, it still remains invasive and not really adapted for a population screening. Indeed, because of the intravenous installation, this test needs to be performed in an hospital or in a place with a specialist. Even though insulin sensitivity tests become more accurate and less invasive, progress is still needed to achieve large population detection. This last outcome should arise from ongoing technology development at the University of Canterbury (Christchurch, New Zealand) and in New Zealand for needle free glucose and insulin test devices.

Appendices

Appendix A : Chapter 3

The SC-OG-ICING-2 model is represented in Figure 3.1 and is defined by the Equations A.1 to A.13 below :

$$\dot{q}_{sto1}(t) = -k_{21} \cdot q_{sto1}(t) + D \cdot \delta(t) \quad (\text{A.1})$$

$$\dot{q}_{sto2}(t) = -k_{empt}(q_{sto}) \cdot q_{sto2}(t) + k_{21} \cdot q_{sto1}(t) \quad (\text{A.2})$$

$$\dot{q}_{gut} = -k_{abs} \cdot q_{gut}(t) + k_{empt}(q_{sto}) \cdot q_{sto2}(t) \quad (\text{A.3})$$

$$Ra(t) = f \cdot k_{abs} \cdot q_{gut}(t) \quad (\text{A.4})$$

$$k_{empt}(q_{sto}) = k_{min} + \frac{k_{max} - k_{min}}{2} \cdot \{ \tanh[\alpha \cdot (q_{sto} - b \cdot D)] - \tanh[\beta \cdot (q_{sto} - c \cdot D)] + 2 \} \quad (\text{A.5})$$

$$q_{sto}(t) = q_{sto1}(t) + q_{sto2}(t) \quad (1)$$

$$\alpha = \frac{5}{2 \cdot D \cdot (1 - b)} \quad (\text{A.6})$$

$$\beta = \frac{5}{2 \cdot D \cdot c} \quad (\text{A.7})$$

$$\dot{I}_{sc}(t) = -k_2 \cdot I_{sc}(t) + \delta(t - T) \cdot I_{bolus} \quad (\text{A.8})$$

$$\dot{Q}_{local}(t) = -k_3 \cdot Q_{local}(t) + k_2 \cdot I_{sc}(t) - k_{di} \cdot Q_{local}(t) \quad (\text{A.9})$$

$$\dot{G}(t) = -p_G \cdot (G(t) - G_{fast}) - \frac{S_I \cdot G(t) \cdot Q(t)}{1 + \alpha_G \cdot Q(t)} + \frac{Ra(t) + EGP - CNS}{V_G} \quad (\text{A.10})$$

$$\dot{I}(t) = -n_K \cdot I(t) - n_L \cdot \frac{I(t)}{1 + \alpha_I \cdot I(t)} - n_I \cdot (I(t) - Q(t)) + \frac{(k_3 \cdot Q_{local}(t) + (1 - x_L) \cdot u_{en}(G))}{V_I} \quad (\text{A.11})$$

$$\dot{Q} = n_I \cdot (I(t) - Q(t)) - n_C \cdot \frac{Q(t)}{1 + \alpha_g \cdot Q(t)} \quad (\text{A.12})$$

$$u_{en}(G) = \begin{cases} u_{min} & \text{if } G(t) < G_{fast} \\ f(G) = k_{sec} \cdot G(t) + k_{off} & \text{otherwise} \\ u_{max} & \text{if } f(G) \geq u_{max} \end{cases} \quad (\text{A.13})$$

Tables A.1 and A.2 represent respectively the summary of all the parameters and variables used in the SC-OG-ICING-2 model.

Table A.1 :
Summary of the parameters of the entire model.

Parameter	Signification	Value	Units
p_G	Insulin-independent glucose uptake rate	0.04	min^{-1}
G_{fast}	Fasting blood glucose level	4.8	mmol.L^{-1}
S_I	Insulin sensitivity	10.8×10^{-4}	$\text{L} \cdot (\text{mU} \cdot \text{min})^{-1}$
α_G	Insulin binding saturation parameter	0.0154	$\text{L} \cdot \text{mU}^{-1}$
P	Exogenous glucose inflow rate	see Section 3.2	$\text{mmol} \cdot \text{min}^{-1}$
EGP	Endogenous Glucose Production rate	0.96	$\text{mmol} \cdot \text{min}^{-1}$
CNS	Central Nervous System glucose uptake rate	0.3	$\text{mmol} \cdot \text{min}^{-1}$
V_G	Plasma glucose distribution volume	12.2	L
n_K	Kidney clearance rate of plasma insulin	0.06	min^{-1}
n_L	Liver clearance rate of plasma insulin	0.0324	min^{-1}
α_I	Hepatic clearance saturation parameter	0.0017	$\text{L} \cdot \text{mU}^{-1}$
n_I	Insulin diffusion rate	0.006	min^{-1}
x_L	Fractional first pass of hepatic insulin extraction	0.67	-
u_{en}	Endogenous pancreatic insulin rate	$f(G)$	$\text{mU} \cdot \text{min}^{-1}$
u_{ex}	Exogenous insulin input rate	see Section 3.3	$\text{mU} \cdot \text{min}^{-1}$

V_I	Plasma and interstitial insulin distribution volume	4	L
n_C	Cellular insulin clearance rate from interstitium	0.032	min^{-1}
u_{min}	Minimum endogenous pancreatic insulin secretion rate	16.7	$\text{mU}\cdot\text{min}^{-1}$
u_{max}	Maximum endogenous pancreatic insulin secretion rate	267	$\text{mU}\cdot\text{min}^{-1}$
k_{sec}	Glucose sensitivity of the endogenous pancreatic insulin secretion rate	14.9	$(\text{mU}\cdot\text{L})\cdot(\text{mmol}\cdot\text{min})^{-1}$
k_{off}	Endogenous pancreatic insulin secretion offset	-49.9	$\text{mU}\cdot\text{min}^{-1}$
k_{21}	Rate of grinding	1	min^{-1}
k_{empt}	Rate of gastric emptying	$f(g_{sto})$	min^{-1}
k_{abs}	Rate constant of intestinal absorption	0.205	min^{-1}
f	Intestinal absorption fraction	0.8	-
k_{min}	Minimum rate of gastric emptying	0.013	min^{-1}
k_{max}	Maximum rate of gastric emptying	0.043	min^{-1}
b	"Intersection point"	0.85	-
c	"Intersection point"	0.25	-
k_2	Transport rate into interstitium	0.0104	min^{-1}
k_3	Interstitium insulin transport rate into plasma	0.06	min^{-1}
k_{di}	Rate of loss from interstitium	0.0029	min^{-1}
I_{bolus}	Amount of injected insulin	2000	mU
T	Time delay	15	min

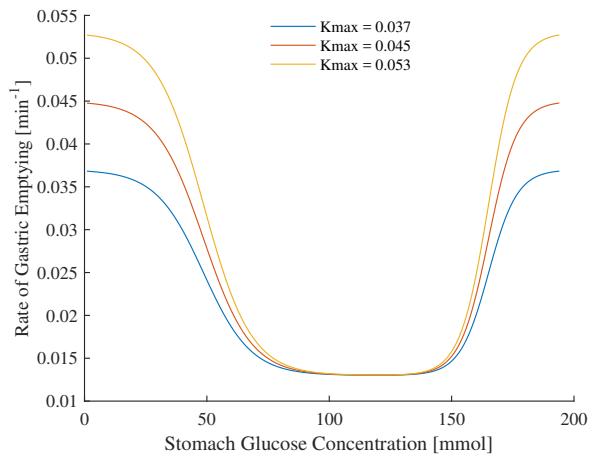
Table A.2 :
Summary of the variables of the entire model.

Variable	Signification	Initial value	Units
G	Blood glucose concentration	4.8	$\text{mmol}\cdot\text{L}^{-1}$
I	Plasma insulin concentration	13.4185	$\text{mU}\cdot\text{L}^{-1}$
Q	Interstitial insulin concentration	7.4255	$\text{mU}\cdot\text{L}^{-1}$
q_{sto1}	Amount of stomach glucose in the solid compartment	194.3	mmol
q_{sto2}	Amount of stomach glucose in the liquid compartment	0	mmol
q_{gut}	Amount of gut glucose	0	mmol

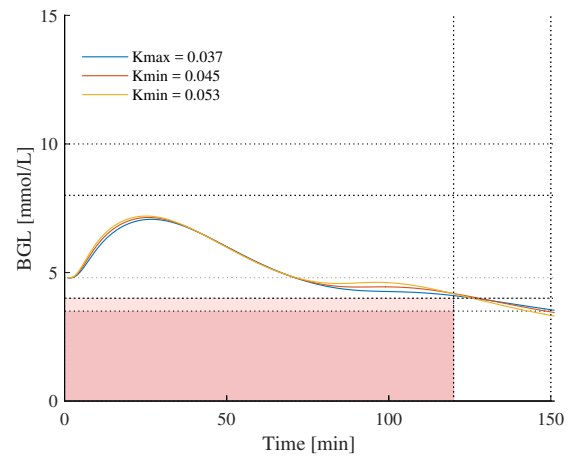
R_a	Plasma rate of appearance of ingested glucose	0	$\text{mmol}\cdot\text{min}^{-1}$
I_{sc}	Amount of insulin in the subcutaneous space	2000	mU
Q_{local}	Amount of insulin a local interstitium	0	mU

Appendix B : Chapter 4

▷ Maximum rate of gastric emptying k_{max}



(a) Shape of k_{empt} according to different values of the parameter k_{max} .



(b) BG evolution according to different values of the parameter k_{max} .

Figure 1 :

Influence of the parameter k_{max} on BG evolution and on shape of k_{empt} .

▷ **Rate constant of intestinal absorption k_{abs}**

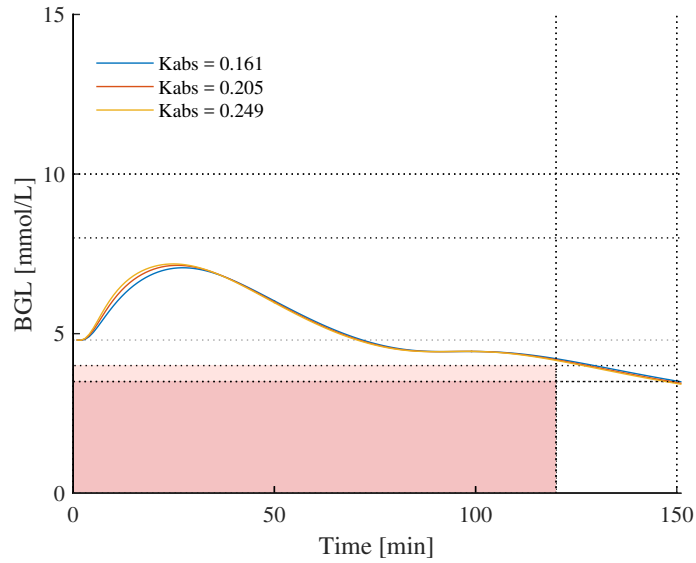


Figure 2 :

BG evolution according to different values of the parameter K_{abs} .

▷ **Rate of loss from the local interstitium k_{di}**

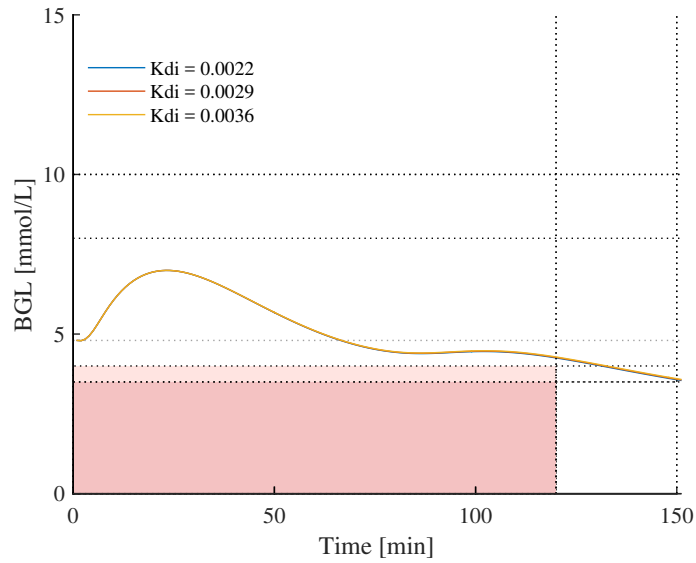
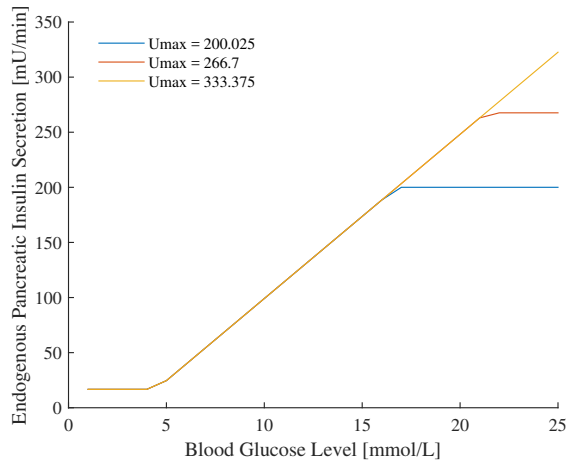


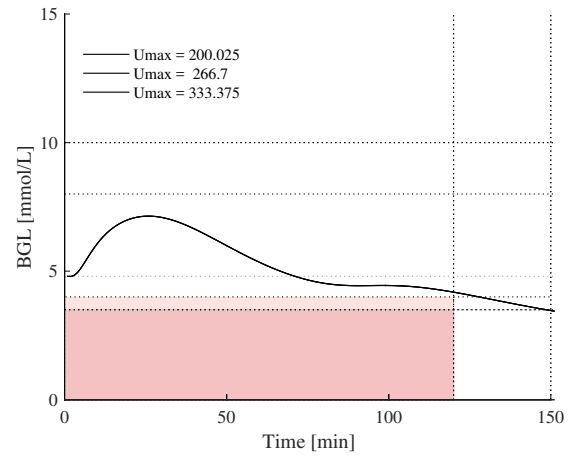
Figure 3 :

BG evolution according to different values of the parameter K_{di} .

▷ **Maximum endogenous pancreatic insulin secretion rate u_{max}**



(a) Shape of u_{en} according to different values of the parameter u_{max} .



(b) BG evolution according to different values of the parameter u_{max} .

Figure 4 :
Influence of the parameter u_{max} on BG evolution and on shape of u_{en} .

Bibliography

- [1] International Diabetes Federation, "*About diabetes: facts and figures*", <http://www.idf.org/about-diabetes/facts-figures>.
- [2] Organisation Mondiale de la Santé, "*centre des médias*", <http://www.who.int/diabetes/infographic/fr/>.
- [3] C. Bommer, V. Sagalova, E. Heeseemann, J. Manne-Goehler, R. Atun, T. Bärnighausen, J. Davies, S. Vollmer, "*Global Economic Burden of Diabetes in Adults: Projections From 2015 to 2030*", American Diabetes Association, Diabetes Care (Vol. 41, No. 5, pp. 963-970), May 2018.
- [4] Campbell, "*Biologie*", Pearson, 9th edition.
- [5] E. Ferrannini, "*Insulin resistance is central to the burden of diabetes*", Diabetes Metab Revue (Vol. 13, No. 2), 1997.
- [6] World Health Organization, "*Definition and Diagnosis of Diabetes Mellitus and Intermediate Hyperglycemia*".
- [7] N. A. Othman, "*Analysis and Optimisation of ModelBased Insulin Sensitivity and Secretion Tests*", University of Canterbury, Christchurch, 29 April 2015.
- [8] Docherty P., "*Evaluation and Development of the Dynamic Insulin Sensitivity and Secretion Test for Numerous Clinical Applications*", University of Canterbury, Christchurch, 7 March 2011.
- [9] K. A. McAuley, J. E. Berkeley, P. D. Docherty, T. F. Lotz, L. A. Te Morenga, G. M. Shaw, S. M. Williams, J. G. Chase, J. I. Mann, "*The dynamic insulin sensitivity and secretion test—a novel measure of insulin sensitivity*", Metabolism, 2011.
- [10] T. F. Lotz, J. G. Chase, K. A. McAuley, G. M. Shaw, P. D. Docherty, J. E. Berkeley, S. M. Williams, C. E. Hann, J. I. Mann, "*Design and Clinical Pilot Testing of the Model-Based Dynamic Insulin Sensitivity and Secretion Test (DISST)*", Journal of Diabetes Science and Technology (Vol. 4, No. 6), November 2010.
- [11] Pronovost M., "*Chapitre 2 : Organisation moléculaire des structures du vivant*", http://mpronovost.profweb.ca/BIONP1/bionp1_molecules_glucides.html, 2015.
- [12] T. McKee, J. McKey, "*Biochemistry : The Molecular Basis of Life*", Oxford.

- [13] *"An Introduction to Nutrition : A Closer Look at Carbohydrates"*, <http://2012books.lardbucket.org/books/an-introduction-to-nutrition/s08-01-a-closer-look-at-carbohydrates.html>, 2012.
- [14] Wikipedia, *Glycogène*, <https://fr.wikipedia.org/wiki/Glycog%C3%A8ne>, last update on 3 January 2018.
- [15] S. Edwards, *"Sugar and the Brain"*, <http://neuro.hms.harvard.edu/harvard-mahoney-neuroscience-institute/brain-newsletter/and-brain-series/sugar-and-brain>, Harvard Medical School : Department of Neurobiology.
- [16] R. Jumpertz, M. S. Thearle, J. C. Bunt, J. Krakoff, *"Assessment of Non-insulin Mediated Glucose Uptake: Association with Body Fat and Glycemic Status"*, *Metabolism* (Vol. 59, No. 10), October 2010.
- [17] Wikipedia, *"Hypoglycemia"*, <https://en.wikipedia.org/wiki/Hypoglycemia>, last update on 1 June 2017.
- [18] American Diabetes Association, *"Hypoglycemia (Low Blood Glucose)"*, <http://www.diabetes.org/living-with-diabetes/treatment-and-care/blood-glucose-control/hypoglycemia-low-blood.html>.
- [19] Wikipedia, *"Hyperglycémie"*, <https://fr.wikipedia.org/wiki/Hyperglycémie>, last update on 6 December 2017.
- [20] Association Belge du Diabète, *"Complications"*, <https://www.diabete-abd.be/le-diabete-cest-quoi/complications.aspx>.
- [21] Doctissimo Santé, *"Glycémie et diabète : les chiffres clés"*, <http://www.doctissimo.fr/html/dossiers/diabete/articles/901-diabete-chiffres-faits.htm>, last update on 14 November 2013.
- [22] Wikipedia, *"Insulin"*, <https://en.wikipedia.org/wiki/Insulin>, last update on 23 March 2018.
- [23] Wikipedia, *"Insuline"*, <https://fr.wikipedia.org/wiki/Insuline>, last update on 28 February 2018.
- [24] Wikipedia, *"Peptide C"*, https://fr.wikipedia.org/wiki/Peptide_C, last update on 27 November 2017.
- [25] Delisle I., *"Sécrétion endocrine du pancreas et sa régulation : Implication en pathologie et thérapeutique (diabète exclu) "*.
- [26] Berthelot, *"TPE DIABETE : Découverte d'un traitement qui sauve des vie"*, <https://diabetetpeberthelot.webnode.fr/news/les-premieres-formes-dinsuline-artificielle/>, 30 January 2015.

- [27] Wikipedia, "*Chromatography*", <https://en.wikipedia.org/wiki/Chromatography>, last update on 21 May 2018.
- [28] Larousse, "*Production d'insuline par génie génétique*", http://www.larousse.fr/encyclopedie/animations/Production_dinsuline_par_g%C3%A9nie_g%C3%A9n%C3%A9tique_m%C3%A9dicament_recombinant/1100478, 2006.
- [29] Site du Collège National de Pharmacologie Médicale, "*Médicament : Insuline*", <https://pharmacomedicale.org/medicaments/par-specialites/item/insulines>, 31 mai 2017.
- [30] Wikipedia, "*Régulation de la glycémie*", https://fr.wikipedia.org/wiki/R%C3%A9gulation_de_la_glyc%C3%A9mie, last update on 28 April 2018.
- [31] C. G Pretty, A. J. Le Compte, J. G. Chase, G. M. Shaw, J.-C. Preiser, S. Penning, T. Desaive, "*Variability of insulin sensitivity during the first 4 days of critical illness: implications for tight glycemic control*", *Annals of Intensive Care*, 2012.
- [32] V. Uyttendaele, J. L. Dickson, G. M. Shaw, T. Desaive, J. G. Chase, "*Untangling glycaemia and mortality in critical care*", *Critical Care* (Vol. 21, No. 152), 2017.
- [33] Wong X., "*Model-Based Therapeutics for Type 1 Diabetes Mellitus*", University of Canterbury, Christchurch, 23 June 2008.
- [34] Fédération Française des Diabétiques, "*Le diabète gestationnel*", <https://www.federationdesdiabetiques.org/information/diabete-gestationnel>.
- [35] Diabète Québec, "*Le diabète de type 1*", <https://www.diabete.qc.ca/fr/comprendre-le-diabete/tout-sur-le-diabete/types-de-diabete/le-diabete-de-type-1>, Avril 2014.
- [36] D. M. Nathan, M. B. Davidson, R. A. DeFronzo, R. J. Heine, R. R. Henry, R. Pratley, B. Zinman, "*Impaired Fasting Glucose and Impaired Glucose Tolerance*", *Diabetes Care* (Vol. 30, No. 3, pp.753-759, Mars 2007).
- [37] L. Holder-Pearson, S. Bekisz, J. Knopp, P. Docherty, J. G. Chase, T. Desaive, "*Model-based Modified OGTT Insulin Sensitivity Test Design*", University of Canterbury, Christchurch, 2018.
- [38] Diabetes.co.uk, "*Fasting Blood Sugar Levels*", https://www.diabetes.co.uk/diabetes_care/fasting-blood-sugar-levels.html.
- [39] C. Kyle, "*When to use fasting glucose to diagnose people with type II diabetes*", https://bpac.org.nz/BT/2012/December/12_fastingGlucose.aspx, bpac^{NZ}, December 2012.
- [40] E. MannucciA. OgnibeneI. SposatoM. BrogiG. GalloriG. BardiniF. CremascoG. MesseriC. M. Rotella, "*Fasting plasma glucose and glycated haemoglobin in the screening of diabetes and impaired glucose tolerance*", *Acta Diabetologica* (Vol. 40, No. 4, pp. 181–186), December 2003.

- [41] Diabetes.co.uk, "*Oral Glucose Tolerance Test*", <https://www.diabetes.co.uk/oral-glucose-tolerance-test.html>.
- [42] Wikipedia, "*Glucose Tolerance Test*", https://en.wikipedia.org/wiki/Glucose_tolerance_test#Dose_of_glucose_and_variations, last update on 21 May 2018.
- [43] C. Thoma, "*Very Low Calorie Diets Type 2 Diabetes Reversal Part 4: Glucose Tolerance*" <http://www.builtformotion.co.nz/reversing-type-2-diabetes-blog/very-low-calorie-diets-type-2-diabetes-reversal-part-4-glucose-tolerance>, 26 June 2015.
- [44] Lotz T., "*High Resolution Clinical Model-Based Assessment of Insulin Sensitivity*", University of Canterbury, Christchurch, 27 April 2007.
- [45] Fédération Française de Diabétiques, "*L'HbA1c ou hémoglobine glyquée*", <https://www.federationdesdiabetiques.org/information/glycemie/hba1c>.
- [46] P. Drury, "*The new role of HbA1c in diagnosing type 2 diabetes*", Best Practice Journal, 2012.
- [47] Wikipedia, "*Glycated Hemoglobin*", https://en.wikipedia.org/wiki/Glycated_hemoglobin, last update on 7 June 2018.
- [48] S. S. Fajans, W. H. Herman, E. A. Oral, "*Insufficient sensitivity of hemoglobin A1C determination in diagnosis or screening of early diabetic states*", *Metabolism Clinical and Experimental* (Vol. 60), 2011.
- [49] C. M. Bennett, M. Guo and S. C. Dharmage, "*HbA1c as a screening tool for detection of Type 2 diabetes: a systematic review*", *Diabetic Medicine*, 2017.
- [50] NZSSD, "*Position Statement on the diagnosis of, and screening for, Type 2 Diabetes*", September 2011.
- [51] Wikipedia, "*Glucose Clamp Technique*", https://en.wikipedia.org/wiki/Glucose_clamp_technique, last update on 29 October 2017.
- [52] Wartburg L., "*What's a glucose clamp, anyway ?*", <https://www.diabeteshealth.com/whats-a-glucose-clamp-anyway/>, DiabetesHealth, 6 November 2017.
- [53] DeFronzo R.A., Tobin J.D., Andres R., "*Glucose clamp technique: a method for quantifying insulin secretion and resistance* ", *American Physiology Society*, 1 September 1979.
- [54] C. Cobelli, E. Carson, "*Introduction to modelling in physiology and medicine*", A volume in the academic press series in Biomedical Engineering (Elsevier).
- [55] P. D. Docherty, J. G. Chase, T. F Lotz, T. Desaive, "*A graphical method for practical and informative identifiability analyses of physiological models: A case study of insulin kinetics and sensitivity*", *Biomedical Engineering Online*, 2011.

- [56] G. Pillonetto, G. Sparacino, C. Cobelli, *"Numerical non-identifiability regions of the minimal model of glucose kinetics: superiority of Bayesian estimation"*, Math Biosci, 2003.
- [57] P. D. Docherty, J. G. Chase, L. Te Morenga, T. F. Lotz, J. E. Berkeley, G. M. Shaw, K. A. McAuley, J. I. Mann, *"A Spectrum of Dynamic Insulin Sensitivity Test Protocols"*, Journal of Diabetes Science and Technology (Vol. 5, No. 6), November 2011.
- [58] P. D. Docherty, J. E. Berkeley, T. F. Lotz, L. Te Morenga, L. M. Fisk, G. M. Shaw, K. A. McAuley, J. I. Mann, J. G. Chase, *"Clinical Validation of the Quick Dynamic Insulin Sensitivity Test"*, Biomedical Engineering (Vol. 60, No. 5), May 2013.
- [59] Pretty C., *"Analysis, classification and management of insulin sensitivity variability in a glucose-insulin system model for critical illness"*, University of Canterbury, Christchurch, 24 January 2012.
- [60] C. G. Pretty, A.J Le Compte, J. G. Chase, G. M. Shaw, J.-C. Preiser, S. Penning, T. Desaive, *"Variability of insulin sensitivity during the first 4 days of critical illness: implications for tight glycaemic control"*, Annals of Intensive Care (Vol. 2, No. 17), 2012.
- [61] Lina J, Razak N., Pretty C., Le Compte A., Docherty P., Parente J., Shaw G., Hann C., Chase G., *"A Physiological Intensive Control Insulin-Nutrition-Glucose (ICING) Model Validated in Critically Ill Patients"*, 2011.
- [62] J. L. Dickson, K. W. Stewart, C. G. Pretty, M. Flechet, T. Desaive, S. Penning, B. C. Lambermont, B. Benyó, G. M. Shaw, J. G. Chase, *"Generalisability of a Virtual Trials Method for Glycaemic Control in Intensive Care"*, 2017.
- [63] J. G. Chase, J.-C. Preiser, J. L. Dickson, A. Pironet, Y. S. Chiew, C. G. Pretty, G. M. Shaw, B. Benyo, K. Moeller, S. Safaei, M. Tawhai, P. Hunter, T. Desaive, *"Next-generation, personalised, model-based critical care medicine: a state-of-the art review of in silico virtual patient models, methods, and cohorts, and how to validate them"*, Biomedical Engineering (Vol. 17, No. 24), 2018.
- [64] J G. Chase¹, F. Suhaimi, S. Penning, J.-C. Preiser, A. J. Le Compte, J. Lin, C. G. Pretty, G. M Shaw, K. T. Moorhead, Thomas Desaive, *"Validation of a model-based virtual trials method for tight glycaemic control in intensive care"*, Biomedical Engineering OnLine (Vol. 9, No. 84), 2010.
- [65] J. Lin, U. Jamaludin, P. Docherty, N. N. Razak, A. Le Compte, C. G. Pretty, C. E. Hann, G. M. Shaw, J. G. Chase, *"Modeled Insulin Sensitivity and Interstitial Insulin Action from a Pilot Study of Dynamic Insulin Sensitivity Tests"*.
- [66] Dalla Man C., Camilleri M., Cobelli C., *"A System Model of Oral Glucose Absorption : Validation on Gold Standard Data"*, Biomedical Engineering (Vol. 53, No. 12), December 2006.
- [67] J.Wong, J. G. Chase, C. E. Hann, G. M. Shaw, T. F. Lotz, J. Lin, A. J. Le Compte, *"A Subcutaneous Insulin Pharmacokinetic Model for Computer Simulation in a Diabetes Decision Support Role: Model Structure and Parameter Identification"*, Journal of Diabetes Science and Technology (Vol. 2 and No. 4), July 2008.

- [68] J.Wong, J. G. Chase, C. E. Hann, G. M. Shaw, T. F. Lotz, J. Lin, A. J. Le Compte, "A *Subcutaneous Insulin Pharmacokinetic Model for Computer Simulation in a Diabetes Decision Support Role: Validation and Simulation*", Journal of Diabetes Science and Technology (Vol. 2 and No. 4), July 2008.
- [69] T. F. Lotz, J. G. Chase, K. A. McAuley, G.M. Shaw, X. W. Wong, J. Lin, A. J. Le Compte, C.E. Hann, J. I. Mann, *Monte Carlo analysis of a new model-based method for insulin sensitivity testing*, Computer methods and programs in biomedicine, 2008.
- [70] Portal Instruments, <https://www.portalinstruments.com/>.
- [71] Roche, <https://www.roche.com/careers.htm>.